

In gemeinsamer Betreuung der
Freien Universität Berlin
und
L'Université Louis Pasteur de Strasbourg

Influence of glial cells on postnatal differentiation
of rat retinal ganglion cells

Dissertation

zur Erlangung des akademischen Grades
doctor rerum naturalium

vorgelegt von
Christian Göritz

beim Fachbereich Biologie, Chemie, Pharmazie
der Freien Universität Berlin

Berlin im Dezember 2004

1. Gutachter: Dr. Frank W. Pfrieder
2. Gutachter: Prof. Dr. Ferdinand Hucho

Disputation: February 25th, 2005

Für Franz Haase

LIST OF CONTENTS

I. INTRODUCTION	1
1.1 Importance of glia neuron interaction for brain development.....	1
1.1.1 Axon pathfinding at the optic chiasm.....	2
1.1.2 Differentiation of nodes of Ranvier.....	5
1.1.3 Influence of glia on synaptogenesis.....	8
1.1.3.1 Role of cholesterol in synapse formation	10
1.1.3.1.1 Neurosteroids.....	11
1.1.3.1.2 Building material	12
1.1.3.1.3 Microdomains/rafts.....	13
1.2 My project	14
II. MATERIAL AND METHODS.....	15
2.1 Cultures of purified CNS neurones	15
2.2 Preparation of GCM	17
2.3 Electrophysiological recordings	17
2.4 Filipin staining.....	18
2.5 Immunocytochemistry	19
2.6 RNA preparation	21
2.7 Gene expression analysis.....	21
2.8 SDS-polyacrylamid-gel electrophoresis (SDS-PAGE)	23
2.9 Immunoblotting	24
2.10 Radioactive labeling and lipid analysis	25
III. RESULTS	27
3.1 Multiple mechanisms mediate glia-induced synaptogenesis in RGCs.....	27
3.1.1 Time course of GCM- and cholesterol-induced changes in the number of..... synapses.....	27
3.1.2 Time course of GCM- and cholesterol-induced increase in neuritic	30
cholesterol content.....	
3.1.3 Dendrite differentiation as rate-limiting step for GCM- and	31
cholesterol-induced synaptogenesis	
3.1.4 Evidence for laminin as dendrite-promoting factor.....	34
3.1.5 Effects of GCM removal on synaptic activity	38
3.2 Influence of soluble glial factors and cholesterol on gene expression	
of cultured postnatal RGCs	41
3.2.1 Microarray analyses and data assessment	41
3.2.2 Expression changes in RGCs related to soluble glia derived factors	44

3.2.2.1 GCM regulated cholesterol synthesis and homeostasis in cultured RGCs and caused downregulation of genes involved in steroid metabolism and fatty acid synthesis	47
3.2.2.2 GCM upregulates matrix Gla protein and heme oxygenase 1 in cultured RGCs.....	52
3.2.3 Comparison of GCM and cholesterol-induced expression changes.....	54
3.2.3.1 Cholesterol treatment mimicked the GCM induced reduction of neuronal cholesterol synthesis	57
3.2.3.2 Cholesterol did not affect MGP and HO1 gene expression but downregulates HO1 on protein level in RGCs	58
I V . DISCUSSION	60
4.1 Multiple mechanisms mediate glia-induced synaptogenesis in RGCs.....	60
4.1.1 Dendrite differentiation limits the rate of glia-induced synaptogenesis, requires cholesterol and is promoted by laminin.....	60
4.1.2 Cholesterol is required for ongoing synaptogenesis and the stability of evoked release	62
4.2 Influence of soluble glial factors and cholesterol on gene expression of cultured postnatal RGCs.....	63
4.2.1 RGCs synthesize cholesterol and fatty acids, and regulate their homeostasis in reaction to external supply	63
4.2.2 Dendritic localization of MGP and HO1	65
V. SUMMARY	68
V I . REFERENCES	74
V I I . ACKNOWLEDGEMENTS	92
V I I I . CURRICULUM VITAE	93

ABBREVIATIONS

ABC-G1	ABC transporter G1
Acat 2	acetyl-Coenzyme A acetyltransferase 2
adu	analog-to-digital units
AMPA	amino-3-hydroxy-5-methylisoxazol-4-propionic acid
ApoE	apolipoprotein E
BDNF	brain derived neurotrophic factor
BMP	bone morphogenetic protein
BSA	bovine serum albumin
CV	coefficient of variance
cGMP	cyclic guanosine monophosphate
CNS	central nervous system
CNTF	ciliary neurotrophic factor
CO	carbon monoxide
DHEA	dehydroepiandrosterone
DMEM	Dulbecco's modified eagle's medium
D-PBS	Dulbecco's phosphate buffered saline
EBBS	Earle's balanced salt solution
ECL	enhanced chemoluminescence
EDTA	ethylene-diamine-tetraacetic acid
EPSC	excitatory postsynaptic currents
EST	expressed sequence tag
FCS	fetal calf serum
GABA	γ -aminobutyric acid
GCM	glia-conditioned medium
GLA	carboxyglutamic acid
GluR2/3	glutamate receptor 2/3
HO1	heme oxygenase 1
HSP 32	heat-shock protein 32
INSIG	insulin induced gene
LDL	low density lipoprotein
MARIA	muscarinic acetylcholine receptor-inducing activity
MGP	matrix Gla protein

Na _v channel	voltage-dependent Na ⁺ channel
NF155	155 kDa splice isoform of neurofascin
NMDA	N-methyl-D-aspartate
NMJ	neuromuscular junction
PDL	poly-D-lysine
PNS	peripheral nervous system
RGC	retinal ganglion cell
sGC	soluble guanylyl cyclase
SNAP 25	soluble synaptosomal-associated Protein of 25 kD
SNARE	soluble NSF attachment protein receptor
SQS	squalene synthase
SRE	sterol regulatory element
SREBP	sterol regulatory element binding protein
STAR	steroidogenic acute regulatory protein
TBS	tris buffered saline
TBS-T	tris buffered saline with Tween-20
TNF α	tumor necrosis factor α
TLC	thin layer chromatography

I . I N T R O D U C T I O N

The development of the nervous system is guided by a balanced action of intrinsic factors defined by the genetic program and of epigenetic factors characterized by cell-cell interactions via contact-dependent or secreted signals. It is well established that the interplay of neurons and glial cells is highly relevant for many aspects of nervous system development.

1.1 Importance of glia neuron interaction for brain development

The nervous system consists mainly of two types of cells, neurons and glial cells or neuroglia. Glial cells are further divided into three different classes (Fields & Stevens-Graham, 2002): Schwann cells and oligodendrocytes are the myelin forming cells of the peripheral nervous system (PNS) and central nervous system (CNS), respectively. These cells wrap layers of myelin membrane around axons to allow for fast impulse conduction. Second, there are astrocytes, which are closely associated with neurons in the brain but do not form myelin. The name refers to their stellate form observed in histological preparations, but their morphology varies widely. Astrocytes form endfeet which connect to blood capillaries and wrap synapses. These interconnections allow them to regulate extracellular concentrations of ions, metabolites and neurotransmitters and to provide neurons. Microglia make up the third category of glial cells in the brain. In contrast to oligodendrocytes and astrocytes, which derive from ectodermal precursors within the nervous system, microglia derive from bone marrow monocyte precursors (Kaur et al., 2001). Like their counterparts in the hematopoietic system, microglia respond to injury or disease by engulfing cellular debris and triggering inflammatory responses.

For a long time, glial cells were regarded as somewhat passive companions to neurons. Today, however, more than a century after their description by Virchow (1856), there is increasing evidence that neurons and glia cells have an intimate and plastic morphological and functional relationship (Pfrieger & Barres, 1996). So intimate is the association between astrocytes and neurons, for example, that monitoring activity of these nonneuronal cells is a reliable surrogate for measuring neural activity (Dani et al., 1992; Porter & McCarthy, 1996; Rochon et al., 2001).

Neuron-glia interactions control several processes of brain development such as neurogenesis (Lim & Alvarez-Buylla 1999), myelination (Girault & Peles, 2002; Bhat, 2003), synapse formation (Slezak & Pfrieger, 2003; Ullian et al., 2004), neuronal

migration (Nadarajah & Parnavelas, 2002), proliferation (Gomes et al., 1999) and differentiation (Garcia-Abreu et al., 1995). Several soluble factors secreted by either glial or neuronal cells, such as neurotransmitters, hormones and growth factors, have been implicated in nervous system morphogenesis (Gomes, 2001).

In the following, I will describe axon pathfinding at the optic chiasm and the differentiation of nodes of Ranvier as examples of well established neuron-glia interactions during development.

1.1.1 Axon pathfinding at the optic chiasm

The correct wiring of the nervous system relies on the ability of axons and dendrites to locate and recognize their appropriate synaptic partners. Axons are guided along specific pathways by attractive and repulsive cues in the extracellular environment. In the mammalian visual system, for example, retinal ganglion cell (RGC) axons form the optic nerve. Axons from each eye grow towards one another to meet at the ventral midline of the diencephalon where they establish an X-shaped intersection called the optic chiasm (Fig. 1). During mouse development, the formation of the optic chiasm appears to occur in two separate phases. In the first phase, early generated RGC axons originating from dorsal-central retina reach the developing ventral diencephalon at embryonic day E12-E12.5 and grow across the ventral midline to establish the correct position of the X-shaped optic chiasm (Colello & Guillery, 1990; Godement et al., 1990; Sretavan, 1990). A number of these early axons, instead of crossing the midline, project into the ipsilateral side of the brain, forming a transient ipsilateral projection (Fig. 1). RGC axons from more peripheral parts of the retina enter the chiasm later, at E13-E14, and make specific pathfinding choices such that the adult-like pattern of chiasmatic axon routing into the ipsilateral and contralateral optic tracts is established by E15-E16 (Sretavan & Reichardt, 1993; Marcus et al., 1995).

One of the cellular specializations localized to the site at which the chiasm will form is a palisade of radial glia draped along either side of the midline, occupying the midline zone at which retinal axons diverge (Fig. 1) (Marcus et al., 1995; Reese et al., 1994; Marcus & Mason, 1995). RGC axons segregate into the ipsilateral and contralateral components during the time when their growth cones contact the midline radial glia (Marcus et al., 1995), suggesting that midline glia could provide important guidance information. Such an interaction has been shown in the *Drosophila* ventral nerve cord and the vertebrate spinal

cord, where midline glia mediate differential axon guidance (Kaprielian et al., 2001). To control axons crossing at the ventral midline, in both systems, midline glia release Netrins, acting as attractants (Harris et al., 1996; Mitchell et al., 1996; Serafini et al., 1996), and Slits, acting as repellents (Kidd et al., 1999; Brose & Tessier-Lavigne, 2000). Axons modulate their responsiveness to these two signals during midline crossing. Crossing axons are initially attracted by Netrin and insensitive to Slit, which draws them to the midline. After reaching the midline they become insensitive to Netrin and upregulate the Slit receptor Robo in axons, which propels them out of the midline (Kidd et al., 1998). This acquired sensitivity to Slit also prevents later recrossing. Other axons, not destined to cross, are sensitive to Slit from the beginning and so never reach the midline. However, to guide RGC axons through the optic chiasm, Netrin is expressed highly at the optic nerve head and acts as an attractant (Deiner et al., 1997). Whereas Slit 1 and 2 are expressed by cells surrounding the chiasm and repel ipsilateral and contralateral axons alike (Erskine et al., 2000; Plump et al., 2002). This has led to the idea that Slit-expressing cells form a repulsive corridor to guide all RGC axons through the chiasm. This model is supported by genetic experiments that disrupt Slit/Robo signaling in fish and mice. Zebrafish carrying a mutation in the *astray/robo2* gene have profound defects in retinal axon pathfinding (Fricke et al., 2001). Double mutant mice for Slit 1 and 2 genes show a large additional chiasm developed anterior to the true chiasm (Plump et al., 2002). Recently, other glia-derived axon guiding signals at the optic chiasm have been described. Williams et al., (2003) could show that the axonal decision about crossing the midline to project contralaterally or uncrossing the midline to form ipsilateral projections is mediated by Ephrin-B2. They found that Ephrin-B2 is expressed in the midline radial glia exactly during the period of ipsilateral projections, and that blocking Ephrin-B2 function eliminates the ipsilateral projection. On the other side, they found that the expression of the Ephrin-B2 receptor EphB1 was restricted to a small number of ganglion cells located exclusively in the ventrotemporal retina. This expression pattern suggests that EphB1 may be present exclusively on ipsilateral axons (Fig. 1).

These data show that interactions between glial cells and neurons are essential for the correct wiring of the nervous system. Glia cells set important landmarks and actively guide axons to their appropriate synaptic partners.

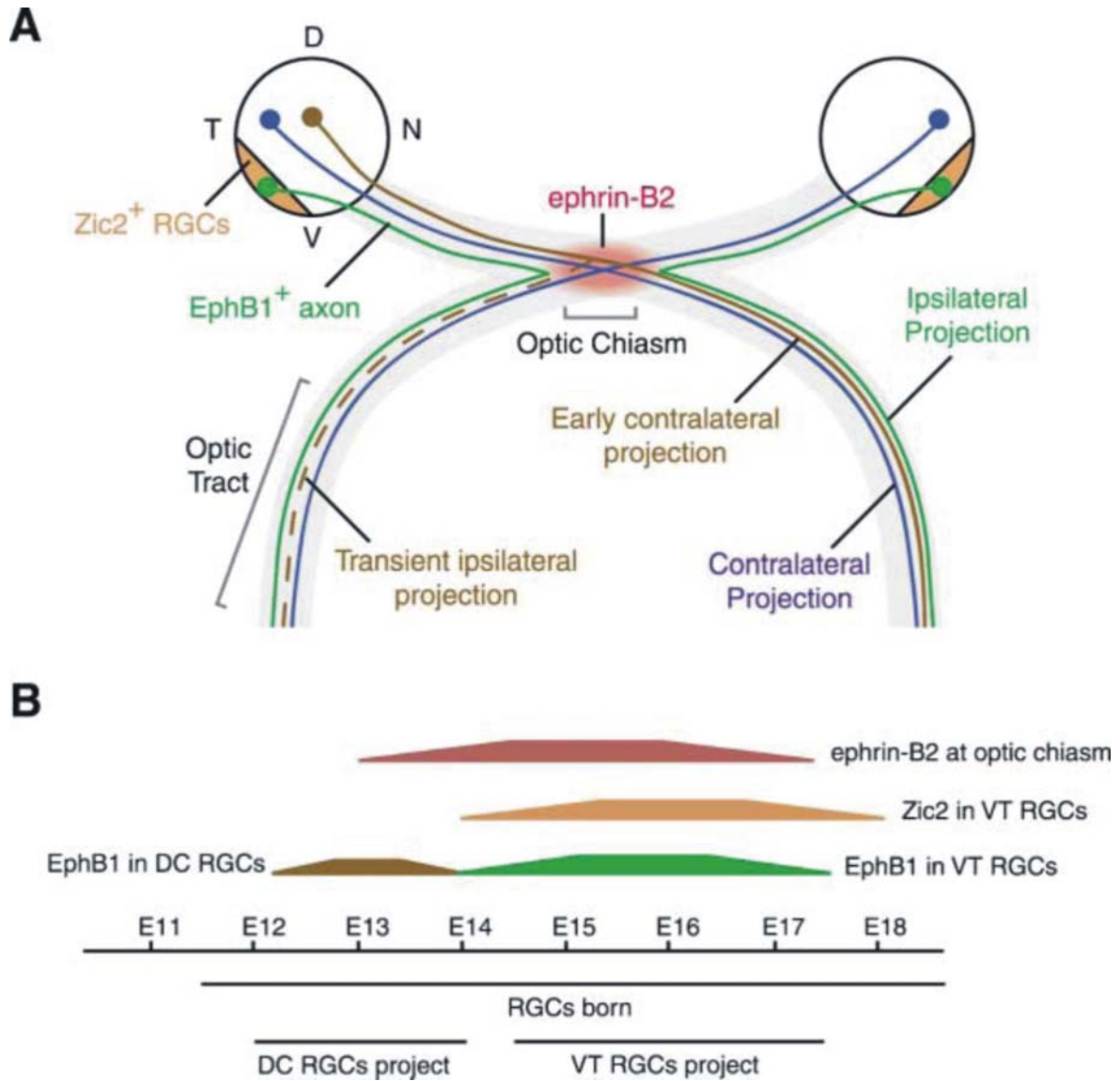


Figure 1: Model of axon sorting at the mouse optic chiasm

(A) Zic2-expressing RGCs give rise to ipsilaterally projecting axons, which express EphB1, allowing them to sense ephrin-B2 at the optic chiasm and turn into the ipsilateral tract. Axons that do not express EphB1 cross at the optic chiasm, joining the contralateral optic tract. D, dorsal; V, ventral; N, nasal; T, temporal. (B) Timeline. RGCs are generated from E11.5 until birth. The first RGCs are born in the dorsocentral (DC) retina. Most project contralaterally, but a few make transient ipsilateral projections. The permanent ipsilateral RGCs arise from the ventrotemporal (VT) retina and are generated from E14.5 to E17.5. These axons express Zic2 and EphB1. Ephrin-B2 is found at the chiasm from E13.5 to E17.5. From Rasband et al., (2003) based on the findings of Williams et al., (2003) and Herrera et al., (2003).

1.1.2 Differentiation of nodes of Ranvier

The development of myelinated axons represents one of the most complex interactions among glia cells and neurons. Many vertebrate axons are surrounded by a myelin sheath allowing rapid and efficient saltatory propagation of action potentials. In myelinated fibers, the contacts between neurons and oligodendrocytes or Schwann cells display a very high level of spatial and temporal organization. This organization requires a tight developmental control and the formation of a variety of specialized zones of contact between different areas of the myelinating cell membrane, and between the myelinating glia cell and the axon (Scherer & Arroyo, 2002). At regular intervals, myelinated axons show gaps in the sheathing myelin, called nodes of Ranvier. These sites interrupt the high-resistance, low-capacitance barrier of myelin and are responsible for the rapid transduction of action potentials by voltage-dependent Na^+ (Na_v) and potassium channels. Each node of Ranvier is flanked by paranodal regions where heliocoidally wrapped glial loops are attached to the axonal membrane by septate-like junctions. The segment between nodes of Ranvier is termed the internode. Its outermost part, in contact with paranodes, is referred to as the juxtaparanodal region (Fig. 2) (Arroyo & Scherer, 2000).

The initial physical contact of the myelinating glial cells with the axon triggers dynamic changes in the distribution and localization of Na^+ and K^+ channels. Prior to the glial cell contact, these channels are uniformly distributed along the axon. Contact of oligodendrocytes or Schwann cells cause an enrichment of Na_v channels at the node of Ranvier, which reach an estimated density of $1500/\mu\text{m}^2$ compared to less than $100/\mu\text{m}^2$ in the adjacent non-nodal regions (Rosenbluth, 1999). These channels display a unique molecular composition, in that they are composed of an α -subunit which is responsible for ion pore formation, and two β -subunits which mediate interactions with the extracellular and intracellular components (Isom, 2002). During development, the Na_v channel subtypes expressed at the node undergo a transition from $\text{Na}_v1.2$ to $\text{Na}_v1.6$, such that only $\text{Na}_v1.6$ channels are seen at the adult nodes of Ranvier (Boiko et al., 2001; Rios et al., 2003). In the unmyelinated proximal segment of the rat optic nerve, $\text{Na}_v1.2$ stays further on diffusely expressed (Boiko et al., 2001). Thus Na_v channel subtypes are differentially targeted within the same axon in a manner regulated by contact with myelinating glia. Two publications show that oligodendrocytes secrete so far unidentified soluble factors sufficient to trigger regulatory spaced axonal clustering of $\text{Na}_v1.2$ channels in cultured RGCs, but not of $\text{Na}_v1.6$ channels (Kaplan et al., 1997 and 2001).

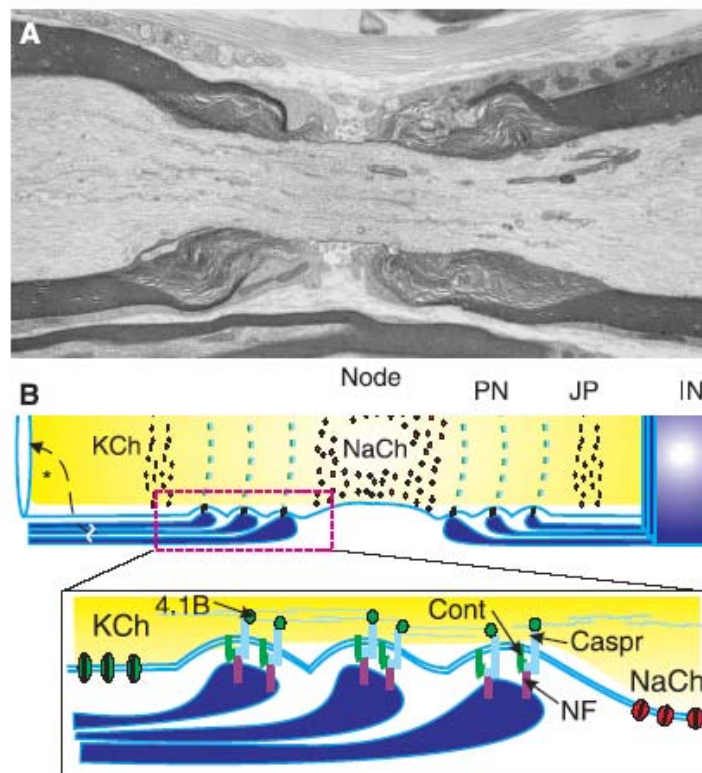


Figure 2: Organizational structure of nodes of Ranvier

(A) Electron micrograph of a longitudinal section through the node of Ranvier in the spinal dorsal root of rat. (B) Four specific domains are defined by axon-glia interactions at the node of Ranvier: the Na^+ channel-enriched node of Ranvier, the adjacent paranode (PN), the juxtaparanodal region (JP), which contains delayed rectifier K^+ channels, and the internode (IN). At the paranode, the transmembrane protein Caspr is found on the axon surface in association with the glycosyl-phosphatidyl-inositol anchored cell adhesion molecule, contactin (Cont). This molecular complex interacts with the glial cell adhesion molecule, neurofascin 155 (NF) and anchors the intercellular junction to the axonal cytoskeleton through the actin-associated protein 4.1B, which binds to the cytoplasmic domain of Caspr. From Fields & Stevens-Graham, (2002).

The requirement of glial cells for Na_v channel clustering was also demonstrated by the early postnatal selective ablation of oligodendrocytes in transgenic mice (Mathis et al., 2000). In these mice, no Na_v channel clustering was visible. Nodal Na_v channels appear to be part of multimolecular complexes including several intracellular [ankyrin G, β IV spectrin and syntenin-1 (Kordeli et al., 1995; Berghs et al., 2000; Lambert et al., 1997; Koroll et al., 2001)] and transmembrane proteins [NrCAM and neurofascin 186 kDa (Davis et al., 1996)]. These complexes have been implicated in the clustering or localization of Na_v channels to the node (Berghs et al., 2000; Komada & Soriano, 2002) and possibly interact with Schwann cell microvillus in the PNS or astrocyte endfeet in the CNS (Isom, 2002; Salzer, 2003).

On either side of the node of Ranvier, the compact myelin lamellae open up into a series of cytoplasmic loops that spiral around, closely appose and form a series of septate like junctions with the axon. These paranodal junctions have been proposed to perform several functions at this axo-glial interface, including anchoring of the glial myelin loops to the axon, creating an ionic diffusion barrier into the periaxonal space and serving as a fence to maintain the axonal domains and preventing lateral diffusion of the various membrane protein complexes (Bhat, 2003). The paranodal loops of oligodendrocytes and Schwann cells contain the 155 kDa splice isoform of neurofascin (NF155) (Tait et al., 2000), that binds to the Caspr-contactin complex on the axonal side (Charles et al., 2002). Since these three molecules are interdependent, it is very likely that Caspr/paranodin, contactin/F11 and NF155 form the core of the axoglial cell adhesion apparatus (Girault & Peles, 2002) (Fig. 2). Caspr/paranodin (Menegoz et al., 1997; Einheber et al., 1997) and contactin/F11 (Rios et al., 2000) are highly enriched in the paranodal axolemma. The association between Caspr/paranodin and contactin/F11 is necessary to address Caspr/paranodin to the plasma membrane in transfected cells (Faivre-Sarrailh et al., 2000) and its targeting to the axon *in vivo* (Rios et al., 2000). Knockout mice lacking Caspr/paranodin or contactin/F11 display ataxia, motor deficits and a dramatically reduced nerve conduction velocity (Bhat et al., 2001; Boyle et al., 2001). In these mutants the ultrastructure of the paranodes is severely altered: the glial paranodal loops are disorganized and the gap between glial and axonal membranes is increased (Bhat et al., 2001; Boyle et al., 2001).

Altogether these data show that the domain organization of nodes of Ranvier including accumulation of nodal and paranodal markers in the axolemma are all dependent on glia cells. The process of node formation is regulated by soluble signals from myelinating glia

as well as direct contact and interactions between proteins expressed on the surface of axons and oligodendrocytes or Schwann cells.

1.1.3 Influence of glia on synaptogenesis

As described above, there is good evidence that glial cells play a profound role at specific steps during neuronal differentiation. The hypothesis that astrocytes play a role in synapse formation stems from a temporal correlation between synaptogenesis and the differentiation of this glial cell type (Pfrieger & Barres, 1996). Most CNS neurons innervate their target areas at least one week before they form most of their synapses. Interestingly, synaptogenesis is delayed until about the same time as astrocytes are generated. This correlation was described for different brain areas (Jacobson, 1991; Parnavelas et al., 1983; Skoff, 1990; Rakic et al., 1986). Figure 3 illustrates the temporal correlation between synaptogenesis and glial differentiation, exemplified by the rodent retinocollicular pathway.

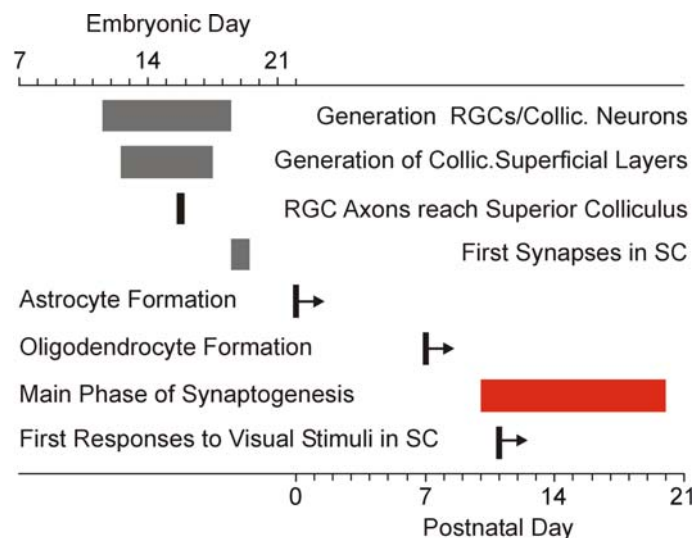


Figure 3: Temporal correlation between synaptogenesis and glial differentiation, exemplified by the rodent retinocollicular pathway. RGC axons reach their target in the superior colliculus (SC) between embryonic day 16 and the day of birth, postnatal day 0. But the majority of synapses are formed between the postnatal day 10 and 20 (Lund & Lund, 1972; Warton & McCart, 1989). Precisely during this delay period, between target innervation and synapse formation, astrocytes are born and proliferate in the superior colliculus. From Slezak & Pfrieger (2003).

Several glial factors with influence on synapse differentiation have been found within the last five years. Beattie et al., (2002), have shown that glia-derived tumor necrosis factor α (TNF α) raises the surface expression of glutamate receptors in hippocampal neurons from postnatal rats *in vitro* and in acute slices. Another study has shown that activity-dependent neurotrophic factor, which is released by astrocytes, acts as maturation signal for synapses (Gozes & Brenneman, 2000; Blondel et al., 2000). A glia-derived signal that controls the expression of specific transmitter receptors has been detected in the chick retina (Belmonte et al., 2000). Cultured Müller glia secrete a protein, termed muscarinic acetylcholine receptor-inducing activity (MARIA), which induces the expression of a specific subtype (M2) of muscarinic receptors in retinal neurons of chick embryos *in ovo*. Finally, there is a link between astrocytes and the most prominent synaptogenic factor agrin, a motoneuron-derived signal that is essential for the formation of neuromuscular junctions (NMJs) (Sanes & Lichtman, 1999) and that may play a role in synaptogenesis in the CNS (Böse et al., 2000). Contact with mouse glia reduced mRNA encoding for agrin in cultured rat hippocampal neurons, while soluble glial factors halved the expression of a specific isoform, but left the total level unaffected (Lesuisse et al., 2000). Notably, a very interesting study showed recently that neurotrophins support survival and growth of cultured frog spinal cord neurons, but inhibit agrin synthesis and thus NMJ formation, whereas soluble Schwann cell-derived factors override this inhibition and switch motoneurons to a synaptogenic state (Peng et al., 2003). An astrocyte-induced increase in synaptogenesis has been reported in different culture preparations including neuronal cell lines (Hartley et al., 1999), hippocampal neurons derived from stem cells of adult rats (Toda et al., 2000; Song et al., 2002) and neurons from spinal cord (Li et al., 1999), cortex (van den Pol & Spencer, 2000), hippocampus (den Pol & Spencer, 2000; Verderio et al., 1999) and hypothalamus (den Pol & Spencer, 2000) from embryonic or perinatal rats. It should be noted, however, that these studies did not exclude that astrocytes increased synapse numbers indirectly by enhancing neuronal survival or neuritic growth.

Direct evidence that astrocytes enhance synapse formation has been obtained by a series of studies on highly purified RGCs (Pfrieger & Barres, 1997; Mauch et al., 2001; Nädler et al., 2001; Ullian et al., 2001). These studies became possible by the establishment of a glia-free preparation of postnatal RGCs (Barres et al., 1988) and the opportunity to culture these cells for several weeks under serum- and glia-free conditions (Meyer-Franke et al., 1995). First, Pfrieger & Barres, (1997), showed that cultured RGCs form ultrastructurally defined synapses in the absence of glia. Thus, initial synapse formation

appears to be an intrinsic property of these neurons that does not require external signals. However, RGCs cultured in the absence of astrocytes, even for several weeks, exhibited very little spontaneous synaptic activity. In contrast, RGCs exhibited high levels of synaptic activity when they were cultured in the presence of a feeding layer of astrocytes or in glia-conditioned medium (GCM) (Pfrieger & Barres, 1997). Even when RGCs were co-cultured with purified collicular neurons, their normal targets, little synaptic activity was observed unless astrocytes were present. Importantly, the culture medium contained several neurotrophic factors that ensured equally high neuronal survival rates and extensive neuritic growth regardless of the presence of astrocytes. Two subsequent studies examined in parallel the effects of astrocytes on the number of synapses that formed between RGCs *in vitro*. As measured by immunostaining with pre- and postsynaptic markers, as well as by electron microscopy, astrocytes were found to induce a 7-fold increase in synapse number between RGCs (Nägler et al., 2001; Ullian et al., 2001). These synapses were presynaptically functional as shown by FM1-43 imaging, a measure of vesicular recycling. They were also postsynaptically functional, as shown by the amplitudes of mini-excitatory postsynaptic currents. Shortly after, at least one synaptogenic factor contained in GCM was identified as cholesterol (Mauch et al., 2001). This somewhat surprising finding provoked the hypothesis that cholesterol is an astrocyte-derived factor that limits the extent of synaptogenesis (Göritz et al., 2002; Pfrieger, 2003). Recently, Ullian et al., (2003) reported that, similar as described for RGCs, Schwann cells induce the formation of functional glutamatergic synapses between spinal motor neurons in culture. This study also showed that soluble astrocyte-derived factors could mimic the synapse-inducing effect of Schwann cells on motoneurons and conversely that Schwann cell-derived factors induce synapse formation in cultured RGCs. However, the nature of these synapse inducing factors remains unclear.

1.1.3.1 Role of cholesterol in synapse formation

The brain contains five to ten times more cholesterol than any other organ and this sterol represents 2-3% of the total weight and 20-30% of all lipids in the brain. Cholesterol is an essential component of biological membranes that determines their biophysical properties by its unique structure. The polar hydroxyl group on one end and the long hydrophobic tail on the other anchor its orientation in the phospholipid monolayer, and its flat shape allows for a neat fit between the hydrophobic tails of fatty acid chains. Cholesterol lowers the

permeability of membranes, possibly by compacting phospholipids, and regulates their fluidity in a temperature-dependent manner by changing the order of fatty acyl chains.

How can cholesterol promote synapse formation? There are three possible explanations: First, cholesterol may serve as a precursor for steroids, which have been shown to promote synaptogenesis (Sakamoto et al., 2001). Second, cholesterol may serve as a building material for different synaptic components. And finally, cholesterol may act by determining the functional properties of membrane-resident proteins like ion channels and neurotransmitter receptors due to creation of microdomains (Bastiaanse et al., 1997; Burger et al., 2000; Bruses et al., 2001; Suzuki et al., 2001).

1.1.3.1.1 Neurosteroids

Steroids, which are synthesized in the central or peripheral nervous system, are called neurosteroids. Neurosteroids are synthesized by oligodendrocytes, Schwann cells, astrocytes and neurons (Zwain & Yen, 1999), either *de novo* from cholesterol or from steroidal precursors imported from peripheral sources (Baulieu, 1998). They include steroids like pregnenolone and dehydroepiandrosterone (DHEA), their sulfates, and reduced metabolites as well as progesterone (Baulieu, 1998). These compounds can act as allosteric modulators of neurotransmitter receptors, such as GABA_A (Majewska et al., 1986), NMDA (Wu et al., 1991) and sigma receptors (Monnet et al., 1995) or via members of the nuclear hormone receptor superfamily. Nuclear hormone receptors are ligand-inducible transcription factors that bind to hormone responsive elements in DNA to activate or repress the expression of specific genes (Aranda & Pascual, 2001).

It has been shown by electron microscopy that estrogens increases dendritic spine density on CA1 pyramidal neurons, and in parallel increases synapse density on spines without any decrease in shaft synapses (Woolley & McEwen, 1992), implying that new spine synapses are formed. Confocal microscopic imaging showed that estrogen treatment up-regulates immunoreactivity for the largest NMDA receptor subunit, NR1, on dendrites and cell bodies of CA1 pyramidal neurons (Gazzaley et al., 1996). Murphy & Segal (1996) revealed that estrogen induces spines on dendrites of dissociated hippocampal neurons in culture by a process that is blocked by an NMDA receptor antagonist and not by an AMPA/kainate receptor blocker. It has been supposed that these effects are mediated by nuclear and extranuclear estrogen receptors (McEwen et al., 2001). Ultrastructural studies have revealed non-nuclear estrogen receptor α immunoreactivity on dendritic spines, axon terminals and glial processes within hippocampal principal cells (Milner et al., 2001).

These receptors are postulated to mediate rapid non-genomic effects (McEwen et al., 2001) via coupled second messenger systems (Levin, 1999; Kelly & Wagner, 1999; Simoncini et al., 2000). Interestingly, *in vivo* and *in vitro* studies using administration of progesterone to pups and cultured cerebellar slices of newborn rats, respectively, showed that progesterone promotes dendritic growth and spine formation of Purkinje cells (Sakamoto et al., 2001). Further analysis by electron microscopy revealed that progesterone induces an increase of synapse density on Purkinje cells, which have been shown to express nuclear progesterone receptors (Sakamoto et al., 2001). This suggests that progesterone promotes both dendritic outgrowth and synaptogenesis in Purkinje cells through nuclear receptor-mediated mechanisms.

1.1.3.1.2 Building material

The simplest explanation of how cholesterol promotes synapse formation would be that it is an essential component of the synaptic machinery and that its availability limits the assembly of synaptic structures. Due to its effects on the biophysical properties of membranes (Yeagle, 1985), cholesterol affects the function of membrane-resident signaling components including ion channels, transporters and receptors (Spector & Yorek, 1985; Yeagle, 1989; Barrantes, 1993; Bastiaanse et al., 1997; Burger et al., 2000). Measurement of cholesterol transbilayer distribution in brain synaptosomes by leaflet-selective quenching of fluorescent cholesterol analogs, has shown that the inner leaflet of synaptic membranes contains a eight-fold higher cholesterol concentration than its outer counterpart and that this distribution is affected by disease (Wood et al., 1990) and aging (Igbavboa et al., 1996). Moreover, ApoE and the LDL receptor influence the transbilayer distribution of cholesterol in synaptic membranes (Igbavboa et al., 1997; Hayashi et al., 2002). Another approach to visualize cholesterol distribution relies on the fact that the polyene antibiotic filipin forms complexes with sterols carrying a hydroxyl group at the third carbon atom. These complexes appear as protuberances in freeze-fractured membranes visualized by electron microscopy (Severs & Robenek, 1983). In frog NMJs, sterol-filipin complexes are localized in the transmitter release zone, but absent from the adjacent area (Nakajima & Bridgman, 1981; Ko & Propst, 1986). A similar distribution was observed at ribbon-type synapses between photoreceptors and bipolar neurons of chick retina (Cooper & McLaughlin, 1984). Notably, Surchev et al. (1995) showed that the density of sterol complexes in presynaptic membranes increases during postnatal development, using freeze-fracture electron microscopy. Egea et al. (1989) reported that potassium-induced acetylcholine release enhances the density of sterol-filipin complexes in

freeze-fracture replicas of synaptosomes from Torpedo electric organ. This effect was abolished in low calcium and by botulinus toxin indicating that the rearrangement was induced by the release process itself rather than by depolarization or calcium influx. Studies on isolated synaptic vesicles from rodent brain or Torpedo electric organ revealed that their cholesterol to phospholipid ratios range from 0.4 to 0.6 (Breckenridge et al., 1973; Nagy et al., 1976; Wagner et al., 1978; Deutsch & Kelly, 1981) showing that synaptic vesicle membranes contain more cholesterol than other intracellular organelles including mitochondria or the endoplasmatic reticulum (Yeagle, 1985; Schmitz & Orso, 2001). The high cholesterol content in the synaptic vesicle membrane suggests a link between vesicle biogenesis (Hannah et al., 1999) and the cellular cholesterol level. This is supported by a study that aimed to identify cholesterol-binding proteins using a new photoaffinity-probe (Thiele et al., 2000). The authors compared patterns of cholesterol-binding proteins in two PC12 lines that differed in their neurosecretory competence and identified synaptophysin as cholesterol-binding component of synaptic vesicles. Importantly, they could establish that the cholesterol level controls the availability of secretory vesicles in PC12 cells: lowering the cellular cholesterol content by methyl- β -cyclodextrin diminished the steady-state pool of synaptic-like microvesicles and their rate of biogenesis, but did not affect endocytosis in general.

1.1.3.1.3 Microdomains/rafts

The above mentioned studies indicate that cholesterol is not equally distributed along membranes and that certain molecules bind to it. An interesting hypothesis extends these observations and claims that biological membranes contain a number of small microdomains, enriched in cholesterol and sphingolipid content, which are essential for various cell functions (Simons & Ikonen, 1997). These cholesterol-rich domains (rafts) have been implicated in numerous cellular processes including signal transduction, membrane trafficking, cell adhesion and molecular sorting (Paratcha & Ibanez, 2002; Simons & Toomre, 2000; Brown & London, 1998; Ikonen, 2001). The fundamental principle, by which lipid rafts may exert their functions, is to separate or concentrate specific membrane proteins and lipids in microdomains (Harder et al., 1998). Two studies provide direct evidence for a role of rafts and cholesterol in exocytosis (Lang et al., 2001; Chamberlain et al., 2001). Lang et al. (2001) observed in the neuron-like cell line PC12 that docking and fusion of secretory granules occur at syntaxin- and synaptosomal-associated protein of 25 kDa (SNAP25)-positive clusters that are sprinkled across the plasma membrane. Lowering

the plasmalemal cholesterol content by methyl- β -cyclodextrin dispersed syntaxin clusters and inhibited KCl-induced release of dopamine and of green fluorescent protein-labeled neuropeptide Y, as monitored by amperometry and fluorescence microscopy, respectively. The relevance of cholesterol for exocytosis has been confirmed by Chamberlain et al. (2001), who observed as well that reduction of the cellular cholesterol level reduces dopamine release from PC12 cells. Together, both studies show that SNARE-dependent exocytosis occurs at cholesterol-rich domains in the plasma membrane (Lang et al., 2001; Chamberlain et al., 2001). Several studies indicate that neurotransmitter receptors and other postsynaptic components are associated with rafts. Nicotinic acetylcholine receptors from cultured chick ciliary ganglion neurons were found in raft-like microdomains, which are cholera toxin-positive and detergent resistant. Moreover, receptor clusters were dispersed by methyl- β -cyclodextrin-dependent cholesterol depletion, but not by actin depolymerization (Bruses et al., 2001). Another study shows detection of AMPA-type glutamate receptors in detergent-insoluble rafts from rat brain synaptosomes (Suzuki et al., 2001). The intercellular adhesion, necessary for the stability of synapses, may also depend on cholesterol considering evidence that different types of cell adhesion molecules are localized in rafts. For example, glycosphosphatidylinositol-linked proteins (Buttiglione et al., 1998; Lang et al., 1998), NCAM (He & Meiri, 2002; Niethammer et al., 2002), integrins (Leitinger & Hogg, 2002), and cadherins (Crossin & Krushel, 2000; Angst et al., 2001; Tsui-Pierchala et al., 2002) have been shown to anchor in rafts. Another interesting aspect has been raised by the observation that the kinesin-mediated transport of vesicles along microtubule requires cholesterol and sphingomyelin-rich rafts in the vesicular membrane *in vitro* (Klopfenstein et al., 2002).

These results indicate possibilities how glia-derived cholesterol affect synapse formation and function and underline the importance of cholesterol for neurotransmission (Pfrieger, 2003).

1.2 My project

The aim of my project was to investigate how cholesterol supports synapse formation and function and whether other glia-derived factors are involved in synaptogenesis in cultured RGCs. Further, I was searching for neuronal target genes involved in glia-dependent postnatal differentiation of rat RGCs.

II. MATERIAL AND METHODS

2.1 Cultures of purified CNS neurones

RGCs were isolated by sequential immunopanning as described (Barres et al., 1988). Postnatal day 7 (P7) Wistar rats (animal facility, Faculte de Medicine, Universite Louis Pasteur, Strasbourg) were killed and retinae were dissected out, cleaned and digested [30 min in D-PBS with 33 U/ml Papain (Worthington Biochemical Corporation, Lakewood, NJ, USA) and 200 U/ml DNase (Sigma) at 37°C]. Digestion was stopped by incubation in 0.15% Ovomucoid [0.15% (w/w) trypsin inhibitor (Roche Molecular Biochemicals) in D-PBS with 0.15% (w/w) BSA (Sigma A8806)]. Tissue was successively triturated in 0.15% Ovomucoid with 330 U/ml DNase and 1:75 rabbit-anti rat macrophage serum (Axell, Westbury, NY, USA) using 1 ml pipette tips with 0.2 to 2 mm tip diameter. The cell suspension was centrifuged for 13 min at 128 g and the cell pellet was resuspended in 1% Ovomucoid solution. After another centrifugation step, the cells were resuspended in 0.02% BSA in D-PBS and filtered through a nylon mesh (Nitex, 20 µm, Tetco, Monterey-Park, CA, USA). RGCs were purified by sequential immunopanning, therefore three panning plates were prepared the day before. The first two plates [(Petri dish Ø 15 cm, Falcon, Becton-Dickinson) incubated for at least 12 h at 4°C with goat anti rabbit IgG (10 µg/ml, Biotrend, Cologne) in Tris/HCl (50 mM, pH 9.5)] were subtraction plates, while the third plate [(Petri dish Ø 10 cm, Falcon, Becton-Dickinson) incubated with goat anti mouse IgM (10 µg/ml, Biotrend, Cologne) in Tris/HCl (50 mM, pH 9.5)] was a selection plate. Plates were washed (PBS) and blocked with 0.2% BSA in D-PBS. Additionally, the selection plate was incubated with mouse anti rat Thy-1 (5 ml culture medium of T11D7e hybridoma cells, American Type Culture Collection, Manassas, VA, USA) for at least 2 h at room temperature. The filtered cell suspension was plated in succession on the two subtraction plates for 36 and 33 min, respectively before filtration and positive selection for Thy-1 on the last plate for 45 min. The plate was washed (D-PBS) until only adherent cells were visible. To take off the selected cells, they were incubated for 10 min in equilibrated Earle's balanced salt solution (EBSS, without Ca²⁺ and Mg²⁺, Sigma) with 2.5 mg/ml trypsin (Sigma) at 37°C and 5% CO₂. Trypsin digestion was stopped by incubation with 30% heat inactivated fetal calf serum (FCS, Gibco) and cells were removed mechanically by pipetting. Cells were counted using a haemocytometer (Assistant, Sondheim) and plated for dense cultures at 200 cells/mm² on poly-D-lysine

(PDL) [MW 30 – 70 kDalton, 10 µg/ml in water (Sigma)] on tissue culture dishes (35 mm Falcon, BD Biosciences). For microcultures cells were plated at 20 cells/mm² on tissue culture dishes (35 mm Falcon, BD Biosciences) containing microdots of PDL (70 - 150 kDalton; 100 µg/ml in water; Sigma) that were formed by a custom-built microatomizer. RGCs were cultured in serum-free NB⁺ medium (see Tab.1, Meyer-Franke et al., 1995). Three times a week, half of the culture medium was replaced by fresh NB⁺. Five days after plating, Cholesterol (5 µg/ml; Sigma) was added to neuronal cultures from a 1000x ethanolic stock solution as described (Mauch et al., 2001). For some experiments Laminin-1 (ultrapure, mouse; BD Biosciences), merosin (human, Gibco) or laminin fragments from the α1 (aa 2091-2108; CSRARKQAASIKVAVSADR; Sephel et al., 1989) and the γ1 chain (aa 1575-1564; RNIAEIIKDI; Liesi et al., 1989) (Bachem) were added to the culture medium at 0.25 µg/ml.

Table 1: NB⁺ medium for cultivation of RGCs (modified from Meyer-Franke et al.,1995)

Components	Concentration
Neurobasal medium (Invitrogen)	
B-27 supplement (Invitrogen)	2% (v/v)
human brain-derived neurotrophic factor (BDNF) (PeproTech/TEBU)	25 ng/ml
rat ciliary neurotrophic factor (CNTF) (PeproTech/TEBU)	10 ng/ml
forskolin (Sigma)	10 µM
glutamine (Invitrogen)	2 mM
insulin (Sigma)	5 µg/ml
N-acetylcysteine (Sigma)	60 µg/ml
penicillin (Invitrogen)	100 units/ml
progesterone (Sigma)	62 ng/ml
putrescine (Sigma)	16 µg/ml
sodium selenite (Sigma)	40 ng/ml
bovine serum albumin (BSA); crystalline grade #A4161, Sigma)	100 µg/ml
sodium pyruvate (Invitrogen)	1 mM
streptomycin (Invitrogen)	100 µg/ml
triiodothyronine (Sigma)	40 ng/ml
holo-transferrin (Sigma)	100 µg/ml

2.2 Preparation of GCM

GCM was obtained from cortical glial cells that were prepared similarly as described (Pfrieger & Barres, 1997; McCarthy and de Vellis, 1980). P7 rats were killed by decapitation and cortices were dissected out and cleaned. The preparation of cell suspension followed the same steps as described for RGCs (2.1). After resuspension in BSA, cells were centrifuged and the cell pellet was resuspended in DMEM/FCS culture medium (see Tab.2). Cells were cultured in PDL-coated [PDL, MW 30 – 70 kDalton, 10 µg/ml in water (Sigma)] tissue culture flasks (25 cm², TPP) in a medium that does not support survival of neurones (see Tab.2). After one week, culture flasks were washed with PBS and glial cells were then cultured in NB+ (see Tab.1) except that BDNF, CNTF and B27 were omitted. Three times a week, half of the GCM was harvested and replaced by fresh NB+. GCM was centrifuged for 5 min at 3000 g to remove cellular debris and added to 5 d old RGC cultures by replacing 5 out of 7 parts of culture medium with 3 parts of GCM and 2 parts of fresh NB+.

Table 2: Cortex culture medium DMEM/FCS

Components (all Invitrogen)	Concentration
DMEM without glutamine and phenol red, with 1000 mg/ml glucose	
FCS, heat inactivated, sterile filtered	10%
glutamine	2 mM
penicillin	100 units/ml
sodium pyruvate	1 mM
streptomycin	100 µg/ml

2.3 Electrophysiological recordings

For recordings, I selected neurons that grew singly or in small groups (< 12 cells) in microcultures. Whole-cell currents were recorded at room temperature (20 - 24°C) on an inverted microscope (Axiovert 135TV, Zeiss) with patch pipettes made of borosilicate glass [2 – 5 MΩ, (World Precision Instruments) prepared using a pipette puller (P97, Sutter Instruments)] using an Axopatch 200B amplifier (Axon Instruments), a data acquisition board (PCI-MIO-16E1, National Instruments) and custom-written Labview programs (National Instruments). The intracellular recording solution contained 100 mM

potassium gluconate, 10 mM KCl, 10 mM EGTA, 10 mM HEPES adjusted to pH 7.4 with KOH (all Sigma). The extracellular solution contained 120 mM NaCl, 3 mM CaCl₂, 2 mM MgCl₂, 5 mM KCl, 10 mM HEPES adjusted to pH 7.4 with NaOH (all Sigma). The membrane potential was clamped at -70 mV. Currents were low-pass filtered at 5 kHz and digitized at 20 kHz. For each cell, spontaneously occurring postsynaptic currents were recorded during 30 seconds. Then, evoked synaptic responses were elicited by extracellular field stimulation [constant current pulses, 30-70 mA/1 ms (Isolator-11, Axon Instruments) delivered via two platinum electrodes (distance ~4 mm)] at 1 Hz with three trains of 20 pulses each (Nagler et al., 2001). Whole-cell currents were recorded continuously during stimulation to monitor asynchronous transmitter release (Goda & Stevens, 1994) occurring at least 20 ms after the stimuli (Nagler et al., 2001). For simplicity, I will refer to synaptic currents that are synchronously evoked and occur within 20 ms after a stimulus as evoked currents and to those occurring in residual interstimulus interval of 980 ms as asynchronous currents. To determine the size of miniature excitatory postsynaptic currents (EPSCs) (quantal size), spontaneous (autaptic) EPSCs from singly growing RGCs were analyzed, as in these cells action-potential evoked transmitter release is suppressed by the voltage-clamp (Nagler et al., 2001).

Synaptic currents were analysed offline with custom-written Labview routines in a blinded fashion. Spontaneous and asynchronous synaptic currents were detected automatically based on size and timing criteria. The frequency of asynchronous events was corrected for the rate of spontaneous synaptic currents. The charge transfer amplitudes were calculated automatically. For charge transfer amplitudes the baseline-corrected membrane current was integrated over 8 ms starting at the onset of a synaptic event. For evoked currents, the onset was determined visually. Since evoked synaptic currents often overlapped with the large sodium current that was activated by extracellular stimulation, charge transfer of transmission failures was subtracted from evoked EPSCs.

2.4 Filipin staining

To determine the neuronal cholesterol content in neurites, cultured neurons were fixed (4 % paraformaldehyde for 30 min) and incubated for 2 hours with filipin (10 µg/ml, stock-solution: 1 mg/ml in 95% ethanol, Sigma), an antibiotic that selectively binds to sterols with a hydroxy group at the 3rd C-atom (Norman et al., 1972). Filipin fluorescence was then excited by monochromatic light (356 nm, provided by a xenon-lamp and a

monochromator, Polychrome Junior, TILL Photonics) and fed into the epi-illumination port of an upright microscope (Axioskop II FS, Zeiss). Fluorescence was viewed through an appropriate emission filter (Filter Set 2, Zeiss) and a 40x objective (water-immersion, N.A. 0.8, Zeiss). Images were acquired by an air-cooled monochrome CCD camera (1280 x 1024 pixels, 8-bit digitization width, PCO Computer Optics, Kelheim, Germany). The measured fluorescence intensity is correlated to the concentration of cholesterol in the cell (Muller et al., 1984). For analysis, filipin fluorescence intensity was determined manually in background area devoid of cells. To determine the intensity in neurites in an unbiased manner, four neuritic areas crossing the vertical and horizontal middle axis of each image were marked manually, the mean intensity over 3 x 3 pixels in each of these areas was calculated and then the average intensity of all areas was calculated. Extensive tests showed that it was impossible to compare intensities of filipin fluorescence between independent staining experiments probably due to the instability of the compound. To avoid possible artefacts and allow for comparison of data, the intensities of filipin fluorescence in neurites of RGCs after different periods of GCM- or cholesterol-treatment were normalized to the average of respective intensities from untreated control cultures that were run in parallel.

2.5 Immunocytochemistry

Microcultures were processed for immunocytochemistry as described (Meyer-Franke et al., 1995). Cells growing on tissue culture plates were washed (PBS), fixed (7 min in methanol at -30 °C), blocked [30 min at room temperature; 50% goat serum in antibody buffer containing 150 mM NaCl, 50 mM Tris, 1% BSA (Sigma A2153), 100 mM l-lysine, 0.04% sodium azide, pH 7.4], and incubated overnight with primary antibodies (diluted in antibody buffer). Presynaptic terminals and postsynaptic receptor clusters were stained with a mouse monoclonal anti-synapsin I antibody (Cl 46.1, 1:500, Synaptic Systems) and a rabbit polyclonal antibody against glutamate receptor 2/3 (GluR2/3) (1:200, Upstate Biotech; 0.2% Triton X added during primary incubation) and visualized with Alexa 488 (Molecular Probes) and Cy3-conjugated secondary antibodies (0.1% Triton X added; 1 hour room temperature; Jackson ImmunoResearch Labs), respectively. Dendrites and microtubule were visualized by mouse monoclonal antibodies against MAP2 (HM-2; 1:400; Sigma) and against α -tubulin (3A2, 1:1000, Synaptic Systems) respectively. Matrix Gla protein (MGP) was stained with a rabbit polyclonal antibody derived against the

C-terminal peptide ERYAMVYGYNAAYNRYFRQRRGAKY (a kind gift from Gerard Karsenty, Baylor College of Medicine, Houston). Heme oxygenase 1 (HO1) was detected using a monoclonal mouse antibody (HO-1-2, 1: 500, Stressgen). Immunofluorescence was viewed using an Hg lamp as light source (HBO100, Zeiss), appropriate filter sets (Cy3: XF33, Cy2: XF100; Omega Optical/Photomed) and a 40 x objective (Zeiss). Images were acquired by an air-cooled monochrome CCD camera (1280 x 1024 pixels, 8-bit digitization width, PCO Computer Optics, Kelheim, Germany). Control experiments showed absence of background staining by secondary antibodies (data not shown). The densities of synapsin-, GluR2/3 and doubled-stained puncta on neurites was determined by a semi-automatic Labview routine. First it was differentiated between fluorescent puncta on neurites and on somata for each microisland. To accomplish this, somata were outlined manually in phase-contrast images and fluorescent puncta were detected using a somata-outlining mask. To detect fluorescent puncta, images were first processed with a Laplacian filter to enhance puncta-like features. This involved discrete convolution of the image with the following matrix:

$$\begin{bmatrix} -1 & -1 & -1 & -1 & -1 \\ -1 & -1 & -1 & -1 & -1 \\ -1 & -1 & 25 & -1 & -1 \\ -1 & -1 & -1 & -1 & -1 \\ -1 & -1 & -1 & -1 & -1 \end{bmatrix}$$

The filtered image was then sectioned with a fixed threshold [median intensity of the filtered image plus antibody-specific offsets; synapsin: 150 analog-to-digital units (adu); GluR2/3: 130 adu]. Puncta were selected based on pixel area (synapsin: 4-250; GluR2/3: 2-250 pixels) and their mean fluorescence intensity (from unprocessed image; threshold intensity at 0.95 cumulative relative frequency of all intensities plus antibody-specific offsets; synapsin: 40 adu; GluR2/3: 30 adu). Double-stained puncta had to meet intensity criteria of both stains and show at least two pixels overlap. To determine the neuritic area in each image, phase contrast images were processed by a Prewitt filter, segmented (threshold intensity at 0.95 cumulative relative frequency of all intensities in the filtered image) and eroded to remove single-pixel particles. All white pixels in the soma-excluded area were then counted. Puncta densities are stated per 100 x 100 pixels. MAP2 immunostainings were analysed manually by counting the number of MAP2 positive neurites per soma whose length exceeded the soma diameter.

2.6 RNA preparation

For gene expression analysis, RGCs were purified by sequential immunopanning from P6 wistar rats and cultured at 177-218 cells/mm² on PDL coated tissue culture dishes in NB⁺ as described under 2.1. After 6 days in culture the cells were treated for 30 hours as given in table 3.

Table 3: Treatment of RGCs for gene expression analysis (added to 2 ml of NB⁺).

Condition	Treatment
Control to GCM treatment	2.5 ml DMEM ⁺ , 2 μ l BDNF (50 μ g/ml, final conc. 44 ng/ml)
GCM	2.5 ml GCM, 2 μ l BDNF (50 μ g/ml, final conc. 44 ng/ml)
Control to cholesterol treatment	2 μ l EtOH (100%)
Cholesterol	2 μ l Cholesterol in EtOH (5 mg/ml, final conc. 5 μ g/ml)

RNA was prepared using the RNeasy Mini Kit (Qiagen). Cells were scrapped off with a rubber policeman in 350 μ l RNeasy lysis buffer containing 1% β -mercaptoethanol, followed by addition of 350 μ l 70% ethanol. Samples were mixed gently, applied to an RNeasy mini-column and processed following the manufacturer's protocol. Purified total RNA was eluted in 60 μ l H₂O and stored at -80°C. Prior to use, RNA was quantified by absorbance at 260 and 280 nm. Quality was checked by capillary electrophoresis using the RNA 6000 Nano Assay in combination with the Agilent 2100 Bioanalyzer (Agilent Technologies, Germany). For this 1 μ l sample RNA together with 1 μ l ladder was loaded onto an RNA 6000 Nano chip and processed following the manufacturer's protocol.

2.7 Gene expression analysis

Gene expression analysis was performed using the Affymetrix GeneChip system. This system is based on oligonucleotide probes, which are synthesized on arrays. Biotin-labeled RNA fragments were hybridized to probe arrays and detected with a combination of streptavidin phycoerythrin conjugate and an antibody against streptavidin coupled to fluorescence. Hybridized gene chips were scanned at the excitation wavelength of 488 nm. The amount of light emitted at 570 nm is proportional to the bound target at each location

on the probe array. The sample amplification, labeling, hybridization and scanning were performed as described in the Affymetrix protocol. Briefly, mRNA was reverse transcribed using T7-oligo(dT) primer and complemented by second strand cDNA synthesis. After a cleanup of double-stranded cDNA, biotin-labeled antisense RNA was generated by T7 RNA polymerase and biotinylated ribonucleotides. Before chip hybridization, the biotin-labeled antisense RNA was purified, quantified and fragmented. Metal-induced hydrolysis was used for statistical fragmentation. Samples were hybridized on the Affymetrix GeneChip Rat Expression Set 230, which consists of two arrays A and B. The GCM or cholesterol treated samples were hybridized in parallel with controls, and processed during the same time. Equivalent amounts of biotinylated antisense RNA were hybridized for compared samples. Each experiment was repeated three times with independent cell preparations.

All primary expression data were analyzed using the Affymetrix 4.0 Microarray Suite (MAS) software. This software determines a detection call for each probe set. The detection algorithm uses probe pair intensities to generate a detection p-value and assigns a present, marginal, or absent call. Each probe pair in a probe set is considered as having a potential vote in determining whether the measured transcript is detected (present) or not detected (absent). The vote is described by a value called the discrimination score. The score is calculated for each probe pair and is compared to a user-definable threshold τ . Probe pairs with scores higher than τ vote for the “presence” of the transcript. Probe pairs with scores lower than τ vote for the “absence” of the transcript. Additionally, a signal value is calculated which assigns a relative measure of abundance to the transcript. The signal is calculated using the One-Step Tukey’s Biweight Estimate which yields a robust weighted mean that is relatively insensitive to outliers. Furthermore this software allows calculating a comparison analysis. In a comparison analysis, two samples, hybridized to two gene chip probe arrays of the same type, are compared against each other in order to detect and quantify changes in gene expression. Two sets of algorithms are used to generate change significance and change quantity metrics for every probe set. As for the single array analysis, the Wilcoxon’s Signed Rank test is used in comparison analysis to calculate a change p-value and an associated change related to user-defined cut-offs. A second algorithm produces a quantitative estimate of the change in gene expression in the form of signal log ratio. As for the signal, this number is calculated using a one-step Tukey’s Biweight method by taking a mean of the log ratios of probe pair intensities across the two arrays. A base 2 log scale is used. Finally, for each gene the values for signal,

detection, detection p-value, signal log ratio, change and change p-value were calculated. These data were copied into an MS Access database and matched with the annotation files. The following formulas were used to calculate the fold change from signal log ratio values:

Fold change = $2^{\text{Signal Log Ratio}}$ for Signal Log Ratio > 0 and

Fold change = $(-1) * 2^{-(\text{Signal Log Ratio})}$ for Signal Log Ratio < 0.

In addition, the coefficient of variance (CV) of each gene was calculated over three independent experiments, to select for relevant changes. Results were selected by relevance criteria given under results point 3.2.1. All positive selected genes were checked for their identity in a discontinuous BLAST search, using the sequence derived form (Zhang & Madden, 1997). Identified ESTs were included in the results and indicated. All selected genes were grouped by their function or localization as indicated by the literature.

2.8 SDS-polyacrylamid-gel electrophoresis (SDS-PAGE)

SDS-PAGE was done as described by Laemmli (1970), using the Miniprotean II system (Biorad). Gels were prepared with different concentrations of Acrylamid (Tab. 4), depending on the size of investigated proteins.

Table 4: Composition of SDS-polyacrylamid minigels

Components (all Sigma)	separation gel 5%	separation gel 10%	collection gel 4%
H ₂ O	2.85 ml	2.03 ml	1.5 ml
30% Acrylamid/Bisacrylamid (29:1)	0.83 ml	1.65 ml	0.33 ml
1.5 M Tris/HCl pH 8.8	1.25 ml	1.25 ml	-
0.5 M Tris/HCl pH 6.8	-	-	0.63 ml
10% SDS	50 µl	50 µl	25 µl
10% Ammoniumperoxodisulfat	25 µl	25 µl	12.5 µl
Temed	2.5 µl	2.5 µl	2.5 µl

RGCs growing in dense or microcultures were washed and harvested in sample buffer [0.125 M Tris/HCl pH6.8, 2.5% SDS, 0.025% bromphenol blue, 10% (v/v) glycerol] on ice using an rubber policeman. For reducing conditions, 1% (v/v) β-mercaptoethanol was added and samples were incubated at 99°C for 5 min. Determination of molecular weight

was performed by a molecular weight marker mix (Precision Plus Protein Standard, BioRad) in a separated slot onto the same gel together with samples. Electrophoresis was performed in running buffer (25 mM Tris, 192 mM glycine and 0.1% SDS) by 80 V during the first 15 min and continued by 100 V.

2.9 Immunoblotting

Separated proteins were transferred from SDS-Page gels to nitrocellulose membranes (Amersham Biosciences) using the Mini Trans-Blot Transfer Cell (BioRad). Transfer was performed in transfer buffer (25 mM Tris, 19.2 mM glycine, 20% methanol) at 100 V for one to two hours, depending on the size of transferred proteins. Subsequently, membranes were incubated in blocking buffer [5% low fat milk powder (Regilait) or 5% BSA (Sigma A2153, for MAP2) in TBS-T (20 mM Tris/HCl pH 7.6, 137 mM NaCl, 0.1% tween 20)] for one hour at room temperature. Membranes were reacted with specific antibodies including polyclonal anti phospho-MAP2 [Thr1620/1623, (1:10.000) or Ser136, (1:1000), Cell Signaling Technology], monoclonal anti MAP2 (1:1000, clone HM-2, Sigma), polyclonal anti GluR2/3 (1:1000, Upstate), monoclonal anti tubulin (1:10.000, clone 3A2, Synaptic Systems), monoclonal anti HO1 (1:5000, clone HO-1-2, Stressgen) and polyclonal anti Histon H3 (1:1000, Abcam) diluted in blocking buffer over night at 4°C. After primary antibody incubation the membranes were washed with TBS-T, two times short, one time 15 min and two times 5 min, followed by incubation with suitable secondary antibodies coupled to horse radish peroxidase (Dianova) for one hour at room temperature. Membranes were washed with TBS-T as described above and detected using ECL-reagent and Hyperfilm (Amersham Biosciences). To compare levels of phosphorylated versus total MAP2, blots reacted with phospho-specific antibodies were stripped by incubation in Restore WB Stripping buffer (Pierce) for 20 min, reblocked in blocking buffer for one hour and reacted with an anti MAP2 antibody as described above. Efficient removal of phospho-specific antibodies was confirmed by incubation with ECL reagent and film exposure after stripping. To detect laminin- γ 1, GCM was spun down (5 min at 15800g) to remove cell debris and then mixed with sample buffer with or without β -mercaptoethanol. Immunoblots of GCM were reacted with a chain-specific monoclonal antibody (1:1000, cat.# MAB1920, Chemicon). Concentration of laminin- γ 1 was determined by comparison to purified laminin-1 (BD Biosciences) on the same gel.

2.10 Radioactive labeling and lipid analysis

RGCs were cultured at 200 cells/mm² under control conditions for seven days before cells were washed with D-PBS and cultured for another two days in NB⁺ where B27 was omitted, in the presence of 0.8 µCi 1-¹⁴C-Acetate (13 nmol, Sigma). After 48 hours of incubation with the radioactive precursor, culture medium was removed and cells were washed with PBS and scraped off in water using a rubber policeman. For pulse-chase labeling, cells were washed with D-PBS before adding fresh NB⁺ medium (without B27) and additional treatment as given in Tab. 5. After further 68 hours culture medium was removed for lipid extraction, cells were washed with PBS and scraped off in water.

Table 5: Treatment of RGCs after pulse labeling (added to 2 ml of NB⁺ without B27).

Condition	Treatment
Control	1,7 ml DMEM ⁺ , 1 µl BDNF (50 µg/ml, final conc. 27 ng/ml)
GCM treatment	1,7 ml GCM, 1 µl BDNF (50 µg/ml, final conc. 27 ng/ml)
Cholesterol treatment	1,7 ml DMEM ⁺ , 1 µl BDNF (50 µg/ml, final conc. 27 ng/ml), 3.7 µl Cholesterol in EtOH (5 mg/ml, final conc. 5 µg/ml)

For sample adjustment, DNA content was determined from cell homogenate. Cells were homogenized by syringe with 27G cannula and sonication for 10 min and 3 x 5 µl were taken off from each sample for DNA content measurement. Cell homogenate (5 µl) was mixed with 194.5 µl TE buffer (10 mM Tris/HCl, pH 7.5, 1 mM EDTA) and 0.5 µl PicoGreen reagent (Molecular Probes) and incubated for at least 5 min at room temperature. DNA content was determined by measuring sample fluorescence at an excitation wavelength of 480 nm and an emission wavelength of 526 nm using a spectrometer (Photon Technology International), and calculated in correlation to a standard curve. For each sample, three probes were determined together with a blank value, which was subtracted from the mean sample value.

For lipid extraction, sample volumes of cell suspension and culture medium were adjusted to equivalent DNA content. Lipids from cell suspension were extracted by hexan/isopropanol as described by Hara & Radin (1978). Cell suspension was mixed with 20 fold sample volume of hexan/isopropanol (3:2) and incubated for 30 min at 4°C, interrupted by shaking all 10 min. Suspensions were centrifuged (5 min at 15800g) and supernatants were collected in glass-tubes. Lipids from culture medium were extracted by chloroform/methanol as described by Oram (1986). First, medium was centrifuged (3 min

at 15800 g) to remove cell debris and mixed with 5-fold volume of chloroform/methanol (2:1) by strong shaking. After centrifugation for 2 min at 1500 g, the upper aqueous phase was removed and the lower organic phase was mixed 1:1 with water. The suspension was again centrifuged (5 min at 1500 g) and the organic phase was convicted to a new glass-tube using a Pasteur pipette. Solvents from cell and medium extraction were vaporized by a nitrogen stream and extracted lipids were solved in small volumes of chloroform for transfer to thin layer chromatography (TLC)-plates.

Lipids were separated by TLC using pebble-gel-plates (60 Å, F254, Merck) and a combination of two different solvent systems. Prior to use, plates were heated for 30 min at 120°C. After cooling to room temperature samples were absorbed to the plates using glass micropipettes (Hirschhorn Laborgeräte). For the later identification of separated lipids, radioactive labeled and unlabeled lipids were absorbed on the same plate in line with samples. The following lipid standards were used: ^3H -cholesterol; cholesteryl [1- ^{14}C] oleat; L-3-phosphatidylcholine, 1,2-di [1- ^{14}C] palmitoyl (Amersham Biosciences); cholesterol; cholesterololeate; phosphatidylcholine; 1,2-diacyl-sn-glycero-3-phosphatidylethanolamine; sphingomyelin and 24-OH-cholesterol (Sigma). Separation was performed by two runs, the first in chloroform/methanol/water (60:30:5) until the plate middle, followed by drying and the second run in hexan/diethylether/acetic acid (80:10:1.5) until the upper end of the plate. Labeled lipids were detected by autoradiography, using X-ray films (BioMax MS, Kodak) in combination with an intensifying screen (BioMax TranScreen, Kodak). Total amounts of lipids were visualized by detection with iodine (Mangold, 1960). Therefore, TLC-plates were reacted for several hours with iodine steam, and staining was documented using a digital camera (Powershot G3, Canon).

III. RESULTS

3.1 Multiple mechanisms mediate glia-induced synaptogenesis in RGCs

Starting from the publication of Nägler et al. (2001), which showed that soluble glial-derived factors enhance the formation and efficacy of synapses in cultured RGCs, and of Mauch et al. (2001), which identified cholesterol as one of this glia derived factors, I studied how cholesterol and other secreted factors from glial cells influence synapse development in microcultures of highly purified rat RGCs. To separate effects mediated by GCM and by cholesterol, which is contained in GCM in form of lipoproteins (LaDu et al., 1998; DeMattos et al., 2001), I treated microcultures of RGCs in parallel with GCM or with cholesterol at the same concentration (5 µg/ml) as in GCM (Mauch et al., 2001).

3.1.1 Time course of GCM- and cholesterol-induced changes in the number of synapses

As a first step, measurements in the lab (D Mauch & FW Pfrieger) showed how fast GCM and cholesterol enhance the level of synaptic activity in RGCs, by measuring spontaneous, asynchronous and evoked EPSCs. As shown in Fig. 4, cholesterol and GCM raised the frequencies of spontaneous and asynchronous release and the size of miniature and evoked EPSCs to the same extent and with a similarly slow time course, leading to significant changes after three or more days of treatment.

This raised the question whether cholesterol- and GCM enhanced the number of synapses with the same time course. To resolve this question, I added GCM or cholesterol to five day old microcultures of RGCs and examined after different periods of treatment the number of synapses in neurons growing singly or in small groups on microislands of PDL. Control cells were cultured for the entire period in defined culture medium. Synapses were defined as double labeled puncta, positive for the presynaptic marker synapsin I and the postsynaptic marker GluR2/3. A semi-automated routine analysed the density of immunostained puncta in neurites of RGCs. As shown in Fig. 5, GCM and cholesterol enhanced the number of synapsin-, GluR2/3-positive and of double-stained puncta per neurite area with remarkably similar time courses. As for the effects on synaptic activity shown in Fig. 4, statistically significant changes were reached only after three or more days of treatment.

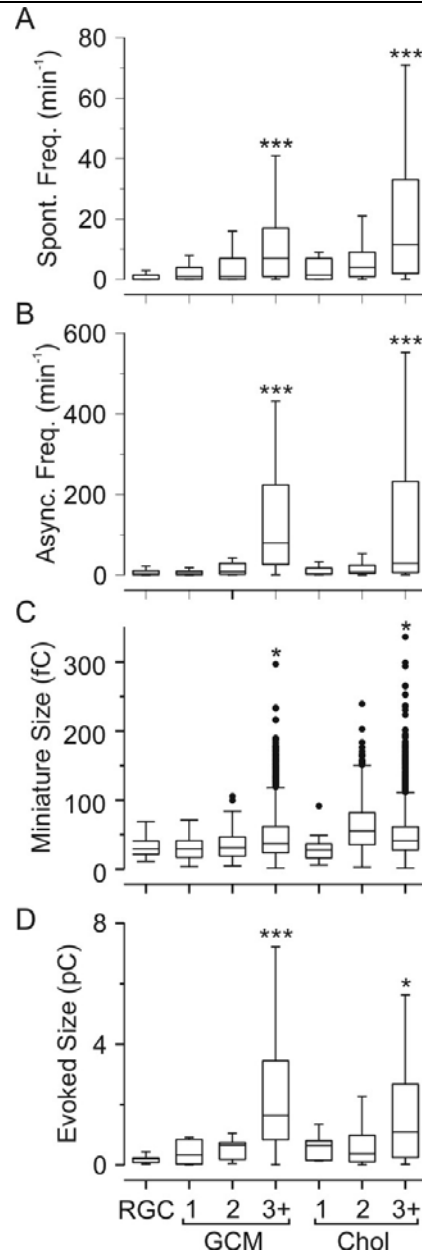


Figure 4: GCM- and cholesterol-induced enhancement of synaptic activity requires at least three days of treatment. Boxplots showing the frequencies of spontaneous (A) and asynchronous EPSCs (B) in RGCs cultured for five days in defined medium and then for 1, 2 or 3 to 7 (3+) days in defined medium (RGC; 60 neurons with activity out of 97 tested), in the presence of GCM (1: 18 of 28; 2: 19 of 34; 3+: 101 of 124) or in the presence of cholesterol (Chol; 1: 14 of 30; 2: 25 of 35; 3+: 112 of 136). In boxplots, horizontal lines represent the median; lower and upper box limits, 1st and 3rd quartile; whiskers, 1.5-fold interquartile range. (C) Charge transfer amplitudes of miniature EPSCs (quantal size) in RGCs cultured as described above in defined medium (RGC; 7 neurons/28 events), in GCM (1: 5/23; 2: 7/105; 3+: 28/901) or in cholesterol (Chol; 1: 5/33; 2: 7/909; 3+: 29/2127). Filled circles indicate values outside the 1.5-fold interquartile range. (D) Charge transfer of evoked EPSCs in RGCs cultured as described above in defined medium (RGC; n = 14 neurons), in GCM (1: 10; 2: 9; 3+: 71) or in cholesterol (Chol; 1: 7; 2: 14; 3+: 67). Asterisks indicate statistically significant changes compared to control cultures (* $p < 0.05$, ** $p < 0.01$, *** $p < 0.001$; A, B: Kruskal-Wallis test; C, D: ANOVA, Dunnett's post-hoc test). Data were recorded by D. Mauch.

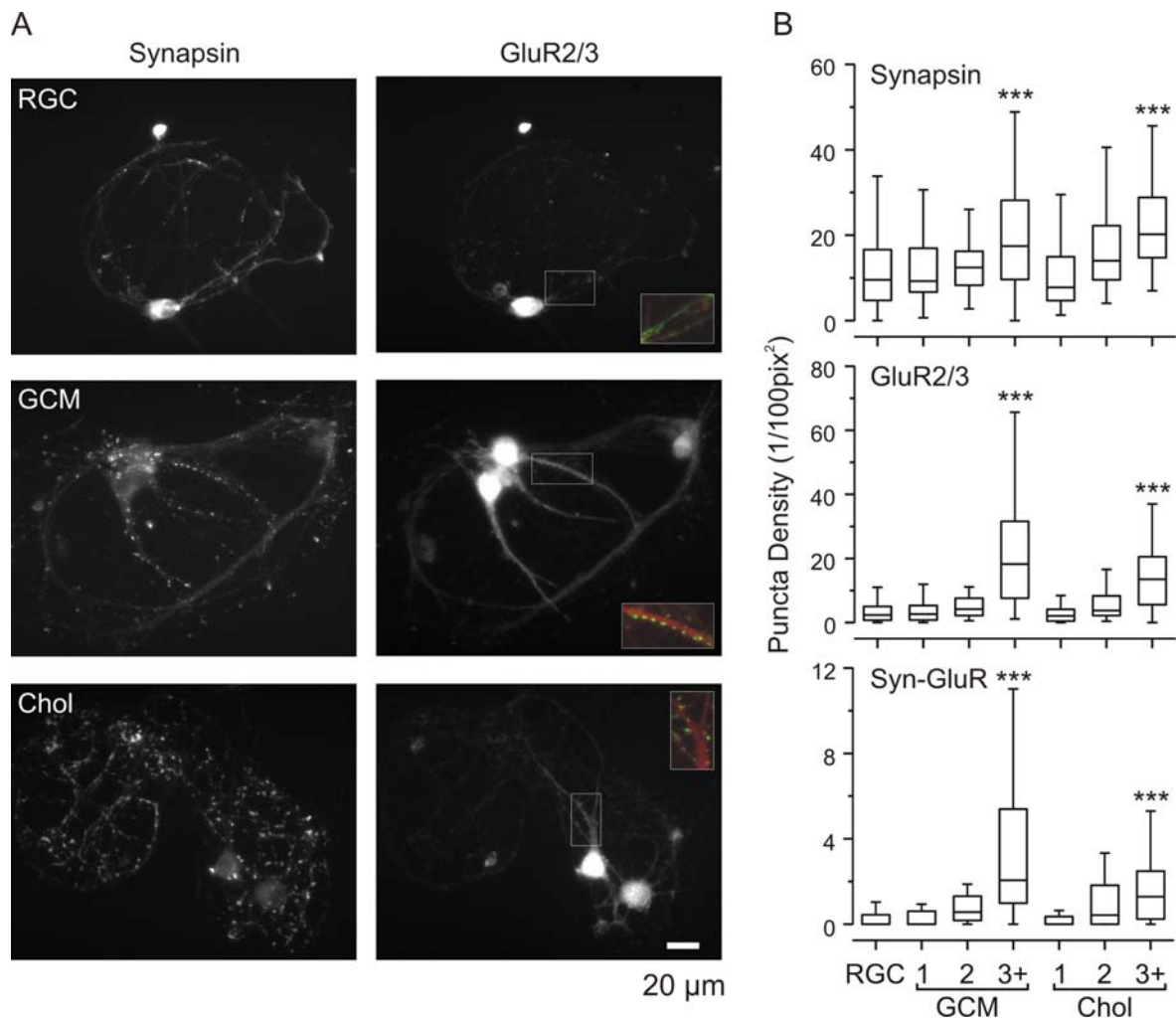


Figure 5: GCM- and cholesterol-induced increase in synapse density requires at least three days of treatment. (A) Fluorescence micrographs of RGCs cultured for five days in defined medium and then for six days in defined medium (top), with GCM (middle) or with cholesterol (bottom) and then stained with antibodies against synapsin I (left column) and GluR2/3 (right column). Inserts show overlays of synapsin I (green) and GluR2/3 (red) fluorescence in indicated areas at 1.5-fold magnification. (B) Densities of synapsin- (top), GluR2/3- (middle) and synapsin-GluR2/3-positive (bottom) puncta on neuritic processes of RGCs cultured for five days in defined medium and then for 1, 2 or at least 3 days in defined medium (RGC; $n = 99$ neurons), in GCM (1: 31; 2: 21; 3+: 54) or in cholesterol (Chol; 1: 32; 2: 21; 3+: 55). Three or more days of treatment with GCM or cholesterol induced statistically significant changes compared to untreated controls (ANOVA, Dunnett's post-hoc test).

I noted two differences between cholesterol- and GCM-treated cells: First, cholesterol induced a significant, but smaller increase in synapse number than GCM. Second, in cholesterol-treated cultures, synapsin-positive puncta were distributed all over neurites, whereas after treatment with GCM these puncta clustered at distinct spots along neurites.

Taken together, GCM and cholesterol enhanced the number of synapses and their spontaneous and evoked activity not immediately, but slowly within several days of treatment. Cholesterol induced a smaller increase in synapse number than GCM, but mimicked all of the GCM effects on synaptic activity.

3.1.2 Time course of GCM- and cholesterol-induced increase in neuritic cholesterol content

The long-delay, with which both GCM and cholesterol promoted synaptogenesis, contrasted with the notion that synapses form within an hour (Ahmari et al., 2000; Friedman et al., 2000; Gomperts et al., 2000) and suggested that both activated an unknown rate-limiting process. As a first candidate, I tested whether the neuronal uptake of cholesterol causes the delay. Using staining with filipin, a fluorescent sterol-binding antibiotic, Mauch et al., (2001) had shown previously that GCM and cholesterol strongly enhance the level of cholesterol in RGCs. Now, I determined the time course of this effect. As shown in Fig. 6, GCM enhanced the cholesterol content of neurites gradually reaching a 10-fold enhancement within 72 hours. Directly added cholesterol had the same effect, but with a strikingly different time course: It caused a 20-fold increase within 48 hours, which then declined to a remarkably similar level as with GCM after 72 hours. The different time courses are probably caused by the different ways of how cholesterol enters neurons: cholesterol contained in GCM is taken up by (regulated) endocytosis of apolipoprotein E-containing lipoproteins, whereas cholesterol that is directly added to the medium is transferred in an unregulated manner to cells by albumin, a component of the culture medium (Brown and Goldstein, 1986). The subsequent decrease in cellular cholesterol content between 48 and 72 hours, by directly added cholesterol, may be due to active cholesterol release from RGCs to protect them from cholesterol overload.

The different rates of cholesterol- and GCM-induced increase in cholesterol content contrasted with the rather similar delay by which both enhanced synapse numbers. This indicated that the increase in cholesterol content does not determine the rate of synaptogenesis.

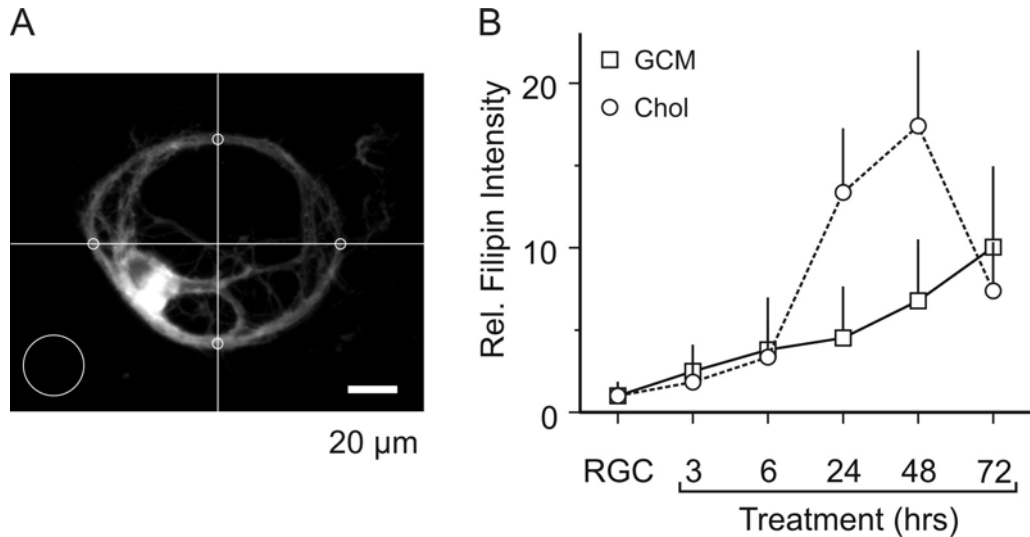


Figure 6: Time course of GCM- and cholesterol-induced increase in neuritic cholesterol content. (A) Fluorescence micrograph of a RGC cultured for five days in defined medium and then for 48 hrs with GCM. Subsequently, the culture was fixed and stained with filipin. Circles indicate regions, where filipin intensity was determined in neurites (small, intersections with center lines) and in background (large). (B) Relative mean intensities of filipin fluorescence in neurites of RGCs cultured for five days in defined medium and then for the indicated times with GCM (black rectangles, solid line; RGC: n = 173 cells; 3: 36; 6: 40; 24: 37; 48: 39; 72: 28) or with cholesterol (red circles, dashed line; RGC: 110; 3: 33; 6: 34; 24: 23; 48: 23; 72: 44). Fluorescence intensities for each time point were normalized to intensities of untreated control cells (RGC). Whiskers indicate standard deviation.

3.1.3 Dendrite differentiation as rate-limiting step for GCM- and cholesterol-induced synaptogenesis

Searching for the rate limiting step in GCM- and cholesterol-induced synaptogenesis, I closer inspected the GluR2/3 immunostaining. This revealed that GCM and cholesterol treatment strongly increased the density of GluR2/3 in neurites, whose tapering form reminded of dendrites (Fig. 5). This observation prompted me to test, whether RGCs formed dendrites in microcultures and whether their development causes the delay in synapse formation. Immunostaining with a MAP2-specific antibody revealed that after 10 to 14 days under control conditions less than 20% of the RGCs tested showed MAP2-positive dendrites (Fig. 7). On the other hand, the majority of RGCs showed MAP2-positive somata and multiple, long and extensively branching neurites extending from their soma (Fig. 7 and Fig. 8). This implied that under control conditions, RGCs grow multiple neurites, but that none of them differentiates into MAP2-positive dendrites. This may

explain the low density of GluR2/3 in neurites (Fig. 5), since glutamate receptors are selectively targeted to mature dendrites (Craig et al., 1993). As next step I treated microcultures with cholesterol or GCM for different periods and counted the number of MAP2-positive dendrites per soma. Both, GCM and cholesterol increased the fraction of RGCs with one or more MAP2-positive dendrites reaching statistically significant changes compared to control cultures after three or more days of treatment (Fig. 7). This time course was remarkably similar to the slow increase in synapse number indicating that dendrite differentiation limits the rate and extent of synaptogenesis in RGCs.

GCM and cholesterol may have increased the content of MAP2 in neurites by enhancing its expression. However, immunoblots of cell extracts showed that RGCs synthesize MAP2 and GluR2/3 under glia free condition and that GCM or cholesterol did not enhance their protein levels (Fig. 9). I also studied whether GCM or cholesterol change the phosphorylation status of MAP2 at sites that have been implicated in neurite outgrowth (Berling et al., 1994; Sanchez et al., 2000), using specific antibodies against MAP2 phosphorylation at serine 136 in the N-terminal region and threonine 1620/1623 in the proline-rich region. As shown in Fig. 9, the phosphorylation status of MAP2 at these sites didn't change within 48 hours of GCM or cholesterol treatment.

Even in the presence of GCM or cholesterol, about 20% of neurons lacked dendrites. Previous observations showed that RGCs impede dendrite development in neighboring cells (Perry & Linden, 1982; Eysel et al., 1985). To determine whether a similar effect occurred in microcultures of RGCs, I counted MAP2 positive dendrites, differentiating between singly growing cells and those with contact to neighbors. Indeed, I found that the percentage of RGCs lacking MAP2-positive dendrites was fourfold higher in neurons growing with one or more neighbors (43%) than in those growing singly on a microisland (12%) indicating an inhibitory effect of neighboring RGCs (Fig. 10).

Together, these results indicate that the low incidence of synapses in RGCs under glia-free conditions is due to a lack of dendrite differentiation. GCM and cholesterol promoted this process, which acted as rate-limiting step for the increase in synapse number and which involved a redistribution of MAP2 and GluR2/3 from the soma to dendrites.

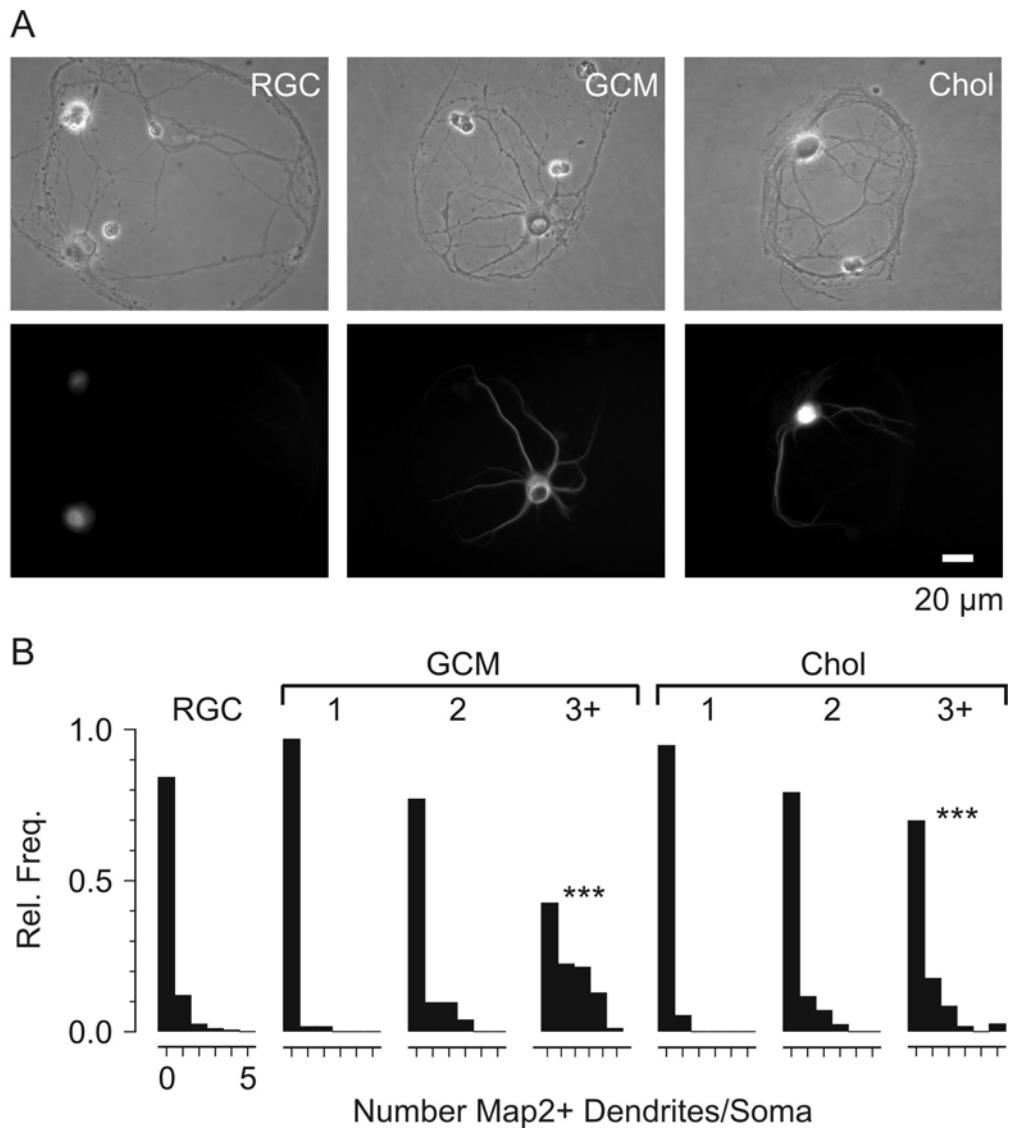


Figure 7: Dendrite formation limits the rate of GCM- and cholesterol-induced synaptogenesis. (A) Phase-contrast (top) and fluorescence (bottom) micrographs of RGCs growing for five days in defined medium and then for three days in defined medium (left), in GCM (middle) and in cholesterol (right). Cultures were stained with antibodies against the dendritic marker MAP2. (B) Relative frequency histograms of the number of MAP2-positive dendrites per soma in RGCs cultured for five days in defined medium and then for 1, 2 or at least 3 days in defined medium (RGC; $n = 138$ neurons), in GCM (1: 20; 2: 27; 3+: 77) or in cholesterol (Chol; 1: 26; 2: 25; 3+: 91). Only three or more days of treatment with GCM or cholesterol induced statistically significant changes compared to untreated cultures (Pearson's χ^2 test).

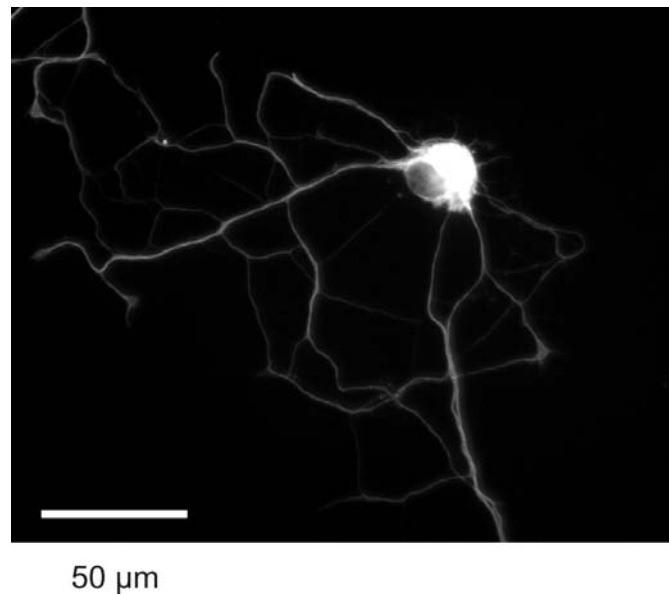


Figure 8: RGCs extend several long, branching processes in the absence of glia-derived factors. Fluorescence micrograph of a representative RGC cultured for seven days in defined medium and then stained with a tubulin-specific antibody. Space bar, 50 μm .

3.1.4 Evidence for laminin as dendrite-promoting factor

Cholesterol induced a statistically significant increase in the number of MAP2-positive dendrites, but it was less efficient than GCM. This may explain the lower number of synapses in cholesterol- compared to GCM-treated RGCs. Both observations indicated that other glial signals may promote dendrite differentiation. Based on previous studies, I tested whether the matrix component laminin induces dendrites. A first hint to laminin came from the study of Meyer-Franke et al. (1995), observing MAP2-positive dendrites in cultures of immunoisolated rat RGCs, but their neurons were plated on laminin-2 (merosin), whereas the microcultures which I used contained PDL. Second, it is well established that laminins are secreted by astrocytes (Liesi et al., 1983; Selak et al., 1985) and promote neurite outgrowth in RGCs and other neurons (Baron-Van Evercooren et al., 1982; Manthorpe et al., 1983; Rogers et al., 1983; Luckenbill-Edds, 1997; Powell & Kleinman, 1997). Treatment of five day old microcultures for three days with a low concentration of laminin-1 (0.25 $\mu\text{g/ml}$) did not change the number of MAP2-positive dendrites per neuron compared to untreated control. However, addition of laminin-1 together with cholesterol increased dendrite differentiation to a very similar degree as GCM (Fig. 11). Laminin-2, which was originally used by Meyer-Franke et al. (1995), fully mimicked this effect (data combined with them for laminin-1, Fig. 11).

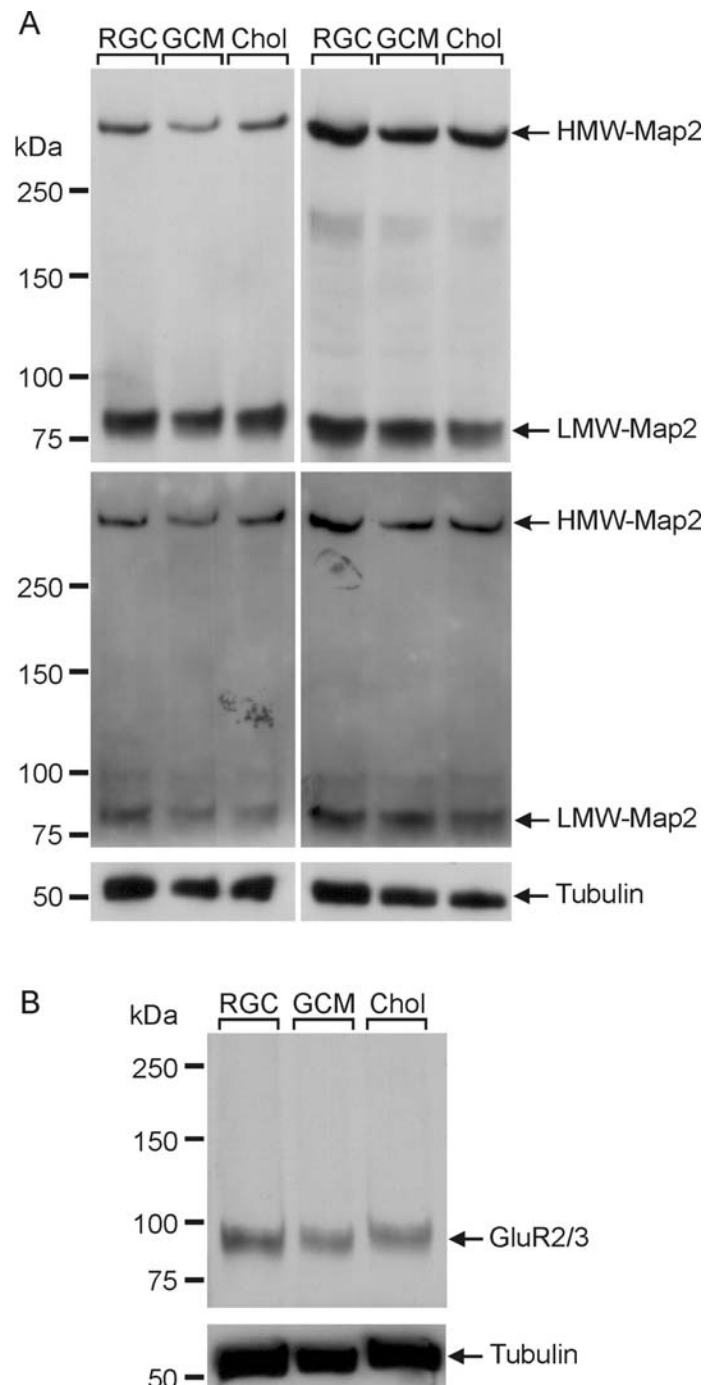


Figure 9: GCM or cholesterol do not change MAP2 and GluR2/3 levels. (A) Immunoblots of RGCs growing for 4 days in defined medium and then for 2 days in the presence of defined medium (RGC), GCM or cholesterol using antibodies against specific phosphorylation sites (top left, thr1620/23; top right, ser136), total MAP2 (middle panel, stripped blots from top panel) and against tubulin (bottom). Arrows indicate high molecular weight (HMW) and low molecular weight (LMW) MAP2. (B) Immunoblot of RGCs cultured for 4 days in defined medium and then for 6 days in the presence of defined medium (RGC), GCM or cholesterol using an antibody against GluR2/3 (top) and tubulin (bottom).

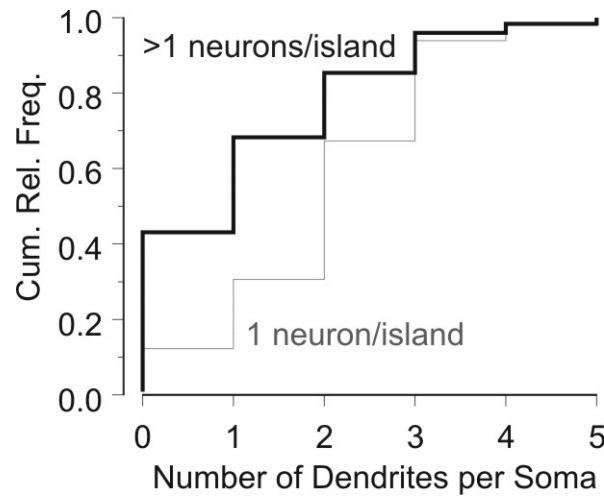


Figure 10: Neighboring RGCs suppress dendrite differentiation in RGCs. Cumulative relative frequency plot of the number of MAP2-positive dendrites per soma for RGCs growing singly on microislands (thin line; $n = 49$ neurons) or together with at least one more neuron (thick black line; $n = 123$ neurons). The two distributions differ significantly ($p < 0.001$; Pearson's χ^2 test). Cells grew for four days under defined conditions and then for 4 to 6 days in the presence of GCM.

Laminins are trimers consisting of α , β and γ chains (Burgeson et al., 1994) and so I tested next which laminin chain mediates the effect. I treated microcultures with synthetic peptide fragments from different laminin chains which are known to enhance neurite growth (Liesi et al., 1989; Sephel et al., 1989). The dendrite-promoting activity of laminin-1 was selectively mimicked by a fragment from the $\gamma 1$ chain, but not by a fragment from the long arm of the $\alpha 1$ chain (Fig. 11). These observations are in line with the results, that both laminin-1 and -2, which have different α chains, promote dendrite differentiation. Immunoblots confirmed that laminin- $\gamma 1$ is present in GCM (Fig. 12) at relatively high concentrations (5 to 10 $\mu\text{g/ml}$). My attempts to deplete laminin from GCM by immunoprecipitation using a polyclonal antibody against laminin 1+2, or to block its effects by addition of this antibody to GCM before treatment of RGCs failed, probably due to the high concentration and its effectiveness at low doses.

Together, these results showed that RGCs require cholesterol to form mature dendrites and that laminins promote dendritogenesis via the $\gamma 1$ chain.

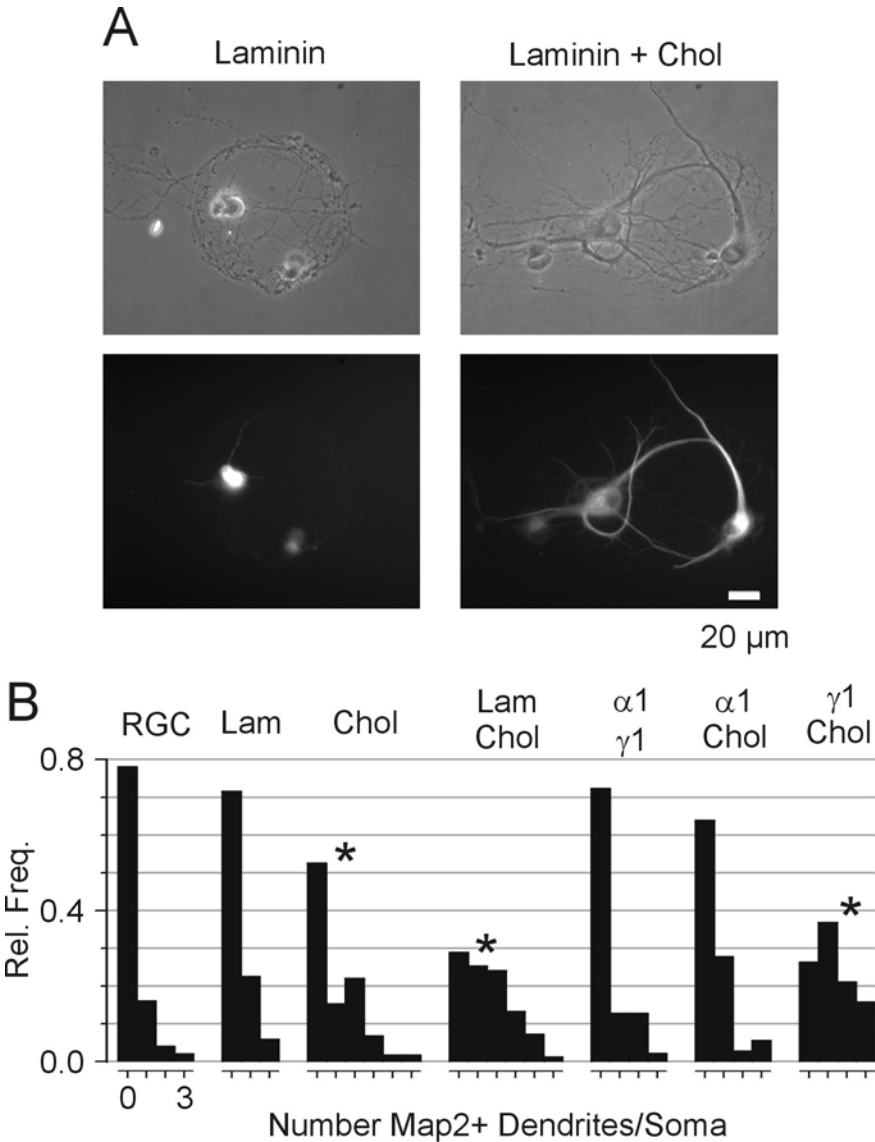


Figure 11: Dendritogenesis requires cholesterol and is promoted by laminin. (A) Phase-contrast (top) and fluorescence (bottom) micrographs of RGCs growing for five days in defined medium and then for three days in defined medium plus laminin (left) or plus laminin (250 ng/ml) and cholesterol (5 μ g/ml) (right). Cultures were stained with a MAP2-specific antibody. Space bar, 20 μ m. (B) Relative frequency histograms of the number of MAP2-positive dendrites per soma of RGCs cultured for four days in defined medium and then for at least 3 days in defined medium (RGC, untreated control; n = 50 cells), with laminin (250 ng/ml; n = 102), with cholesterol (5 μ g/ml; n = 59; p < 0.05), with laminin and cholesterol (n = 83; p < 10⁻⁵), with two fragments from the α 1 and γ 1 chain (250 ng/ml each; n = 47), with the α 1 fragment and cholesterol (n = 36) and with the γ 1 fragment and cholesterol (n = 38; p < 10⁻⁴). Values for each treatment are from two to four independent preparations. Asterisks indicate statistically significant changes compared to untreated control (Pearson's χ^2 test).

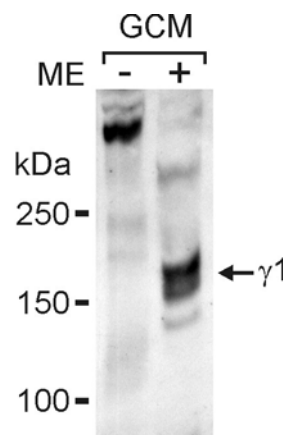


Figure 12: GCM contains a large amount of laminin- γ 1. Immunoblot of GCM using an antibody against the laminin- γ 1 chain. ME (mercaptoethanol) indicates presence/absence of reducing conditions.

3.1.5 Effects of GCM removal on synaptic activity

So far, the results showed that glial cholesterol and laminin promote dendrite differentiation and the formation of synapses, but it remained unclear, whether these effects persisted after their removal or whether glial factors were required to maintain synaptic activity. Therefore I tested, whether the GCM-induced increase in synaptic activity persisted after removal of GCM.

To address this, RGCs were cultured for four days under control conditions and then treated for five days with GCM to stimulate synapse formation and synaptic activity. At this point, the GCM-induced baseline synaptic activity was recorded (Fig. 13A). Then, GCM was removed, cells were washed once with PBS to remove soluble glial factors and cultured in defined medium or in the presence of GCM or of cholesterol (Fig. 13A). After further six days of culture (total 15 days *in vitro*), synaptic activity was recorded to detect its sensitivity to the removal of GCM and its replacement by cholesterol. I observed that in those RGCs, where GCM was removed, the frequency of spontaneous and asynchronous release and the quantal size remained at the baseline level (Fig. 13). In those cultures, where GCM treatment was continued, the frequencies of spontaneous and asynchronous release increased further (Fig. 13) and this increase persisted also, if GCM was replaced by cholesterol (Fig. 13). This indicated that RGCs continue to form synapses *in vitro*, if provided with cholesterol. Remarkably, removal of GCM caused a significant decrease in the size of evoked EPSCs below the baseline level and a significant increase in the fraction

of neurons, where stimulation failed to evoke EPSCs (Fig. 13). Again, these changes did not occur, when GCM was replaced by cholesterol (Fig. 13).

Taken together, these results showed that the continuous presence of cholesterol is required to maintain evoked synaptic transmission and to support ongoing synaptogenesis.

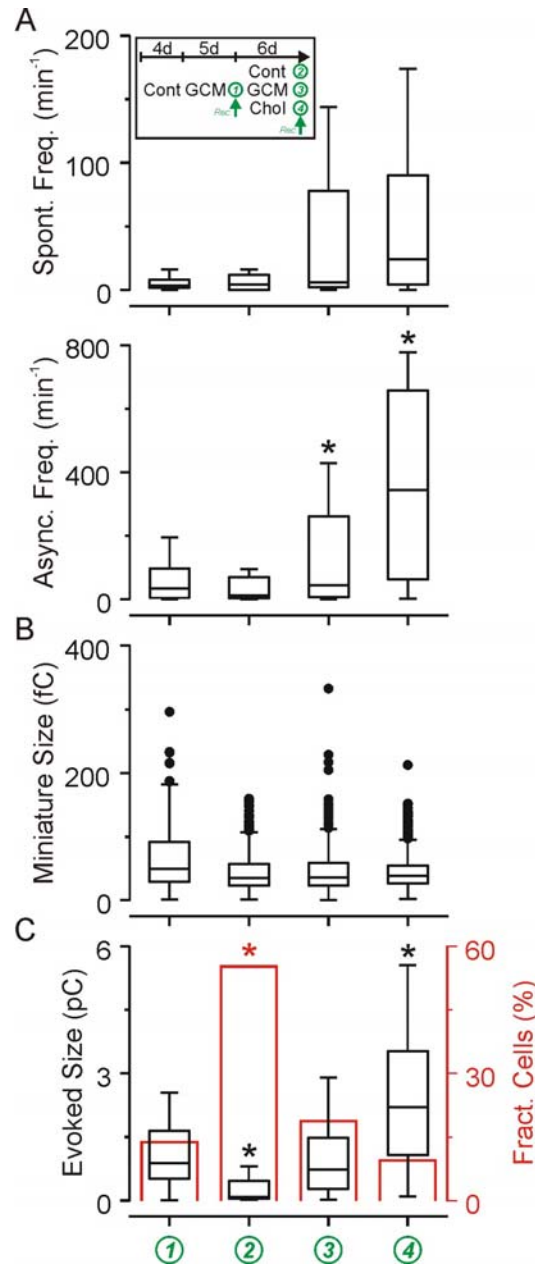


Figure 13: Effects of GCM removal on synaptic activity. (A) insert: Timing of culture treatment and electrophysiological recordings. Immunoisolated RGCs were cultured for 4 days in defined medium and for 5 days with GCM. Then, synaptic activity was recorded to define GCM-induced baseline activity (1). GCM was washed off with PBS and replaced by defined culture medium, GCM or medium plus cholesterol. After six more days, synaptic activity was recorded to define the effects of GCM removal (2), of the continued presence of GCM (3) or of its replacement by cholesterol (4) on synaptic activity. Boxplots in (A) show frequencies of spontaneous (upper panel) and asynchronous (lower) EPSCs. (B) Charge transfer amplitudes of miniature EPSCs. (C) Charge transfer amplitudes of evoked EPSCs (left axis, black boxplots) and fraction of neurons showing spontaneous or asynchronous events but no evoked EPSCs (right axis, red columns). After removal of GCM, the size of evoked EPSCs and the fraction of neurons lacking EPSCs decreased and increased compared to the baseline, respectively. Continued treatment with GCM or cholesterol prevented this decrease. Asterisks indicate statistically significant changes compared to baseline (A, C left axis: Kruskal-Wallis test; C right axis: Pearson's χ^2 test).

3.2 Influence of soluble glial factors and cholesterol on gene expression of cultured postnatal RGCs

So far, I had shown that glia-derived laminin and cholesterol are necessary for dendrite differentiation in purified RGCs, and that this step probably acts rate limiting for synapse formation. Apart from this effect, soluble glial factors may affect further aspects of RGC differentiation. In order to search for new neuronal targets which are influenced by soluble glial signals, I studied the influence of glial factors on RGC gene expression. To separate the influence of cholesterol from that of other soluble glia factors, I compared gene expression in purified RGCs after 30 hours of treatment with GCM or cholesterol with untreated control cells. To study a broad range of genes, I performed gene chip expression analysis using the Affymetrix system, which allows to investigate expression changes of several thousand genes at once. All experiments concerning the gene chip hybridization, data read out and processing were done in the University Hospital of Regensburg in cooperation with the group of Prof. Gerd Schmitz.

3.2.1 Microarray analyses and data assessment

Gene chip arrays are highly sensitive tools. For stringency, control analyses were performed at all steps of sample preparation. First, prepared sample RNA was analyzed for degradation using capillary electrophoresis. Fig. 14A shows the separation profile of total RNA purified from control RGCs as an example. The diagram shows three peaks, a standard peak at 17 seconds, the 18 S rRNA at 35 and the 28 S rRNA at 41 seconds. Both rRNA peaks are clearly distinguishable and no degradation fragments are present. Fig. 14B shows the electrophoresis profile of purified cDNA after reverse transcription of mRNA using T7-oligo(dT) primer. For microarray hybridization, labeled RNA fragments were generated by reverse transcription of cDNA using T7 polymerase and biotin-labeled ribonucleotides followed by metal induced statistical fragmentation. Fig. 14C shows the size distribution of fragmented antisense RNA. Labeled antisense RNA fragments were hybridized on oligonucleotide microarrays (Affymetrix rat expression set 230), representing 31.000 probe sets including 28.000 identified rat genes and ESTs.

The variability of expression data between independent experiments is a critical point and determines their reliability. I performed cross correlation analysis of the hybridization signals of the three independent experiments after GCM treatment as well as under the

corresponding control conditions (Fig. 15). Correlation coefficients ranged between 0.96 and 0.985, showing a high data stability across experiments.

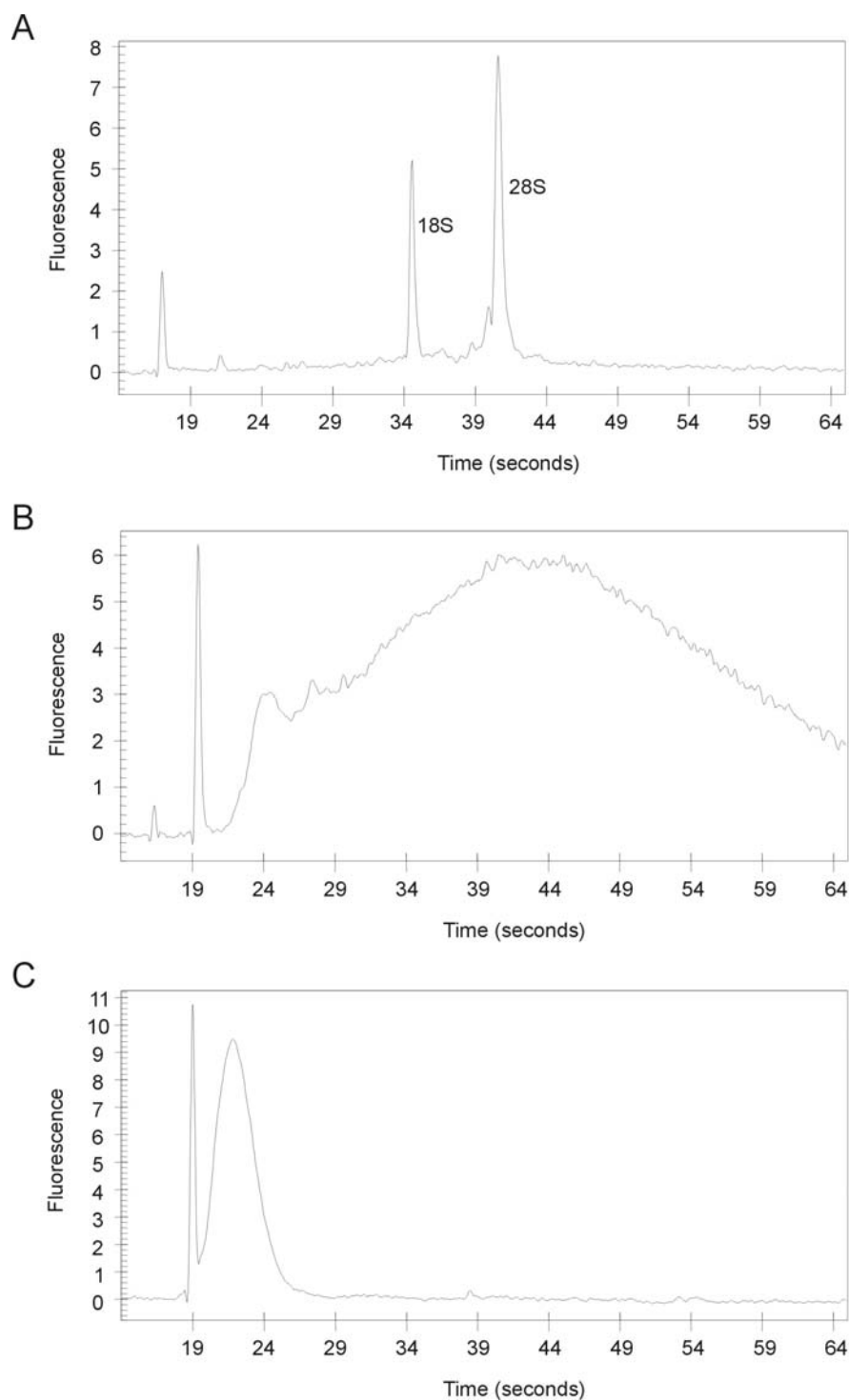


Figure 14: Quality control at different steps of sample preparation: (A) Electrophoretic separation profile of control sample RNA, standard peak at 17 seconds, 18 S rRNA at 35 seconds and 28 S rRNA at 41 seconds. (B) Electrophoresis profile of purified cDNA after reverse transcription. (C) Size distribution of fragmented antisense RNA.

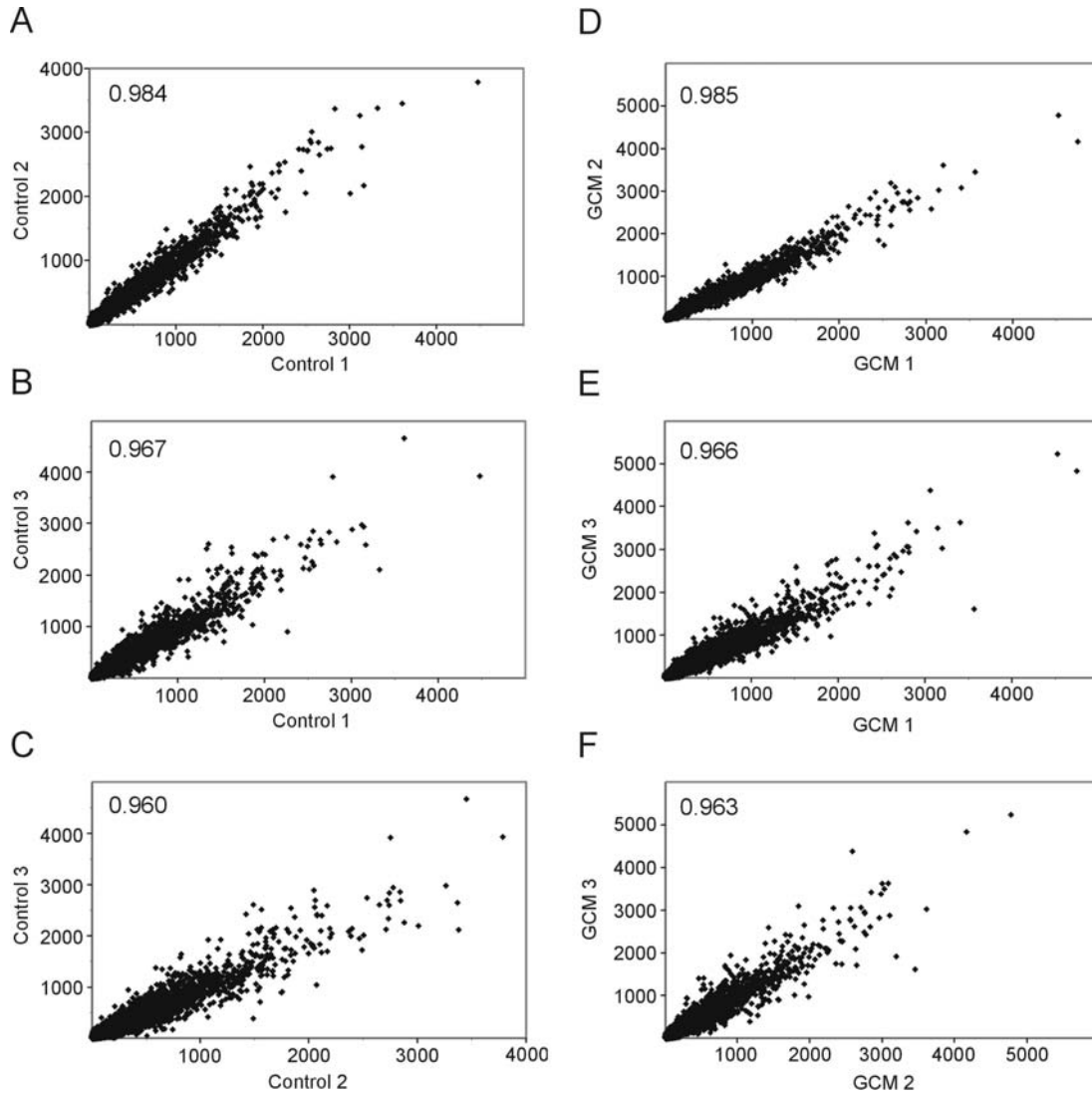


Figure 15: Microarray data are highly reproducible across experiments.

Cross-correlation of hybridization signals. (A-C) Hybridization signals for control RGCs in three independent experiments. (D-F) Hybridization signals for GCM-treated RGCs in three independent experiments. Numbers indicate correlation coefficients.

To detect relevant gene expression changes I set four criteria: First, only genes were selected which are present under control conditions - in the case of downregulation, or under treated conditions - in the case of upregulation, over all three experiments. Second, up- or downregulation of a single gene occurred in all of the three experiments. Third, the mean fold change over all three experiments was higher than 1.34 fold. And fourth, the CV for each gene over the three independent experiments was below 0.6. All genes which fulfilled these criteria were grouped by their function or cellular localization. Exceptions from these criteria were only made in special cases of known relevance as indicated.

3.2.2 Expression changes in RGCs related to soluble glia derived factors

GCM treatment of cultured RGCs for 30 hours resulted in changes of 82 genes, given in table 6. In general, gene regulation occurred in both directions and regulated genes were associated with different functional groups. The regulated genes were involved in sterol biosynthesis and regulation of cholesterol homeostasis, steroid metabolism, fatty acid synthesis, regulation of transcription, growth- and neurotrophic factors, extracellular matrix components, signal transduction or cell adhesion, for example (Tab. 6). The ten most downregulated genes mediated cholesterol synthesis and homeostasis, fatty acid synthesis, and steroid metabolism. On the other side, the top ten upregulated genes were distributed over several functional groups.

Table 6: Gene expression changes in cultured RGCs after 30h of GCM treatment

Gene	Trend	Fold change	CV	Sequence derived form
Sterol biosynthesis and regulation of cholesterol homeostasis				
<i>mevalonate pyrophosphate decarboxylase</i>	↓	3.48	0.16	NM_031062
<i>growth response protein (CL-6) / insulin induced gene 1 (Insig1)</i>	↓	2.3	0.41	NM_022392
<i>acetyl-Coenzyme A acetyltransferase 2 (Acat2)</i>	↓	2.3	0.25	AI412322
<i>isopentenyl-diphosphate delta isomerase</i>	↓	2.24	0.44	NM_053539
<i>farnesyl diphosphate synthase</i>	↓	2.14	0.32	NM_031840
<i>farnesyl diphosphate farnesyl transferase 1 / squalene synthase</i>	↓	2	0.36	NM_019238
<i>2,3-oxidosqualene lanosterol cyclase</i>	↓	1.95	0.18	BM390574
<i>cytochrome P450, subfamily 51</i>	↓	1.91	0.36	NM_012941
<i>sterol-C4-methyl oxidase-like</i>	↓	1.87	0.33	NM_080886
<i>3-hydroxy-3-methylglutaryl-Coenzyme A synthase 1 / HMG-CoA synthase, soluble</i>	↓	1.87	0.27	NM_017268
ESTs, similar to Delta(14)-sterol reductase [Rattus norvegicus]	↓	1.78	0.15	BM390364
ESTs, similar to 24-dehydrocholesterol reductase (DHCR24) [Homo sapiens]	↓	1.74	0.27	BF417479
<i>mevalonate kinase</i>	↓	1.74	0.27	AW433971
<i>acetyl-CoA acetyltransferase / thiolase</i>	↓	1.7	0.06	NM_023104
ESTs, similar to low density lipoprotein receptor [Mus musculus]	↓	1.66	0.46	BI294974
<i>squalene epoxidase</i>	↓	1.66	0.46	NM_017136
<i>3-hydroxy-3-methylglutaryl-Coenzyme A reductase / HMG CoA reductase</i>	↓	1.59	0.19	BM390399
phenylalkylamine Ca ²⁺ antagonist (emopamil) binding protein / 3-beta-hydroxysteroid-delta-8,delta-7-isomerase	↓	1.59	0.19	NM_057137
<i>sterol-C5-desaturase (fungal ERG3, delta-5-desaturase)-like</i>	↓	1.48	0.08	AB052846
ESTs, highly similar to sterol regulatory element binding protein-2 (SREBP-2) [Cricetulus griseus]	↓	1.41	0.86*	AI170663
<i>7-dehydrocholesterol reductase</i>	↓	1.41	0.16	NM_022389
ATP-binding cassette, sub-family G (WHITE), member 1	↑	1.48	0.79*	NM_053502

Gene	Trend	Fold change	CV	Sequence derived form
Steroid metabolism				
<i>ESTs, similar to hydroxysteroid dehydrogenase 17 beta, type 7 (Hsd17b7) [Mus musculus]</i>	↓	2.09	0.09	AI176172
<i>ESTs, weakly similar to steroidogenic acute regulatory protein precursor homolog [Homo sapiens]</i>	↓	2.05	0.18	AI236580
<i>ESTs, highly similar to NAD(P) dependent steroid dehydrogenase-like / aldo-keto reductase family 1, member C4 [Mus musculus]</i>	↓	1.62	0.2	BF407232
Fatty acid synthesis				
<i>stearoyl-Coenzyme A desaturase 1</i>	↓	2.24	0.21	J02585
<i>fatty acid synthase</i>	↓	1.55	0.07	AI179334
<i>fatty acid desaturase 1</i>	↓	1.52	0.27	NM_053445
<i>stearoyl-Coenzyme A desaturase 2</i>	↓	1.48	0.36	BE107760
<i>Thyroid hormone responsive protein (spot14)</i>	↓	1.45	0.49	NM_012703
<i>fatty acid elongase 2</i>	↓	1.35	0.11	BE116152
<i>phosphate cytidyltransferase 2, ethanolamine</i>	↓	1.35	0.29	NM_053568
Energy metabolism				
<i>isocitrate dehydrogenase 1</i>	↓	1.52	0.14	NM_031510
<i>ATP citrate lyase</i>	↓	1.35	0.22	NM_016987
Regulation of transcription / Chromatin associated				
<i>ESTs, similar to E2F transcription factor 3 [Mus musculus]</i>	↑	1.52	0.59	AI060205
<i>ESTs, similar to Wilms tumor 1 associated protein (WTAP) [Mus musculus]</i>	↑	1.52	0.36	AA900400
<i>cysteine-rich protein 3</i>	↑	1.45	0.58	NM_057144
<i>ESTs, highly similar to Thymidylate kinase/deoxythymidylate kinase (DTYMK) [Mus musculus]</i>	↑	1.41	0.33	BI290898
<i>ESTs, similar to interferon regulatory factor 2 (IRF2) [Mus musculus]</i>	↑	1.38	0.53	BI302791
<i>ESTs, similar to modulator of estrogen induced transcription [Rattus norvegicus]</i>	↑	1.35	0.44	BF397936
<i>ESTs, similar to putative transcription factor ZNF131 [Rattus norvegicus]</i>	↑	1.35	0.54	BE110637
Neurotransmission				
<i>transient receptor potential cation channel, subfamily C, member 3 (Trpc3)</i>	↓	1.38	0.53	NM_021771
<i>G protein-coupled receptor 51 / GABA-B receptor 2</i>	↑	1.45	0.39	NM_031802
Growth- and neurotrophic factors				
<i>pancreatitis-associated protein 1 / Reg2</i>	↑	1.55	0.07	NM_053289
<i>ESTs, similar to insulin-like growth factor I [Mus musculus]</i>	↑	1.38	0.36	BE103520
Extracellular matrix components				
<i>matrix Gla protein</i>	↑	2.58	0.28	NM_012862
<i>Tissue inhibitor of metalloproteinase 3</i>	↑	1.38	0.36	AI599265
<i>EST, weakly similar to nidogen 1 (Nid1) [Mus musculus]</i>	↑	1.38	0.53	AI070991
Cytoskeleton organization				
<i>ESTs, similar to platelet-activating factor acetylhydrolase 45kD subunit (Pafah) / lissencephaly-1 protein (LIS-1) [Mus musculus]</i>	↓	1.82	0.52	BG663460
<i>ESTs, weakly similar to actopaxin [Rattus norvegicus]</i>	↓	1.35	0.29	AA899471
<i>kinesin family member 3c</i>	↑	1.38	0.51	BF553488

Gene	Trend	Fold change	CV	Sequence derived form
Protein synthesis, modification transport and degradation				
ESTs, similar to E3 ligase for inhibin receptor [Rattus norvegicus] or HECT domain containing 1 (Ubiquitin-protein ligase) [Mus musculus]	↓	1.45	0.47	AW531948
ESTs, similar to syntaxin 11 (Stx11) [Mus musculus]	↓	1.41	0.28	AW920037
ESTs weakly similar to ribosomal protein S23 [Rattus norvegicus]	↑	1.55	0.37	BE114185
ESTs, moderately similar to polypeptide GalNAc transferase T1 [Rattus norvegicus]	↑	1.41	0	AI103845
ESTs, moderately similar to CGI-09 protein [Homo sapiens]	↑	1.38	0.27	BF560079
Signal transduction				
diazepam binding inhibitor	↓	1.48	0.44	AI175009
ESTs, moderately similar to membrane-spanning 4-domains, subfamily A, member 10 [Mus musculus]	↓	1.45	0.32	AI555523
ESTs, similar to galanin receptor 2 (Galr2) [Mus musculus]	↓	1.35	0.29	AI385327
ESTs, serine/threonine kinase 32C (Stk32c) [Mus musculus]	↓	1.35	0.44	BE097305
interleukin 24	↑	1.35	0.11	NM_133311
ESTs, similar to Rho GTPase activating protein 12 [Rattus norvegicus] / Rho guanine nucleotide exchange factor (Larg) [Mus musculus]	↑	1.35	0.47	AI137762
Cell adhesion				
ESTs, similar to integrin, beta-like 1 / ten beta-integrin EGF-like repeat domains [Mus musculus]	↓	1.45	0.49	BI303923
ESTs, protocadherin 18 [Mus musculus]	↓	1.38	0.4	BF408099
Stress				
Metallothionein 1	↓	1.35	0.11	AF411318
heme oxygenase 1	↑	1.62	0.31	NM_012580
ESTs, similar to sestrin 2 (Sesn2) [Mus musculus]	↑	1.38	0.56	BE109653
Immune response				
ESTs, hypothetical Immunoglobulin and major histocompatibility complex domain containing protein	↓	1.41	0.57	BI294746
ESTs, highly similar to toll-like receptor 1 [Mus musculus]	↓	1.38	0.53	AI070419
ESTs, T-cell receptor alpha/delta locus [Mus musculus]	↓	1.38	0.44	BE098148
Other functions				
ESTs, highly similar to cora cornifin alpha (small proline-rich protein 1) (SPRR1) [Rattus norvegicus]	↑	1.38	0.1	BI286387
ESTs, highly similar to atda diamine acetyltransferase / Spermidine/spermine N(1)-acetyltransferase (SSAT) / Putrescine acetyltransferase [Mus musculus]	↑	1.38	0.2	AA893220
ESTs, moderately similar to HSPC133 protein (DC3) [Homo sapiens]	↑	1.35	0.47	BE113965
Unknown function				
ESTs, similar to nasopharyngeal carcinoma susceptibility protein [Rattus norvegicus] or ankyrin repeat-containing cofactor-1 (ANCO1) [Homo sapiens]	↓	1.48	0.46	BE097847

Gene	Trend	Fold change	CV	Sequence derived form
ESTs, highly similar to T9S3_MOUSE Transmembrane 9 superfamily protein member 3 precursor [Mus musculus]	↓	1.45	0.23	BF545305
ESTs, highly similar to nucleolar protein GU2 [Mus musculus]	↓	1.38	0.2	AI170715
ESTs, similar to male sterility protein 2-like protein [Torpedo marmorata]	↓	1.38	0.2	AI555210
ESTs, similar to EGF-like module containing, mucin-like, hormone receptor-like sequence 1 [Mus musculus]	↓	1.38	0.1	BE100625
ESTs, similar to MYOSIN-IXA homolog [Homo sapiens]	↓	1.35	0.22	AW535406
ESTs, similar to nasopharyngeal epithelium specific protein 1 [Rattus norvegicus]	↑	1.52	0.49	BF419626
ESTs, similar to lymphocyte antigen 6 complex [Mus musculus]	↑	1.41	0.59	BE108597
ESTs, similar to hypothetical Esterase/lipase/thioesterase family active site containing protein [Mus musculus]	↑	1.38	0.44	AI603103

Table 6: Gene expression changes in RGCs after 30 hours of GCM treatment. Arrows indicate up- (↑) or down- (↓) regulation compared to control. Italicized genes are similarly regulated by cholesterol treatment. Stars (*) indicate CV values which are larger than the threshold.

3.2.2.1 GCM regulated cholesterol synthesis and homeostasis in cultured RGCs and caused downregulation of genes involved in steroid metabolism and fatty acid synthesis

The largest functional group of regulated genes concerned cholesterol homeostasis. All investigated genes encoding for enzymes directly involved in cholesterol biosynthesis were downregulated. In addition, the cholesterol synthesis regulating protein INSIG, the cholesterol esterification enzyme Acat2, the cholesterol uptake mediating LDL receptor and the sterol regulatory element binding protein 2 (SREBP-2) were downregulated. On the other hand, the cholesterol releasing ABC transporter G1 (ABC-G1) was upregulated by GCM treatment. These results indicated that GCM treatment diminished neuronal cholesterol synthesis and uptake and enhanced cholesterol release.

To confirm these results on the protein level, I selected squalene synthase (SQS) as the key enzyme at the entrance of the cholesterol synthesis pathway, whose gene was two-fold downregulated. GCM treatment of microculture RGCs drastically reduced the protein level of SQS as shown by immunostaining using a specific antibody against SQS (Fig. 16). For direct evidence of neuronal cholesterol synthesis regulation, I performed labeling of newly synthesized cholesterol using a radioactive precursor. RGCs were incubated with ^{14}C -acetat as cholesterol precursor in absence or presence of GCM. After 48 hours of

incubation, lipids were extracted and separated by TLC. Fig. 17 shows the autoradiogram of the labeled lipid profile. Visible as clear band in line with the cholesterol standard, cultured RGCs synthesized cholesterol under the given culture conditions and GCM treatment reduced this *de novo* synthesis drastically.

To confirm the upregulation of the ABC-G1, I performed quantitative real time RT-PCR in cooperation with the group of Prof. Gerd Schmitz in Regensburg. After five days in culture, RGCs were cultured in the presence of GCM for further five days before RNA was prepared. Analysis by real time PCR revealed a 3.46 fold higher mRNA level for ABC-G1 under GCM treated conditions compared to control cells. Since ABC-G1 is known to be involved in cholesterol and phospholipid efflux (Schmitz et al., 2001), I tested next if the expression enhancement of ABC-G1 is correlated to neuronal cholesterol release. Performing pulse chase labeling using ^{14}C -acetat as lipid precursor followed by lipid analysis of the culture media of untreated and GCM treated RGCs (Fig. 18), I showed that GCM treatment increased the release of endogenous cholesterol to the culture medium compared to untreated conditions. Additionally, treatment with GCM caused also neuronal phosphatidylcholine release.

In addition to the large group of genes mediating cholesterol homeostasis, down-regulated genes were involved in steroid- and fatty acid biosynthesis. Steroid synthesis requires cholesterol as common precursor and partially shares enzymes and regulatory pathways with cholesterol synthesis. The steroidogenic acute regulatory protein (STAR) transports cholesterol from the outer- to the inner mitochondrial membrane where the first steroidogenic enzyme P450scc is localized (Thomson, 2003; Stocco, 2001) but also oxysterol producing enzymes such as cholesterol 27-hydroxylase (Sugawara et al., 1995) which have a significant impact in the regulation of cholesterol metabolism. The two other genes in his group are hydroxysteroid dehydrogenase 17 beta and aldo-keto reductase 1C4.

Fatty acid synthesis is similar transcriptional regulated as cholesterol synthesis, and both pathways were activated by the transcription factor SREBP-1a (Horton et al., 2002). Several key genes involved in fatty acid synthesis and regulation were downregulated by GCM. In addition to fatty acid synthesizing enzymes like fatty acid synthase, -desaturase 1 and -elongase 2, the thyroid hormone responsive protein – responsible for the activation of genes encoding for enzymes of fatty acid synthesis was downregulated by 1.45 fold.

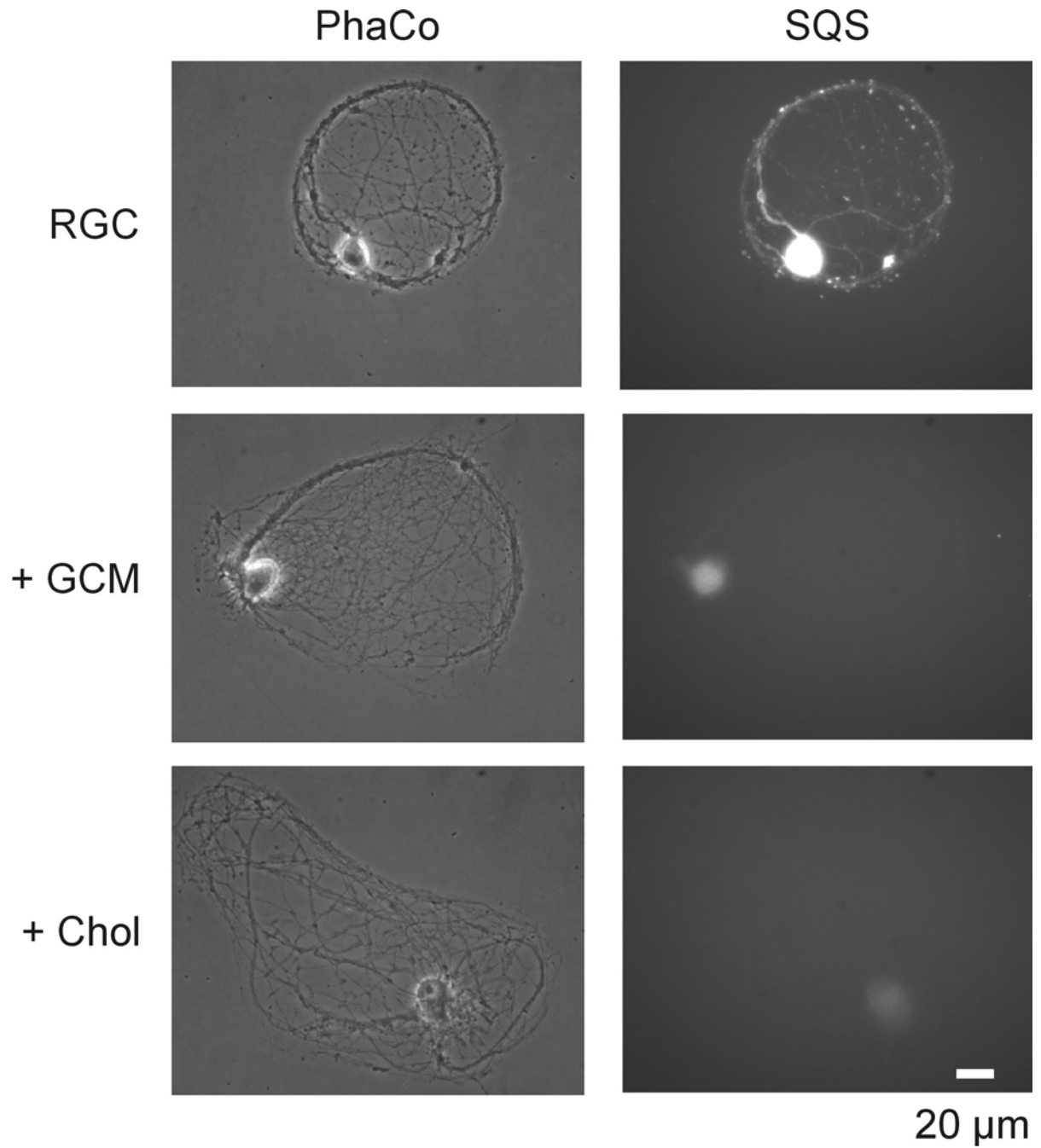


Figure 16: GCM- and cholesterol-induced downregulation of SQS

Phase-contrast (left) and fluorescence (right) micrographs of RGCs, which were cultured for six days in defined medium and then for five days in defined medium (RGC), with GCM or with cholesterol and which were then stained with an antibody against SQS.

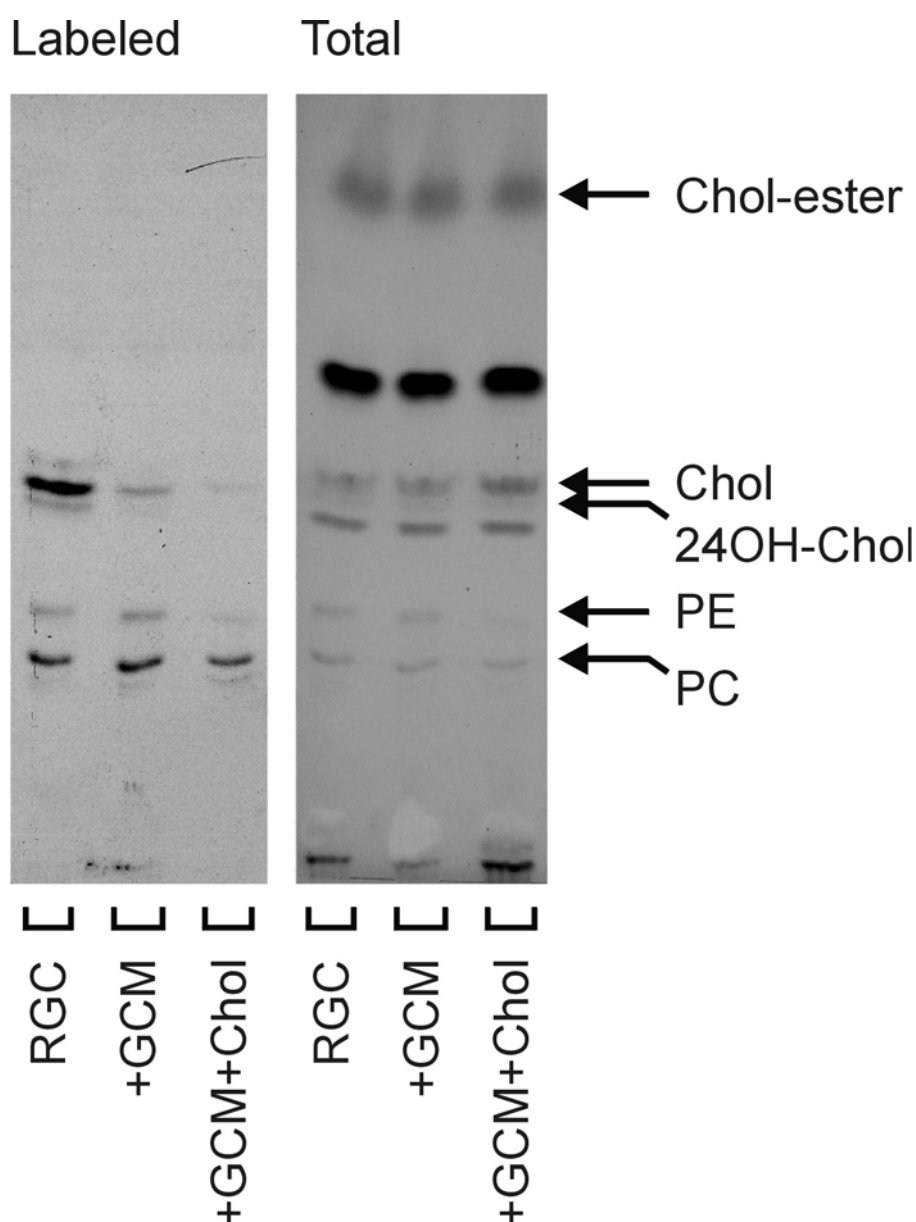


Figure 17: GCM-induced downregulation of cholesterol synthesis in RGCs.

Micrographs show the autoradiogram (left) and total lipid staining (right) of the same TLC plate. RGCs were cultured for seven days in defined medium and then for 48 hours in defined medium (RGC), with GCM or with GCM + cholesterol in the presence of ^{14}C -acetat as cholesterol precursor. Lipids were extracted by hexan/isopropanol from cells and separated by TLC. Arrows indicate positions of lipid standards running together with samples: Chol – cholesterol; 24OH-chol – 24-hydroxy-cholesterol; PE – phosphatidylethanolamine; PC – phosphatidylcholine. Chol-ester – cholesteryl-ester. TLC by K. Nieweg.

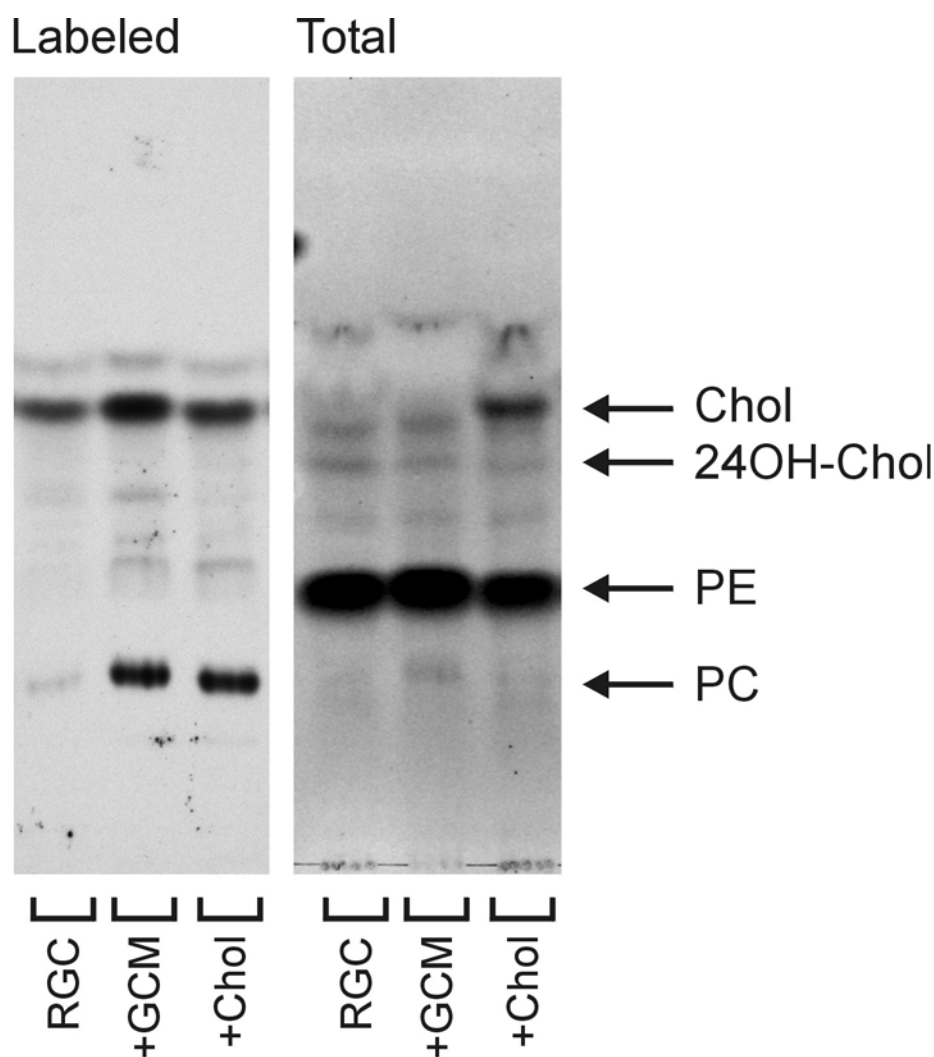


Figure 18: GCM- and cholesterol-induced endogenous cholesterol and phosphatidylcholine release of RGCs.

Micrographs show the autoradiogram (left) and total lipid staining (right) of the same TLC plate. RGCs were cultured for seven days in defined medium and then for 48 hours in defined medium in presence of ^{14}C -acetat as lipid precursor. After washing, cells were cultured for 48 hours in defined medium (RGC), with GCM or with cholesterol. Lipids were extracted by chloroform/methanol from culture medium and separated by TLC. Arrows indicate positions of lipid standards running together with samples: Chol – cholesterol; 24OH-chol – 24-hydroxy-cholesterol; PE – phosphatidylethanolamine; PC – phosphatidylcholine.

Together, these results demonstrated that GCM downregulated the cholesterol biosynthesis in cultured RGCs as shown on gene expression-, protein- and lipid level. Treatment with GCM enhanced the expression of the ABC-G1 transporter and led to endogenous cholesterol and phosphatidylcholine release. Further, genes involved in steroid metabolism and fatty acid synthesis were downregulated by GCM treatment.

3.2.2.2 GCM upregulates matrix Gla protein and heme oxygenase 1 in cultured RGCs

In the following, I will focus on the two most upregulated genes. The highest upregulated neuronal gene in response to GCM treatment encodes for the MGP, a small ubiquitous matrix protein (Price & Williamson, 1985; Luo et al., 1995). This gene is 2.58 fold up-regulated with a small CV (0.28).

A first experiment to localize MGP in RGCs was performed with untreated cells and cells that were treated for five days with GCM, using immunostaining with a specific antibody. Immunofluorescence showed an association of MGP with somata and dendrites of GCM treated RGCs as demonstrated by double labeling with the dendritic marker MAP2, whereas control cells showed only stained somata (Fig. 19).

The second highly upregulated neuronal gene in response to GCM treatment encoded for heme oxygenase 1 (HO1). It showed a change of 1.62 fold and a CV of 0.31. HO1 is a well known enzyme that cleaves the heme ring at the alpha methene bridge to form biliverdin, ferric iron and carbon monoxide (CO) (Tenhunen et al., 1968).

The expression upregulation could be confirmed on protein level. Immunoblotting using a specific antibody against HO1, showed for GCM-treated dense culture RGCs an upregulation of HO1 after three days of treatment compared to control (Fig. 20). Furthermore, intracellular localization of HO1 was investigated by double labeling of microculture RGCs using specific antibodies against HO1 and GluR2/3 (Fig. 21). RGCs growing for five days in defined medium and then for four days in defined medium with GCM, showed a similar distribution for HO1 and GluR2/3 positive staining in somata and dendrites. Control cells, which were cultured for the whole time in defined medium, showed only somata association of HO1 and GluR2/3.

Taken together, the upregulation of MGP and HO1 could be confirmed on the protein level. Both proteins showed dendritic localization.

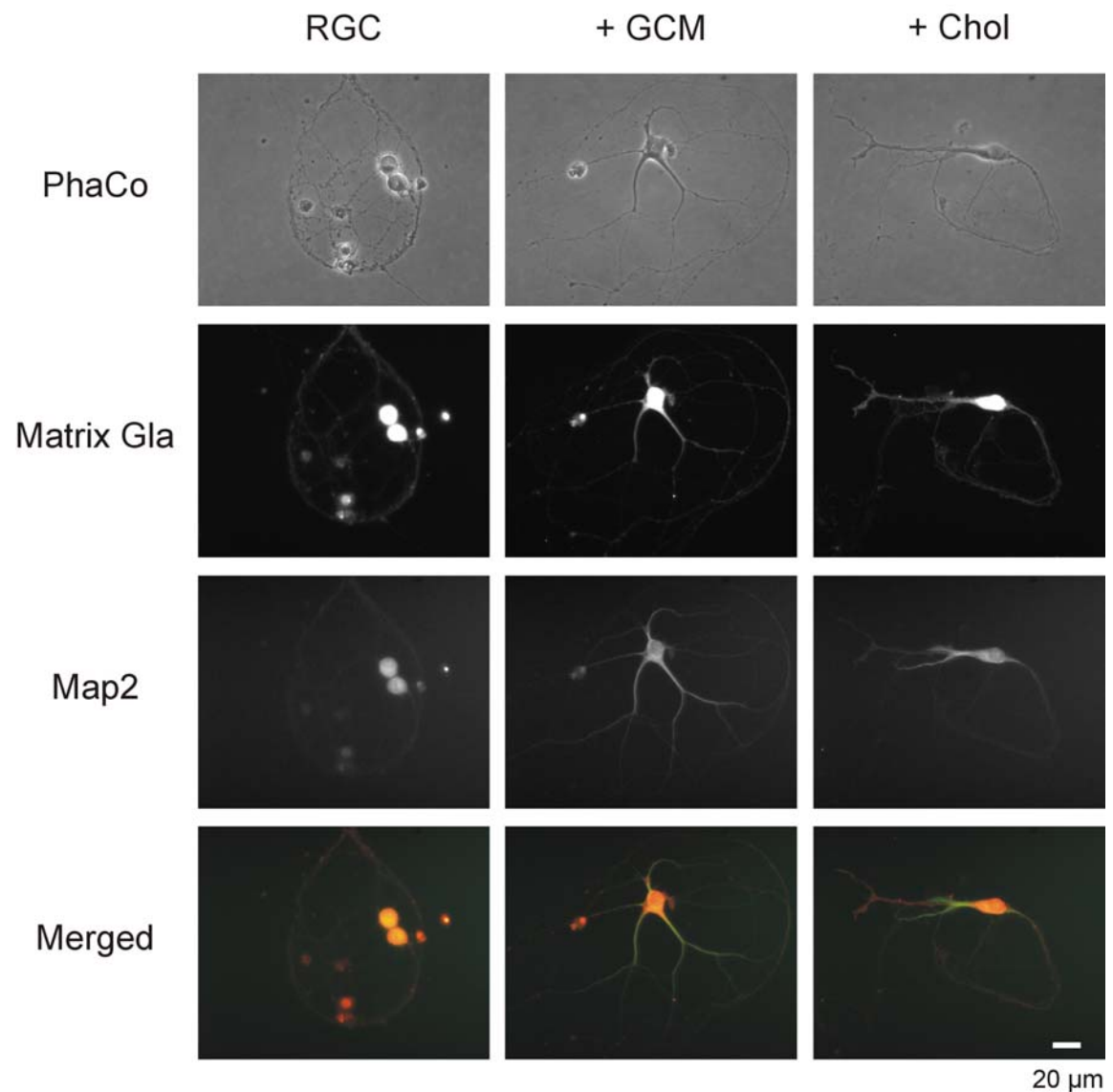


Figure 19: Localization of MGP in RGCs.

Phase-contrast and fluorescence micrographs of RGCs growing for three days in defined medium and then for five days in defined medium (left), with GCM (middle) and with cholesterol (right). Cultures were stained with antibodies against MGP and the dendritic marker MAP2. Merged images show MGP in red and MAP2 in green.

3.2.3 Comparison of GCM and cholesterol-induced expression changes

As shown before, cholesterol itself has a profound influence on RGC differentiation. To search for neuronal genes that mediate these effects and to distinguish the influence of cholesterol from other glial factors, I treated cultured RGCs for 30 hours with cholesterol at the same concentration as it is present in GCM and compared the gene expression pattern with that of untreated control cells. I found that directly added cholesterol regulated the gene expression of 37 genes, given in table 7. As for GCM, regulated genes were associated with different functional groups like sterol biosynthesis and regulation of cholesterol homeostasis, splicing, extracellular matrix components, signal transduction, stress reaction and vesicle transport (Tab. 7).

A comparison of genes that were regulated by cholesterol and GCM treatment showed that the expression of 18 genes changed in a similar manner. These genes belonged exclusively to the functional groups of sterol biosynthesis and regulation of cholesterol homeostasis, steroid metabolism and fatty acid synthesis.

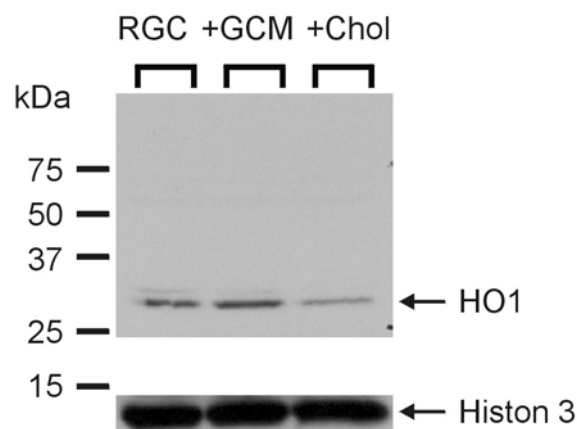


Figure 20: Differential regulation of HO1 by GCM and cholesterol.

Immunoblot of RGCs growing for four days in defined medium and then for three days in the presence of defined medium (RGC), GCM or cholesterol using antibodies against HO1 and Histon 3 (bottom).

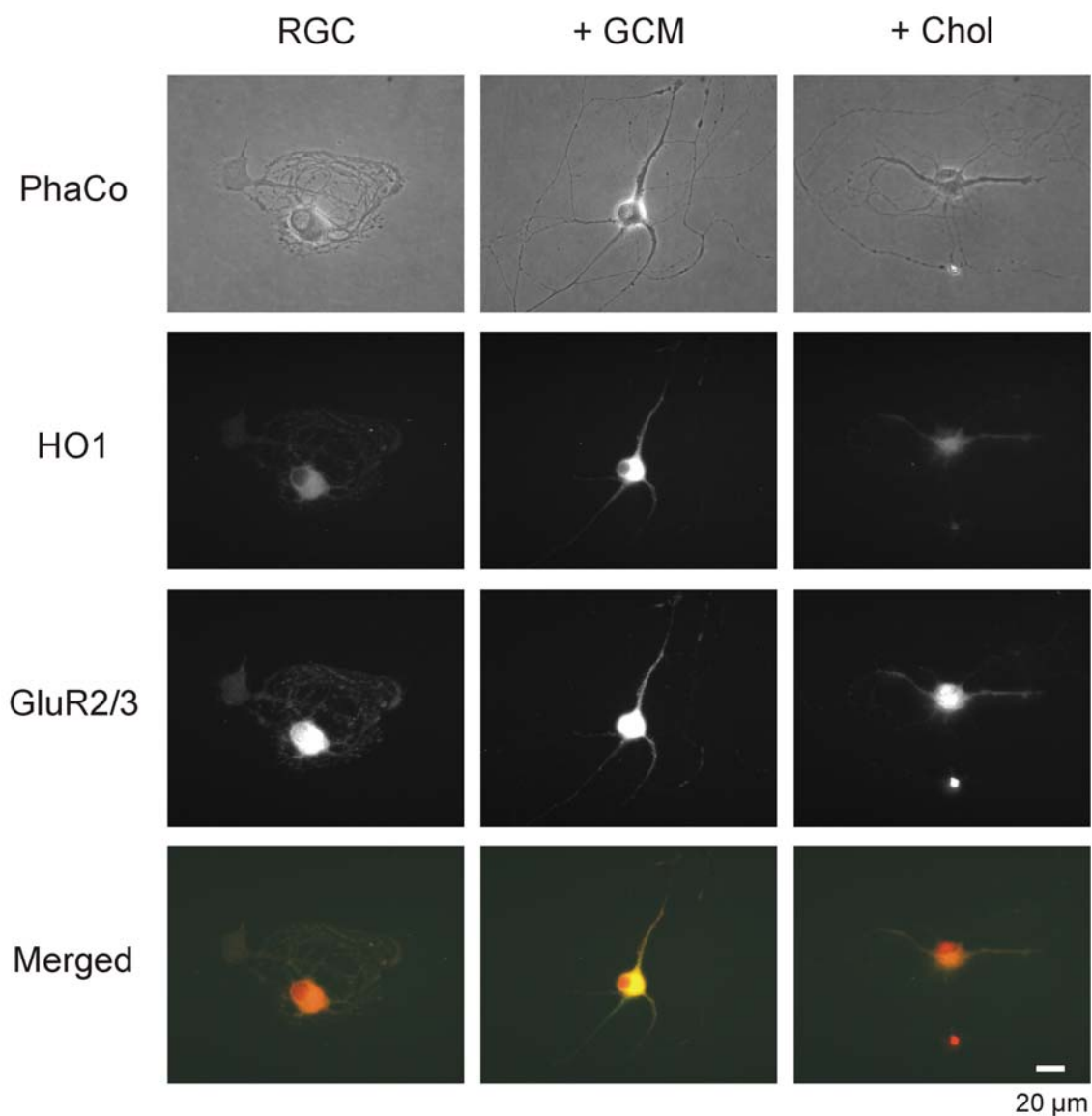


Figure 21: Localization of HO1 in RGCs.

Phase-contrast and fluorescence micrographs of RGCs growing for three days in defined medium and then for five days in defined medium (left), with GCM (middle) and with cholesterol (right). Cultures were stained with antibodies against HO1 and the postsynaptic marker GluR2/3. Merged images show HO1 in green and GluR2/3 in red.

Table 7: Gene expression changes in cultured RGCs after 30h of cholesterol treatment

Gene	Trend	Fold change	CV	Sequence derived form
Sterol biosynthesis and regulation of cholesterol homeostasis				
isopentenyl-diphosphate delta isomerase	↓	2.0	0.14	BI290053
mevalonate pyrophosphate decarboxylase	↓	1.82	0.24	NM_031062
growth response protein (CL-6) / insulin induced gene 1 (Insig1)	↓	1.7	0.33	NM_022392
2,3-oxidosqualene: lanosterol cyclase	↓	1.55	0.52	BM390574
sterol-C4-methyl oxidase-like	↓	1.52	0.49	NM_080886
cytochrome P450, subfamily 51	↓	1.52	0.49	NM_012941
squalene epoxidase	↓	1.48	0.3	NM_017136
7-dehydrocholesterol reductase	↓	1.48	0.36	NM_022389
acetyl-Coenzyme A acetyltransferase 2 (Acat2)	↓	1.48	0.44	AI412322
acetyl-CoA acetyltransferase / thiolase	↓	1.45	0.09	NM_023104
mevalonate kinase	↓	1.41	0.57	NM_031063
3-hydroxy-3-methylglutaryl-Coenzyme A synthase 1 / HMG-Co A synthase, soluble	↓	1.38	0.53	NM_017268
farnesyl diphosphate farnesyl transferase 1 / squalene synthase	↓	1.38	0.53	NM_019238
ESTs, similar to low density lipoprotein receptor [Mus musculus]	↓	1.38	0.66*	BI294974
farnesyl diphosphate synthase	↓	1.35	0.61*	NM_031840
3-hydroxy-3-methylglutaryl-Coenzyme A reductase / HMG-CoA reductase	↓	1.35	0.47	BM390399
Steroid metabolism				
hydroxysteroid dehydrogenase 17 beta, type 7	↓	1.45	0.09	NM_017235
Fatty acid synthesis				
stearoyl-Coenzyme A desaturase 1	↓	1.45	0.64*	J02585
ESTs, highly similar to hypertension-associated protein SA [Rattus norvegicus]	↓	1.38	0.36	BI282211
Energy metabolism				
pyruvate dehydrogenase phosphatase isoenzyme 2	↓	1.41	0.49	AF062741
ESTs, Weakly similar to lactate dehydrogenase D [Mus musculus]	↑	1.38	0.56	AI501131
Chromatin associated / splicing				
ESTs similar to Transformer-2 protein homolog (TRA-2 ALPHA) homolog [Homo sapiens]	↑	1.48	0.22	AI137236
ESTs, similar to SMC4 protein homolog/ Structural maintenance of chromosomes 4-like 1 protein [Microtus arvalis],	↑	1.41	0.59	AW535494
ESTs similar to FUS interacting protein (serine-arginine rich) 1 / TLS-associated protein with SR repeats (TASR)	↑	1.41	0.59	AI070564
ESTs similar to Histone deacetylase 8 (Hdac8) [Mus musculus]	↑	1.35	0.29	BE117008
Neurotransmission				
ESTs similar to glutamate receptor, ionotropic, N-methyl-D-aspartate 3A [Homo sapiens]	↑	1.35	0.29	AI146055
Extracellular matrix components				
netrin 1	↑	1.59	0.37	NM_053731

Gene	Trend	Fold change	CV	Sequence derived form
Cytoskeleton organization				
ESTs, Highly similar to autophagy 5-like [Mus musculus]	↑	1.52	0.36	AW528235
rapostlin	↑	1.41	0.33	BE105446
calpain 8 (Capn8)	↑	1.41	0.49	NM_133309
Signal transduction				
ESTs, similar to Serine/threonine-protein kinase nek1 (NimA-related protein kinase 1) [Mus musculus]	↓	1.38	0.36	AI406369
neuraminidase 3	↑	1.45	0.39	NM_054010
receptor-like tyrosine kinase	↑	1.35	0.54	AB073721
ESTs, Moderately similar to FMT_MOUSE Methionyl-tRNA formyltransferase, mitochondrial precursor (MtFMT) [Mus musculus]	↑	1.35	0.39	AW251803
Stress				
selenoprotein P, plasma, 1	↑	1.48	0.08	AA799627
Vesicle transport				
ESTs, Moderately similar to golgi autoantigen, golgin subfamily a, 4 (Golga4), [Mus musculus]	↑	1.35	0.54	BF568007
Unknown function				
ESTs, Highly similar to CGI-67 serine protease [Rattus norvegicus]	↑	1.62	0.58	AI007882

Table 7: Gene expression changes in RGCs after 30h of cholesterol treatment. Arrows indicate expression up- (↑) or down- (↓) regulation compared to control. Stars (*) indicate CV values which are larger than the threshold.

3.2.3.1 Cholesterol treatment mimicked the GCM induced reduction of neuronal cholesterol synthesis

Similar to GCM, cholesterol treatment caused a downregulation of the sterol synthesis pathway, as well as the downregulation of Acat2 and LDL receptor. Immunostaining for SQS (Fig. 16) as well as radioactive labeling with ^{14}C -acetat as cholesterol precursor (Fig. 17) confirmed cholesterol-induced downregulation of neuronal cholesterol synthesis and of enzymes. The release of endogenous cholesterol by exogenous cholesterol treatment was lower as for GCM (Fig. 18) and just marginally higher as control level. However, the level of endogenous released phosphatidylcholine was considerable higher as under control conditions and similar to GCM treated RGCs (Fig. 18). Similarities concerning expression regulation of genes involved in steroid metabolism and fatty acid synthesis were limited to the genes of hydroxysteroid dehydrogenase 17 beta and stearyl-CoA desaturase.

Taken together, these results demonstrated that exogenously added cholesterol regulated cholesterol synthesis in cultured RGCs similar to GCM. This suggests that

cholesterol contained in GCM in form of lipoproteins caused the detected downregulation of neuronal cholesterol synthesis by GCM.

3.2.3.2 Cholesterol did not affect MGP and HO1 gene expression but downregulates HO1 on protein level in RGCs

Comparing upregulated genes by cholesterol and GCM treatment, I observed no overlap between these two groups. Gene expression of MGP, drastically upregulated by GCM, was unaffected by cholesterol treatment. Double labeling of cholesterol-treated microcultures for MGP and MAP2 revealed a redistribution of MGP from somata to dendrites similar as seen for GCM. However, dendritic labeling was weaker as for GCM-treated cells whereas control cells showed only stained somata (Fig. 19).

HO1, which was highly upregulated by GCM, was unaffected by 30 hours of cholesterol treatment. However, immunoblotting of cell lysate from dense culture RGCs treated for three days with cholesterol, showed a clear downregulation of HO1 on protein level compared to control (Fig. 20). Further, immunostaining of microculture RGCs cultured for four days in the presence of cholesterol confirmed this result (Fig. 21). This regulation appeared in opposite to the noted GCM effect, where treatment for the same time caused a clear upregulation of HO1. However, the association of HO1 with GluR2/3 at dendrites occurred in both, cholesterol and GCM treated RGCs, indicating a redistribution of HO1 from Somata to dendrites.

Together, MGP and HO1 gene expression was not affected by 30 hours of cholesterol treatment in contrast to GCM. Longer cholesterol and GCM treatment induced opposite effects on HO1 protein levels. GCM enhanced the protein level, whereas cholesterol lowered it. GCM and cholesterol induced redistribution of MGP and HO1 from soma to dendrites.

3.2.3.3 Cholesterol enhanced CGI-67 serine protease and Netrin 1 expression

The highest upregulated gene due to cholesterol treatment was an EST similar to CGI-67 serine protease. It was 1.62 fold regulated and had with 0.58 a relatively high CV. Its identification as serine protease stems from sequence analysis and so far nothing is known about its functional role.

The second highest upregulated gene was netrin 1, where cholesterol caused a fold change of 1.59 at the expression level of RGCs compared to control, at a CV of 0.37. Netrin 1 is known as matrix molecule and involved in axon guidance (see introduction).

Both, CGI-67 and netrin 1 were not regulated by GCM treatment. Together, these results showed that directly added cholesterol at the same concentration as in GCM caused gene expression changes that were distinct from those induced by GCM.

IV. DISCUSSION

4.1 Multiple mechanisms mediate glia-induced synaptogenesis in RGCs

The first part of this work reveals that the GCM- and cholesterol-induced increase in synapse number requires several days of treatment and identifies dendrite differentiation as rate limiting step for glia-induced synaptogenesis. Cholesterol was indispensable for the differentiation of dendrites and glia-derived laminin containing the $\gamma 1$ chain acted as dendrite-promoting signal for RGCs. Finally, cholesterol was essential for continuous synaptogenesis and for the functional stability of evoked transmitter release.

4.1.1 Dendrite differentiation limits the rate of glia-induced synaptogenesis, requires cholesterol and is promoted by laminin $\gamma 1$

My observation that GCM and cholesterol induced dendrite differentiation with a remarkably similar time course as the increase in synapse number suggested it as the rate limiting step in glia-induced synaptogenesis. This is in line with reports that dendrite development determines the competence of neurons to form synapses (Fletcher et al., 1994) and that dendritic filopodia play an active role in the establishment of contacts (Ziv & Smith, 1996). My findings corroborate the idea that glial cells are a source of dendrite promoting signals. This has been shown in vitro for RGCs isolated from embryonic chicken (Bauch et al., 1998), for sympathetic neurons from newborn mice (Tropea et al., 1988) and for cortical neurons from embryonic mice (Le Roux & Esquenazi, 2002; Higgins et al., 1997; Keith & Wilson, 2001). In addition, regional differences in the dendrite-promoting activity of glial cells have been reported (Le Roux & Reh, 1994; Dijkstra et al., 1999).

My results suggest that cholesterol and laminin promote the differentiation of dendrites. Under control conditions, most RGCs extended several neurites from their soma, which grew and branched extensively, but lacked MAP2 or GluR2/3. Cholesterol together with laminin induced a redistribution of MAP2 and GluR2/3 receptors to neurites without changing their level of expression. This indicates that they promote the maturation of dendrites. So far, signals and mechanisms that shape the dendritic tree are well established (Gao & Bogert, 2003; Jan & Jan, 2003; Miller & Kaplan, 2003; Scott & Luo, 2001;

Whitford et al., 2002; Wong & Ghosh, 2002), but much less is known about the pathways that regulate their differentiation (Libersat & Duch, 2004).

As mentioned in the introduction, cholesterol could serve as precursor for neurosteroids, as building material or it may act by determining the functional properties of membrane proteins as a component of rafts. It has been shown that progesterone promotes dose-dependent dendritic outgrowth of Purkinje cells, using cerebellar slice cultures from newborn rats (Sakamoto et al., 2001). However, treatment of RGCs with progesterone, pregnenolone and several of their derivatives showed no synaptogenic effects as measured by electrophysiological recordings (D. Mauch, C. Göritz; F.W. Pfrieger, unpublished results). It appears possible that cholesterol serves as building material. The differentiation of dendrites may require large amounts of lipids due to the presence of intracellular organelles like endoplasmatic reticulum and Golgi apparatus (Horton & Ehlers, 2004). A specific dependence of dendrites on the neuronal cholesterol level has been shown previously in primary cortical cultures from embryonic rats, where experimentally induced cholesterol deficiency decreased selectively the number and length of dendrites, but not axonal elongation (Fan et al., 2002). Furthermore, it cannot be excluded at present, that cholesterol promotes dendrite differentiation by clustering of specific signaling components in rafts.

The finding that laminin promotes the differentiation of dendrites is surprising. Laminin is well known to enhance neurite growth in RGCs from different vertebrate species (Manthorpe et al., 1983; Rogers et al., 1983; Smalheiser et al., 1984; Hopkins et al., 1985; Ivins et al., 1998) and in many other neuronal cell types (Luckenbill-Edds, 1997; Powell & Kleinman, 1997; Patton, 2000), but a dendrite-promoting activity of this matrix component has never been reported. This effect may have gone unnoticed, because neurites were not further characterized as axons or dendrites or because the presence of serum in culture medium influenced the neuronal response to laminin (Bates & Meyer, 1994). In glia- and granule cell-deprived organotypic cultures of rat cerebellum, laminin promoted spine proliferation in Purkinje cells, but this effect was not mimicked by laminin fragments (Seil, 1998).

Barres and coworkers proposed recently that around birth, rat RGCs switch from axonal to dendritic growth and that this switch is induced by contact to amacrine cells (Goldberg et al., 2002). Furthermore, it has been shown that during development, axon formation in RGCs becomes independent from laminin (Cohen et al., 1986; Hall et al., 1987; Ivins et al., 1998). Based on my results, I hypothesize that the amacrine-derived

signal changes the way how RGCs respond to laminin: Before birth, laminin induces axons, whereas after birth, it promotes dendrite differentiation. But so far, it remains to be studied which signaling mechanisms are involved in laminin promoted dendrite differentiation.

Treatment of RGCs with laminin fragments revealed that the $\gamma 1$ chain contains the dendrite-promoting activity. However, I should mention that laminin and peptides were used at the same weight per volume, and therefore differ widely in their molar concentrations. Immunohistochemical and in situ hybridization studies showed that this chain is present in the ganglion cell layer in rodents (Dong & Chung, 1991; Libby et al., 2000; Yin et al., 2003), but its exact distribution and cellular source around birth, when RGCs form dendrites (Maslim et al., 1986; Tucker & Matus, 1988; Sernagor et al., 2001) remains to be studied. Other laminins including newly discovered forms (Koch et al., 2000; Yin et al., 2002) may exert dendrite promoting activity, but their function in the retina or other brain regions is unknown.

A fraction of RGCs failed to differentiate dendrites even in the presence of soluble glial factors, and these cells are mainly found on microislands with more than one neuron. This suggests that contact with neighboring RGCs impedes dendrite differentiation. Alternatively, dendrite differentiation in these cells may require signals from other neurons or direct neuron-glia contact. A previous study on cultured cerebellar neurons has shown that granule cells induce dendrites in Purkinje cells (Baptista et al., 1994).

4.1.2 Cholesterol is required for ongoing synaptogenesis and the stability of evoked release

My observation that removal of GCM from cultured RGCs stopped the continuous increase in synaptic activity during the culture period and that this effect was rescued, if GCM was replaced by cholesterol indicates that RGCs require cholesterol for continuous synaptogenesis. After removal of GCM, synaptic activity remained at a baseline level indicating that those synapses that had formed, remained active. Interestingly, removal of GCM diminished selectively the size of evoked EPSCs and increased the number of RGCs lacking evoked synaptic responses and these effects were eliminated when GCM was replaced by cholesterol. This indicates that the functional stability of evoked release requires the presence of cholesterol. This is further supported by previous reports that exocytosis is sensitive to the removal of cholesterol, and probably occurs at cholesterol-rich domains in the plasma membrane (Chamberlain et al., 2001; Lang et al., 2001;

Pfriege, 2003b; Ohara-Imaizumi et al., 2004). Cholesterol may also promote the biogenesis and maturation of synaptic vesicles as suggested previously (Mauch et al., 2001). It appears essential for the biogenesis of secretory vesicles in neurosecretory cell lines (Thiele et al., 2000; Wang et al., 2000) and for the formation of vesicle protein complexes *in vivo* (Mitter et al., 2003; Pfriege, 2003). The idea of an enhanced vesicle production is further supported by the observation that cholesterol enhanced the number of synapsin-positive puncta, which were dispersed along axons. This is in contrast to GCM-treated cells, where synapsin-puncta were concentrated at synaptic sites along dendrites. The dispersed puncta probably represent clusters of surplus synaptic vesicles that cannot be delivered to synapses due to the lower incidence of dendrites. Alternative, cholesterol may have increased the transmitter concentration in synaptic vesicles, for example by enhancing the efficacy of glutamate transporters (Canolle et al., 2004).

4.2 Influence of soluble glial factors and cholesterol on gene expression of cultured postnatal RGCs

My GeneChip experiments revealed 82 genes whose level of expression changed under the influence of GCM and 38 genes for cholesterol treatment. Interestingly, there was only little overlap between the two groups. The 18 genes which were upregulated by GCM and cholesterol are mainly involved in cholesterol biosynthesis and homeostasis. The supply of external cholesterol, directly or contained in GCM, downregulates genes involved in cholesterol synthesis and uptake, and additional GCM upregulate ABC-G1 involved in cholesterol release. MGP and HO1 are the highest upregulated genes provoked by GCM treatment. The neuronal regulation of cholesterol synthesis and release as well as the upregulation of MGP and HO1 by GCM were confirmed on lipid and protein level and will be discussed in the following.

4.2.1 RGCs synthesize cholesterol and fatty acids, and regulate their homeostasis in reaction to external supply

The gene expression profile of RGCs showed that neurons express the complete enzymatic machinery for cholesterol and fatty acid synthesis. Further metabolic labeling emphasized the ability of RGCs to synthesize cholesterol and phosphatidylcholine. Treatment with GCM downregulated genes involved in both, cholesterol and fatty acid synthesis, whereas cholesterol treatment only affected genes of the cholesterol synthesis pathway. Lipid

labeling experiments showed that both, GCM and cholesterol drastically reduced the level of de novo synthesized neuronal cholesterol. In general, regulation of cholesterol biosynthesis takes place at the level of gene transcription, mRNA stability, translation, enzyme phosphorylation and enzyme degradation. Cellular cholesterol levels are also modulated by conversion of cholesterol to cholesteryl esters, bile acids and oxysterols (Liscum, 2002). The transcriptional regulation of lipid homeostasis in vertebrate cells is regulated by a family of membrane-bound transcription factors designated SREBPs (Horton et al., 2002). SREBPs are activated by proteolytical cleavage of membrane bound precursors regulated by a lipid sensing mechanism (Brown & Goldstein, 1997). They directly activate the expression of more than 30 genes dedicated to the synthesis and uptake of cholesterol, fatty acids, triglycerides, and phospholipids, as well as the NADPH cofactor required to synthesize these molecules (Brown & Goldstein, 1997; Horton & Shimomura, 1999; Sakakura et al., 2001). The mammalian genome encodes three SREBP isoforms, designated SREBP-1a, SREBP-1c, and SREBP-2 (Yokoyama et al., 1993; Hua et al., 1993). SREBP-1a is a potent activator of all SREBP-responsive genes, including those that mediate the synthesis of cholesterol, fatty acids, and triglycerides. The Steroidogenic acute regulatory protein, downregulated by GCM, was shown to be regulated by SREBP-1a mediated by sterol regulatory element (SRE) binding sites in its promoter region (Christenson et al., 2001; Shea-Eaton et al., 2001). SREBP-1c preferentially enhances transcription of genes required for fatty acid synthesis (Shimano et al., 1997). This regulation includes the genes for ATP citrate lyase, and fatty acid synthase, necessary to produce palmitate, fatty acid elongase, which converts palmitate to stearate, stearoyl-CoA desaturase, which converts stearate to oleate, and glycerol-3-phosphate acyltransferase, the first committed enzyme in triglyceride and phospholipid synthesis. All these genes were downregulated by GCM, indicating that SREBP-1c activity may be reduced by GCM. Both SREBP-1 splice variants have been shown to mediate the GCM and cholesterol caused downregulation of the LDL receptor by binding to an SRE-1 binding site in its promoter region (Yokoyama et al., 1993). SREBP-2, itself downregulated by GCM, preferentially controls cholesterol synthesis as shown for the entire pathway (Sakakura et al., 2001). My observation that GCM and cholesterol downregulated 15 genes involved in this pathway in a similar manner, suggested that glia derived cholesterol contained in GCM stopped SREBP-2 activation mediated by a cholesterol sensing mechanism (Brown & Goldstein, 1997). Finally, SREBP-1c and SREBP-2 activate three genes required to generate NADPH, which is consumed at multiple stages in these lipid biosynthetic pathways

(Horton et al., 2002). One of them is isocitrate dehydrogenase, which was downregulated by GCM.

The difference regarding gene expression of fatty acids synthesizing enzymes between GCM and cholesterol treatment is possibly caused by the fact that GCM also contains fatty acids, which may act on the SREBP-1c pathway and which are not supplied to cells treated with cholesterol alone. The difference between GCM and cholesterol treatment for neuronal cholesterol release, observed by pulse chase labeling, may be related to the same fact. Since cholesterol is water insoluble, released cholesterol needs to be taken up by, or released with a carrier. Physiologically, active cellular cholesterol release appears together with phosphatidylcholine release and is mediated by specific transporters like ABC-A1 and ABC-G1 (Zheng et al., 2001; Klucken et al., 2000; Schmitz et al., 2001). The latter was upregulated by GCM. The release of cholesterol from untreated RGCs seems to be unphysiological since only cholesterol is released, probably to BSA in the culture medium. Treatment of RGCs with GCM or cholesterol caused additional release of phosphatidylcholine. The higher cholesterol release by GCM compared to cholesterol treatment is probably related to lipoproteins contained in GCM, which mediate transporter dependent cholesterol uptake by apolipoproteins like A-1 (Wang et al., 2000 & 2001; Chambenoit et al., 2001; Ito et al., 2002). Another possibility was suggested by Sun et al. (2003) who showed that co-transfection of ABC-A1 with either stearoyl CoA desaturases 1 or 2, both downregulated by GCM but not by Cholesterol, inhibited ABC-A1-mediated cholesterol efflux but not phospholipid efflux in HEK 293 cells.

4.2.2 Dendritic localization of MGP and HO1

GCM and cholesterol enhanced the expression of several genes, but no overlap between these two groups was observed. Choosing the two most upregulated genes by GCM treatment, I confirmed the expression results on the protein level. Using immunostaining with specific antibodies, I detected a somatodendritic localization of MGP and HO1 in GCM treated microculture RGCs, whereas control cells showed only labeled somata. These findings suggested the specific upregulation of dendrite associated proteins and is a further hint for the observed glia-induced dendrite differentiation. MGP is a small matrix protein containing carboxyglutamic acid (GLA), initially isolated from bone and characterized by Price et al., (1985). It affects differentiation in developing cartilage and bone and has an effect on the mineralization in chondrocytes (Luo et al.,

1997; Yagami et al., 1999). Urist et al., (1984) found that MGP is tightly associated with bone morphogenetic protein (BMP) *in vitro* during protein purification and that strong denaturants are required to break the association. Using the multipotent mouse embryonic cell line C3H10T1/2 Boström et al., (2001) showed that MGP inhibits BMP-induced cell differentiation, by application of BMP2 on MGP transfected cells. Deletion of MGP by antisense transfection or cell preparation from MGP-deficient mice enhanced BMP2 induced differentiation. Together, these results suggest that MGP modulates BMP activity. Highly interesting, BMP-7, a glia-derived factor, promotes dendrite formation in sympathetic (Lein et al., 1995 & 2002) and different types of CNS neurons (Le Roux et al., 1999; Withers et al., 2000). This has also been shown for BMP-2, -5, and -6 at sympathetic neurons *in vitro* (Guo et al., 1998; Beck et al., 2001). My findings that MGP localized at RGC dendrites and was upregulated by GCM, which promotes dendrite differentiation, could be a hint for its involvement in BMP-regulated neuronal differentiation.

The second highly upregulated gene in response to GCM treatment was HO1. This enzyme cleaves the heme ring at the alpha methene bridge to form biliverdin, ferric iron and CO (Tenhunen et al., 1968). HO1 activity can be induced in almost all cell types by cellular stressors, including ultraviolet radiation, hydrogen peroxide, heavy metals, and arsenite, and has also been referred to as heat-shock protein 32 (HSP32) (Keyse & Tyrrell, 1989; Kothary & Candido, 1982) and p32 (Kageyama et al., 1988). Molecular cloning revealed three heme oxygenase genes, the highly inducible isoform HO1 (Shibahara et al., 1985) and two constitutive expressed isoforms termed HO2 (Rotenberg & Maines, 1990) and HO3 (McCoubrey et al., 1997). But the catalyzed reaction of all three enzymes is the same. Unlike HO1, HO2 is selectively concentrated in the brain and testes. Therefore the majority of studies concerning the brain had focused on HO2. I observed that HO1 and GluR2/3 were co-localized at dendrites, which opens the possibility for an involvement in neurotransmission. Recently, CO as one of the products formed by HO reaction has been shown to be involved in neurotransmission by activating the soluble guanylyl cyclase (sGC) (Verma et al., 1993; Zakhary et al., 1997). Interestingly, the GABA-B receptor 2, which is upregulated by GCM but not by cholesterol, could be involved in the regulation of HO activity. Several studies have suggested that metabotropic glutamate receptor (mGluR) activity regulates HO2 activity. Nathanson et al., (1995) found that exogenous CO and mGluR agonists both increase cGMP and Na⁺, K-ATPase activity in cerebellar slices, and mGluR agonists also enhance endogenous CO production. These effects are completely blocked by inhibitors of HO2 and protein kinase C (PKC) (which is activated by mGluR1).

Similarly, Dore et al., (1999), found activation of HO2 in response to phorbol ester treatment of hippocampal and cortical cultures, effects that are blocked by PKC inhibitors. HO2 is activated by glutamate in cerebral vascular endothelium (Parfenova et al. 2001). Glutamate, NMDA, and AMPA injections into mouse spinal cord stimulate cGMP production that is blocked by HO inhibitors and is absent in HO2 knockout animals (Li & Clark 2002). It has to be noted, however, that the HO inhibitors used in these studies (protoporphyrins substituted with metals other than iron) exhibit poor specificity and can directly inhibit sGC (Grundemar & Ny, 1997).

HO1 has also a neuroprotective role by producing an antioxidant precursor. Biliverdin formed by HO is rapidly reduced to bilirubin because of the high levels of biliverdin reductase in most tissues. Bilirubin is neuroprotective (Dore et al., 1999^a) and exerts this effect by redox cycling. Each molecule of bilirubin that acts as an antioxidant is thereby itself oxidized to biliverdin. The high tissue levels of biliverdin reductase immediately reduce the biliverdin back to bilirubin (Baranano & Snyder, 2001). In brain cultures of HO2^{-/-} mice neurotoxicity is markedly detectable (Dore et al., 1999^a). Augmented neurotoxicity is associated with a selective increase in apoptotic death and is reduced by HO2 transfection (Dore et al., 2000). HO2^{-/-} animals also display increased neuronal damage after middle cerebral artery occlusion (Dore et al., 1999^b). Moreover, HO1^{-/-} mice, which are notably debilitated and die when 3-4 months old, do not display augmented stroke damage.

V. SUMMARY

The interplay of neurons and glia cells is highly relevant for many aspects of nervous system development. One important phase is the formation of synapses. Previous studies had shown that soluble glia-derived factors enhance the formation and efficacy of synapses in cultured retinal ganglion cells (RGCs) (Nägler et al., 2001), and identified one of these factors as cholesterol (Mauch et al., 2001). The aim of my project was to investigate how cholesterol supports synapse formation and function and whether other glia derived factors are involved in synaptogenesis in cultured RGCs. In the second part, I was searching for neuronal target genes involved in glia-dependent postnatal differentiation of rat RGCs using GeneChip expression analysis.

Searching for the mechanism of glia- and cholesterol-induced synapse formation, I could show by immunostaining with pre- and postsynaptic markers that glia conditioned medium (GCM) and cholesterol enhanced the number of synapses slowly within several days of treatment. Cholesterol induced a smaller but significant increase in synapse number than GCM. Filipin staining, an indicator of the cholesterol content, revealed a ten-fold enhancement in neuritic cholesterol content within 72 hours of GCM and cholesterol treatment but with a strikingly different time course. This indicated that the increase in cholesterol content does not determine the rate of synaptogenesis. Immunostaining of dendrites using a MAP2 antibody revealed that GCM and cholesterol induced dendrite differentiation with a remarkably similar time course as the increase in synapse number. This indicated that dendrite differentiation, which involved a redistribution of MAP2 and GluR2/3 from the somata to dendrites, was the rate limiting step in glia-induced synaptogenesis. Interestingly, I also found that neighboring cells impede dendrite differentiation. Cholesterol was indispensable for dendrite differentiation but less efficient than GCM, which may explain the lower number of synapses in cholesterol- compared to GCM-treated RGCs. I found that glia-derived laminin containing the $\gamma 1$ chain together with cholesterol promoted dendrite differentiation to the same extent then GCM, suggesting that laminin act as dendrite promoting signal for RGCs. Furthermore, using electrophysiological recordings, I showed by removal of GCM and replacement with cholesterol, that cholesterol is essential for continuous synaptogenesis and for the stability of evoked transmitter release.

To detect neuronal genes whose expression is regulated by glia, I performed GeneChip analysis of GCM- and cholesterol-treated RGCs. My experiments revealed several genes whose level of expression changed under the influence of GCM and cholesterol.

Interestingly, there was very little overlap between the two groups except for genes involved in cholesterol biosynthesis and homeostasis. To test if the neuronal cholesterol synthesis was influenced by these changes I labeled new synthesized lipids, using a radioactive precursor. I observed that GCM and cholesterol treatment clearly down regulated the cholesterol synthesis in neurons, confirming this expression result. GCM highly up regulated the genes of matrix Gla protein and heme oxygenase 1, which could be confirmed on protein level. Immunostaining revealed that both proteins were located in the somatodendritic compartment.

Together, these results revealed new roles of cholesterol and laminin in neuronal differentiation and underline the importance of neuron-glia interactions during brain development.

ZUSAMMENFASSUNG

Für viele Prozesse bei der Entwicklung des Nervensystems ist die Interaktion von Neuronen und Gliazellen wichtig. Eine entscheidende Phase dabei ist die Bildung von Synapsen. Vorangegangene Studien haben gezeigt, dass von Gliazellen sezernierte Faktoren die Bildung und Effizienz von Synapsen in kultivierten retinalen Ganglienzellen (RGZ) erhöhen (Nägler et al., 2001). Einer dieser Faktoren wurde als Cholesterin identifiziert (Mauch et al., 2001). Ziel des ersten Teils meiner Arbeit war es, herauszufinden wie Cholesterin die Synapsenbildung in Kulturen von gereinigten RGZ unterstützt und ob weitere gliale Faktoren dabei involviert sind. Der zweite Teil meiner Arbeit diente der Identifizierung von neuronalen Genen, die bei der postnatalen Differenzierung von RGZ eine Rolle spielen und deren Expression durch Gliazellen beeinflusst wird.

Zur Untersuchung der Mechanismen der glia- und cholesterininduzierten Synapsenbildung führte ich zuerst Immunfärbungen mit pre- und postsynaptischen Markern durch. Ich konnte zeigen, dass Glia-konditioniertes Medium (GKM) und Cholesterin die Anzahl der Synapsen innerhalb von mehreren Tagen langsam erhöhen. Die Behandlung mit Cholesterin erzeugte eine signifikante Erhöhung der Synapsenzahl, die jedoch geringer ausfiel als bei GKM-behandelten Zellen. Anschließende Filipin-Färbungen, ein Indikator für den Cholesteringehalt, ergaben nach 72 Stunden GKM- oder Cholesterinbehandlung einen zehnfachen Cholesterinanstieg in RGZ Neuriten. Dieser wurde jedoch über einen deutlich verschiedenen Zeitverlauf erreicht, was den Anstieg des zellulären Cholesteringehalts als Ursache für die verzögerte Synapsenbildung ausschloss. Die Immunfärbung von Dendriten mit einem Antikörper gegen Map2 ergab, dass GKM und Cholesterin die Differenzierung von Dendriten auslösen, und zwar mit genau derselben zeitlichen Verzögerung wie bei der Synapsenbildung. Dieser Umstand zeigte, dass die Differenzierung von Dendriten die gliainduzierte Synapsenbildung verzögerte und ging einher mit der Umverteilung von Map2 und GluR2/3 vom Soma zu den Dendriten. Weitergehende Untersuchungen ergaben, dass Nachbarzellen die Dendritendifferenzierung behindern. Cholesterin war unentbehrlich für die Dendritendifferenzierung, aber von geringerer Wirkung als GKM, was die kleinere Anzahl der Synapsen bei Cholesterinbehandlung im Vergleich zur GKM-Behandlung erklären könnte. Weitere Untersuchungen ergaben, dass Laminin, welches in GKM enthalten ist, über seine $\gamma 1$ Untereinheit die Dendritendifferenzierung unterstützte und zusammen mit Cholesterin dieselbe Wirkung erzielte wie GKM. Diese Ergebnisse deuten darauf hin, dass Laminin bei RGZ als Signal für die

Dendritendifferenzierung wirkt. Mit Hilfe von elektrophysiologischen Messungen und der Wegnahme von GKM sowie dessen Ersatz durch Cholesterin, konnte ich zeigen das Cholesterin essentiell ist für die Fortdauer der Synapsenbildung und die Stabilität von evozierter Transmitter-Ausschüttung.

Um neuronale Gene, deren Expression durch Gliazellen reguliert wird, zu identifizieren, verglich ich die Expressionsmuster von unbehandelten RGZ mit denen von GKM- oder cholesterinbehandelten. Hierfür benutzte ich GeneChips. Diese Untersuchungen ergaben mehrere Gene, deren Expression sich unter dem Einfluss von GKM oder Cholesterin änderte. Interessanterweise gab es nur wenige Überschneidungen zwischen den beiden Gruppen, mit Ausnahme von Genen die Funktionen in der Cholesterinsynthese und Homeostase ausüben. Um zu untersuchen, ob die Veränderung der Genexpression die neuronale Cholesterinsynthese beeinflusst, markierte ich neu synthetisierte Lipide mit Hilfe eines radioaktiven Vorläufers. Die Ergebnisse bestätigten die Expressionsanalyse und zeigten, dass GKM und Cholesterin die Cholesterinsynthese in RGZ deutlich verringerten. Weiterhin ergab die Behandlung mit GKM eine Erhöhung der Expression des Matrix Gla Proteins und der Heme Oxygenase 1, was auf Proteinebene bestätigt wurde. Immunfärbungen lokalisierten beide Proteine in Somata und Dendriten.

Die Ergebnisse dieser Arbeit zeigten neue Funktionen für Cholesterin und Laminin bei der neuronalen Differenzierung auf und lieferten weitere Beweise für die Bedeutung der Interaktionen zwischen Neuronen und Gliazellen während der Entwicklung des Nervensystems.

RÉSUMÉ

Les interactions entre neurones et cellules gliales jouent un rôle essentiel au cours des diverses phases du développement du système nerveux et en particulier lors de la formation des synapses. Des études réalisées à partir de cultures pures de cellules ganglionnaires rétiniennes (CGR) ont pu ainsi établir que des facteurs gliaux solubles augmentent, pour ces neurones, le nombre de synapses et leur efficacité fonctionnelle (Näglér et al., 2001). De plus, elles ont permis d'identifier le cholestérol comme l'un de ces facteurs dérivé des glies (Mauch et al., 2001). Notre travail a eu pour but de déterminer d'une part comment le cholestérol peut induire la formation de synapses et accroître leur efficacité et d'identifier d'autres facteurs gliaux potentiellement impliqués dans la synaptogénèse des CGR. D'autre part, nous avons recherché par l'utilisation de GeneChips, les gènes cibles impliqués dans la différenciation post-natale des CGR de rat et dont l'expression est influencée par les facteurs dérivées des glies. Nos travaux sur les mécanismes mis en œuvre lors de la synaptogénèse ont permis de montrer, par immuno-marquage des structures pré et post-synaptiques, que le milieu conditionné de glie (MCG) ainsi que le cholestérol induisent une augmentation lente et progressive du nombre des synapses au cours de la durée du traitement. Pour le cholestérol, cette augmentation est plus faible quoique significative par rapport au traitement par le MCG. Après un traitement de 72 heures par le MCG ou le cholestérol, un marquage à la filipine permet la visualisation du cholestérol intracellulaire et montre une augmentation d'un facteur dix de la teneur en cholestérol des neurites. Cependant, il faut remarquer que la cinétique d'augmentation observée est très différente dans les deux cas. Ces résultats semblent indiquer que l'augmentation de la teneur interne en cholestérol ne détermine pas le taux de synaptogénèse. L'immunomarquage des dendrites à l'aide de l'anticorps MAP2 nous a permis d'établir que le MCG et le cholestérol induisent une différenciation dendritique selon une cinétique similaire à celle de l'augmentation du nombre de synapses. Ceci indique que la différenciation dendritique, impliquant une redistribution de MAP2 et du récepteur GluR2/3 du corps cellulaire vers les dendrites, constitue donc l'étape limitante du taux de synaptogénèse induite par la glie. Nous avons pu aussi montrer que la présence de cellules voisines limite la différenciation dendritique. Le cholestérol est indispensable pour la différenciation dendritique mais s'avère moins efficace que le MCG : ce résultat pourrait expliquer le plus faible nombre de synapses obtenues avec les CGR traitées avec le cholestérol comparativement à celles traitées avec le MCG. Nous avons pu établir que la

laminine dérivée des glies, contenant la chaîne $\gamma 1$, induit une différenciation dendritique comparable à celle obtenue à l'aide du MCG lorsqu'elle est associée au cholestérol: ce résultat suggère que la laminine constituerait un signal d'induction dendritique chez les CGR. De plus la mesure de l'activité électrophysiologique nous a permis de montrer, en remplaçant le MCG par le cholestérol, que ce dernier est essentiel pour maintenir la synaptogénèse et la libération des neurotransmetteurs dans la réponse évoquée.

Afin d'isoler les gènes dont l'expression serait régulée par les facteurs gliaux, nous avons réalisé des analyses par GeneChips de CGR traitées au MCG et au cholestérol. Ce travail a permis de mettre en évidence plusieurs gènes dont l'expression est ainsi modifiée par le MCG ou par le cholestérol. De façon surprenante très peu de gènes candidats se retrouvent à la fois dans les deux conditions de traitement, à l'exception des gènes impliqués dans la biosynthèse et l'homéostasie du cholestérol. Afin de déterminer si la biosynthèse neuronale du cholestérol était influencée par les modifications dans l'expression de ces gènes, nous avons marqué à l'aide de précurseurs radioactifs les lipides nouvellement synthétisés. Nous avons ainsi pu établir que le traitement au MCG comme au cholestérol diminue effectivement la synthèse du cholestérol dans les neurones, confirmant donc le travail portant sur l'expression des gènes neuronaux. Enfin le MCG accroît fortement l'expression des gènes codant pour l'expression de la protéine de la matrice Gla et l'hème oxygénase 1. Ce résultat a pu être confirmé au niveau de l'expression protéique: les marquages immunocytologiques ont en effet montré que ces deux protéines sont localisées dans le compartiment somatodendritique des CGR.

L'ensemble de notre travail révèle les rôles nouveaux que joueraient le cholestérol et la laminine au cours de la différenciation neuronale et souligne l'importance des interactions neurone-glie au cours du développement du système nerveux.

VI. REFERENCES

- Ahmari SE, Buchanan J, Smith SJ (2000) Assembly of presynaptic active zones from cytoplasmic transport packets. *Nat Neurosci* 3: 445-451.
- Angst BD, Marcozzi C, Magee AI (2001) The cadherin superfamily: diversity in form and function. *J Cell Sci* 114: 629-641.
- Aranda A, Pascual A (2001) Nuclear hormone receptors and gene expression. *Physiol Rev* 81: 1269-1304.
- Arroyo EJ, Scherer SS (2000) On the molecular architecture of myelinated fibers. *Histochem Cell Biol* 113: 1-18.
- Baptista CA, Hatten ME, Blazeski R, Mason CA (1994) Cell-cell interactions influence survival and differentiation of purified Purkinje cells in vitro. *Neuron* 12: 243-260.
- Baranano DE, Snyder SH (2001) Neural roles for heme oxygenase: contrasts to nitric oxide synthase. *Proc Natl Acad Sci U S A* 98: 10996-11002.
- Baron-Van Evercooren A, Kleinman HK, Ohno S, Marangos P, Schwartz JP, Dubois-Dalcq ME (1982) Nerve growth factor, laminin, and fibronectin promote neurite growth in human fetal sensory ganglia cultures. *J Neurosci Res* 8: 179-193.
- Barrantes FJ (1993) Structural-functional correlates of the nicotinic acetylcholine receptor and its lipid microenvironment. *FASEB J* 7: 1460-1467.
- Barres BA, Silverstein BE, Corey DP, Chun LLY (1988) Immunological, morphological, and electrophysiological variation among retinal ganglion cells purified by panning. *Neuron* 1: 791-803.
- Bastiaanse EM, Hold KM, Van der Laarse A (1997) The effect of membrane cholesterol content on ion transport processes in plasma membranes. *Cardiovasc Res* 33: 272-283.
- Bates CA, Meyer RL (1994) Differential effect of serum on laminin-dependent outgrowth of embryonic and adult mouse optic axons in vitro. *Exp Neurol* 125: 99-105.
- Bauch H, Stier H, Schlosshauer B (1998) Axonal versus dendritic outgrowth is differentially affected by radial glia in discrete layers of the retina. *J Neurosci* 18: 1774-1785.
- Baulieu EE (1998) Neurosteroids: a novel function of the brain. *Psychoneuroendocrinology* 23: 963-987.
- Beattie EC, Stellwagen D, Morishita W, Bresnahan JC, Ha BK, Von Zastrow M, Beattie MS, Malenka RC (2002) Control of synaptic strength by glial TNF α . *Science* 295: 2282-2285.
- Beck HN, Drahushuk K, Jacoby DB, Higgins D, Lein PJ (2001) Bone morphogenetic protein-5 (BMP-5) promotes dendritic growth in cultured sympathetic neurons. *BMC Neurosci* 2: 12.

- Belmonte KE, McKinnon LA, Nathanson NM (2000) Developmental expression of muscarinic acetylcholine receptors in chick retina: selective induction of M2 muscarinic receptor expression in ovo by a factor secreted by muller glial cells. *J Neurosci* 20: 8417-8425.
- Berghs S, Aggujaro D, Dirkx R, Jr., Maksimova E, Stabach P, Hermel JM, Zhang JP, Philbrick W, Slepnev V, Ort T, Solimena M (2000) betaIV spectrin, a new spectrin localized at axon initial segments and nodes of ranvier in the central and peripheral nervous system. *J Cell Biol* 151: 985-1002.
- Berling B, Wille H, Roll B, Mandelkow EM, Garner C, Mandelkow E (1994) Phosphorylation of microtubule-associated proteins MAP2a,b and MAP2c at Ser136 by proline-directed kinases in vivo and in vitro. *Eur J Cell Biol* 64: 120-130.
- Bhat MA (2003) Molecular organization of axo-glia junctions. *Curr Opin Neurobiol* 13: 552-559.
- Bhat MA, Rios JC, Lu Y, Garcia-Fresco GP, Ching W, St Martin M, Li J, Einheber S, Chesler M, Rosenbluth J, Salzer JL, Bellen HJ (2001) Axon-glia interactions and the domain organization of myelinated axons requires neurexin IV/Caspr/Paranodin. *Neuron* 30: 369-383.
- Blondel O, Collin C, McCarran WJ, Zhu S, Zamostiano R, Gozes I, Brenneman DE, McKay RD (2000) A glia-derived signal regulating neuronal differentiation. *J Neurosci* 20: 8012-8020.
- Boiko T, Rasband MN, Levinson SR, Caldwell JH, Mandel G, Trimmer JS, Matthews G (2001) Compact myelin dictates the differential targeting of two sodium channel isoforms in the same axon. *Neuron* 30: 91-104.
- Bostrom K, Tsao D, Shen S, Wang Y, Demer LL (2001) Matrix GLA protein modulates differentiation induced by bone morphogenetic protein-2 in C3H10T1/2 cells. *J Biol Chem* 276: 14044-14052.
- Boyle ME, Berglund EO, Murai KK, Weber L, Peles E, Ranscht B (2001) Contactin orchestrates assembly of the septate-like junctions at the paranode in myelinated peripheral nerve. *Neuron* 30: 385-397.
- Böse CM, Qiu D, Bergamaschi A, Gravante B, Bossi M, Villa A, Rupp F, Malgaroli A (2000) Agrin controls synaptic differentiation in hippocampal neurons. *J Neurosci* 20: 9086-9095.
- Breckenridge WC, Morgan IG, Zanetta JP, Vincendon G (1973) Adult rat brain synaptic vesicles. II. Lipid composition. *Biochim Biophys Acta* 320: 681-686.
- Brose K, Tessier-Lavigne M (2000) Slit proteins: key regulators of axon guidance, axonal branching, and cell migration. *Curr Opin Neurobiol* 10: 95-102.
- Brown DA, London E (1998) Functions of lipid rafts in biological membranes. *Annu Rev Cell Dev Biol* 14: 111-136.
- Brown MS, Goldstein JL (1986) A receptor-mediated pathway for cholesterol homeostasis. *Science* 232: 34-47.

- Brown MS, Goldstein JL (1997) The SREBP pathway: regulation of cholesterol metabolism by proteolysis of a membrane-bound transcription factor. *Cell* 89: 331-340.
- Bruses JL, Chauvet N, Rutishauser U (2001) Membrane lipid rafts are necessary for the maintenance of the (alpha)7 nicotinic acetylcholine receptor in somatic spines of ciliary neurons. *J Neurosci* 21: 504-512.
- Burger K, Gimpl G, Fahrenholz F (2000) Regulation of receptor function by cholesterol. *Cell Mol Life Sci* 57: 1577-1592.
- Burgeson RE, Chiquet M, Deutzmann R, Ekblom P, Engel J, Kleinman H, Martin GR, Meneguzzi G, Paulsson M, Sanes J (1994) A new nomenclature for the laminins. *Matrix Biol* 14: 209-211.
- Buttiglione M, Revest JM, Pavlou O, Karagogeos D, Furley A, Rougon G, Faivre-Sarrailh C (1998) A functional interaction between the neuronal adhesion molecules TAG-1 and F3 modulates neurite outgrowth and fasciculation of cerebellar granule cells. *J Neurosci* 18: 6853-6870.
- Canolle B, Masméjean F, Melon C, Nieoullon A, Pisano P, Lortet S (2004) Glial soluble factors regulate the activity and expression of the neuronal glutamate transporter EAAC1: implication of cholesterol. *J Neurochem* 88: 1521-1532.
- Chambenoit O, Hamon Y, Marguet D, Rigneault H, Rosseneu M, Chimini G (2001) Specific docking of apolipoprotein A-I at the cell surface requires a functional ABCA1 transporter. *J Biol Chem* 276: 9955-9960.
- Chamberlain LH, Burgoyne RD, Gould GW (2001) SNARE proteins are highly enriched in lipid rafts in PC12 cells: implications for the spatial control of exocytosis. *Proc Natl Acad Sci U S A* 98: 5619-5624.
- Charles P, Tait S, Faivre-Sarrailh C, Barbin G, Gunn-Moore F, Denisenko-Nehrbass N, Guennoc AM, Girault JA, Brophy PJ, Lubetzki C (2002) Neurofascin is a glial receptor for the paranodin/Caspr-contactin axonal complex at the axoglial junction. *Curr Biol* 12: 217-220.
- Christenson LK, Osborne TF, McAllister JM, Strauss JF, III (2001) Conditional response of the human steroidogenic acute regulatory protein gene promoter to sterol regulatory element binding protein-1a. *Endocrinology* 142: 28-36.
- Cohen J, Burne JF, Winter J, Bartlett P (1986) Retinal ganglion cells lose response to laminin with maturation. *Nature* 322: 465-467.
- Colello RJ, Guillery RW (1990) The early development of retinal ganglion cells with uncrossed axons in the mouse: retinal position and axonal course. *Development* 108: 515-523.
- Cooper NG, McLaughlin BJ (1984) The distribution of filipin-sterol complexes in photoreceptor synaptic membranes. *J Comp Neurol* 230: 437-443.
- Craig AM, Blackstone CD, Huganir RL, Banker G (1993) The distribution of glutamate receptors in cultured rat hippocampal neurons: postsynaptic clustering of AMPA-selective subunits. *Neuron* 10: 1055-1068.

- Crossin KL, Krushel LA (2000) Cellular signaling by neural cell adhesion molecules of the immunoglobulin superfamily. *Dev Dyn* 218: 260-279.
- Dani JW, Chernjavsky A, Smith SJ (1992) Neuronal activity triggers calcium waves in hippocampal astrocyte networks. *Neuron* 8: 429-440.
- Davis JQ, Lambert S, Bennett V (1996) Molecular composition of the node of Ranvier: identification of ankyrin-binding cell adhesion molecules neurofascin (mucin+/third FNIII domain-) and NrCAM at nodal axon segments. *J Cell Biol* 135: 1355-1367.
- Deiner MS, Kennedy TE, Fazeli A, Serafini T, Tessier-Lavigne M, Sretavan DW (1997) Netrin-1 and DCC mediate axon guidance locally at the optic disc: loss of function leads to optic nerve hypoplasia. *Neuron* 19: 575-589.
- DeMattos RB, Brendza RP, Heuser JE, Kierson M, Cirrito JR, Fryer J, Sullivan PM, Fagan AM, Han X, Holtzman DM (2001) Purification and characterization of astrocyte-secreted apolipoprotein E and J-containing lipoproteins from wild-type and human apoE transgenic mice. *Neurochem Int* 39: 415-425.
- Deutsch JW, Kelly RB (1981) Lipids of synaptic vesicles: relevance to the mechanism of membrane fusion. *Biochemistry* 20: 378-385.
- Dijkstra S, Bar PR, Gispen WH, Joosten EA (1999) Selective stimulation of dendrite outgrowth from identified corticospinal neurons by homotopic astrocytes. *Neuroscience* 92: 1331-1342.
- Dong LJ, Chung AE (1991) The expression of the genes for entactin, laminin A, laminin B1 and laminin B2 in murine lens morphogenesis and eye development. *Differentiation* 48: 157-172.
- Dore S, Goto S, Sampei K, Blackshaw S, Hester LD, Ingi T, Sawa A, Traystman RJ, Koehler RC, Snyder SH (2000) Heme oxygenase-2 acts to prevent neuronal death in brain cultures and following transient cerebral ischemia. *Neuroscience* 99: 587-592.
- Dore S, Sampei K, Goto S, Alkayed NJ, Guastella D, Blackshaw S, Gallagher M, Traystman RJ, Hurn PD, Koehler RC, Snyder SH (1999a) Heme oxygenase-2 is neuroprotective in cerebral ischemia. *Mol Med* 5: 656-663.
- Dore S, Takahashi M, Ferris CD, Zakhary R, Hester LD, Guastella D, Snyder SH (1999b) Bilirubin, formed by activation of heme oxygenase-2, protects neurons against oxidative stress injury. *Proc Natl Acad Sci U S A* 96: 2445-2450.
- Egea G, Marsal J, Solsona C, Rabasseda X, Blasi J (1989) Increase in reactive cholesterol in the presynaptic membrane of depolarized Torpedo synaptosomes: blockade by botulinum toxin type A. *Neuroscience* 31: 521-527.
- Einheber S, Zanazzi G, Ching W, Scherer S, Milner TA, Peles E, Salzer JL (1997) The axonal membrane protein Caspr, a homologue of neurexin IV, is a component of the septate-like paranodal junctions that assemble during myelination. *J Cell Biol* 139: 1495-1506.

- Erskine L, Williams SE, Brose K, Kidd T, Rachel RA, Goodman CS, Tessier-Lavigne M, Mason CA (2000) Retinal ganglion cell axon guidance in the mouse optic chiasm: expression and function of robo and slits. *J Neurosci* 20: 4975-4982.
- Eysel UT, Peichl L, Wässle H (1985) Dendritic plasticity in the early postnatal feline retina: quantitative characteristics and sensitive period. *J Comp Neurol* 242: 134-145.
- Faivre-Sarrailh C, Gauthier F, Denisenko-Nehrbass N, Le Bivic A, Rougon G, Girault JA (2000) The glycosylphosphatidyl inositol-anchored adhesion molecule F3/contactin is required for surface transport of paranodin/contactin-associated protein (caspr). *J Cell Biol* 149: 491-502.
- Fan QW, Yu W, Gong JS, Zou K, Sawamura N, Senda T, Yanagisawa K, Michikawa M (2002) Cholesterol-dependent modulation of dendrite outgrowth and microtubule stability in cultured neurons. *J Neurochem* 80: 178-190.
- Fields RD, Stevens-Graham B (2002) New insights into neuron-glia communication. *Science* 298: 556-562.
- Fricke C, Lee JS, Geiger-Rudolph S, Bonhoeffer F, Chien CB (2001) astray, a zebrafish roundabout homolog required for retinal axon guidance. *Science* 292: 507-510.
- Friedman HV, Bresler T, Garner CC, Ziv NE (2000) Assembly of new individual excitatory synapses: time course and temporal order of synaptic molecule recruitment. *Neuron* 27: 57-69.
- Gao FB, Bogert BA (2003) Genetic control of dendritic morphogenesis in *Drosophila*. *Trends Neurosci* 26: 262-268.
- Garcia-Abreu J, Moura N, V, Carvalho SL, Cavalcante LA (1995) Regionally specific properties of midbrain glia: I. Interactions with midbrain neurons. *J Neurosci Res* 40: 471-477.
- Gazzaley AH, Weiland NG, McEwen BS, Morrison JH (1996) Differential regulation of NMDAR1 mRNA and protein by estradiol in the rat hippocampus. *J Neurosci* 16: 6830-6838.
- Girault JA, Peles E (2002) Development of nodes of Ranvier. *Curr Opin Neurobiol* 12: 476-485.
- Godement P, Salaun J, Mason CA (1990) Retinal axon pathfinding in the optic chiasm: divergence of crossed and uncrossed fibers. *Neuron* 5: 173-186.
- Goldberg JL, Klassen MP, Hua Y, Barres BA (2002) Amacrine-signaled loss of intrinsic axon growth ability by retinal ganglion cells. *Science* 296: 1860-1864.
- Gomes FC, Maia CG, de Menezes JR, Neto VM (1999) Cerebellar astrocytes treated by thyroid hormone modulate neuronal proliferation. *GLIA* 25: 247-255.
- Gomes FC, Spohr TC, Martinez R, Moura N, V (2001) Cross-talk between neurons and glia: highlights on soluble factors. *Braz J Med Biol Res* 34: 611-620.

- Gomperts SN, Carroll R, Malenka RC, Nicoll RA (2000) Distinct roles for ionotropic and metabotropic glutamate receptors in the maturation of excitatory synapses. *J Neurosci* 20: 2229-2237.
- Goritz C, Mauch DH, Nagler K, Pfrieger FW (2002) Role of glia-derived cholesterol in synaptogenesis: new revelations in the synapse-glia affair. *J Physiol Paris* 96: 257-263.
- Gozes I, Brenneman DE (2000) A new concept in the pharmacology of neuroprotection. *J Mol Neurosci* 14: 61-68.
- Grundemar L, Ny L (1997) Pitfalls using metalloporphyrins in carbon monoxide research. *Trends Pharmacol Sci* 18: 193-195.
- Guo X, Rueger D, Higgins D (1998) Osteogenic protein-1 and related bone morphogenetic proteins regulate dendritic growth and the expression of microtubule-associated protein-2 in rat sympathetic neurons. *Neurosci Lett* 245: 131-134.
- Hall DE, Neugebauer KM, Reichardt LF (1987) Embryonic neural retinal cell response to extracellular matrix proteins: developmental changes and effects of the cell substratum attachment antibody (CSAT). *J Cell Biol* 104: 623-634.
- Hannah MJ, Schmidt AA, Huttner WB (1999) Synaptic vesicle biogenesis. *Annu Rev Cell Dev Biol* 15: 733-798.
- Hara A, Radin NS (1978) Lipid extraction of tissues with a low-toxicity solvent. *Anal Biochem* 90: 420-426.
- Harder T, Scheiffele P, Verkade P, Simons K (1998) Lipid domain structure of the plasma membrane revealed by patching of membrane components. *J Cell Biol* 141: 929-942.
- Harris R, Sabatelli LM, Seeger MA (1996) Guidance cues at the *Drosophila* CNS midline: identification and characterization of two *Drosophila* Netrin/UNC-6 homologs. *Neuron* 17: 217-228.
- Hartley RS, Margulis M, Fishman PS, Lee VM, Tang CM (1999) Functional synapses are formed between human NTera2 (NT2N, hNT) neurons grown on astrocytes. *J Comp Neurol* 407: 1-10.
- Hayashi H, Igbavboa U, Hamanaka H, Kobayashi M, Fujita SC, Wood WG, Yanagisawa K (2002) Cholesterol is increased in the exofacial leaflet of synaptic plasma membranes of human apolipoprotein E4 knock-in mice. *Neuroreport* 13: 383-386.
- He Q, Meiri KF (2002) Isolation and characterization of detergent-resistant microdomains responsive to NCAM-mediated signaling from growth cones. *Mol Cell Neurosci* 19: 18-31.
- Higgins D, Burack M, Lein P, Banker G (1997) Mechanisms of neuronal polarity. *Curr Opin Neurobiol* 7: 599-604.
- Hopkins JM, Ford-Holevinski TS, McCoy JP, Agranoff BW (1985) Laminin and optic nerve regeneration in the goldfish. *J Neurosci* 5: 3030-3038.
- Horton AC, Ehlers MD (2004) Secretory trafficking in neuronal dendrites. *Nat Cell Biol* 6: 585-591.

- Horton JD, Goldstein JL, Brown MS (2002) SREBPs: activators of the complete program of cholesterol and fatty acid synthesis in the liver. *J Clin Invest* 109: 1125-1131.
- Horton JD, Shimomura I (1999) Sterol regulatory element-binding proteins: activators of cholesterol and fatty acid biosynthesis. *Curr Opin Lipidol* 10: 143-150.
- Hua X, Yokoyama C, Wu J, Briggs MR, Brown MS, Goldstein JL, Wang X (1993) SREBP-2, a second basic-helix-loop-helix-leucine zipper protein that stimulates transcription by binding to a sterol regulatory element. *Proc Natl Acad Sci U S A* 90: 11603-11607.
- Igbavboa U, Avdulov NA, Chochina SV, Wood WG (1997) Transbilayer distribution of cholesterol is modified in brain synaptic plasma membranes of knockout mice deficient in the low-density lipoprotein receptor, apolipoprotein E, or both proteins. *J Neurochem* 69: 1661-1667.
- Igbavboa U, Avdulov NA, Schroeder F, Wood WG (1996) Increasing age alters transbilayer fluidity and cholesterol asymmetry in synaptic plasma membranes of mice. *J Neurochem* 66: 1717-1725.
- Ikonen E (2001) Roles of lipid rafts in membrane transport. *Curr Opin Cell Biol* 13: 470-477.
- Isom LL (2002) The role of sodium channels in cell adhesion. *Front Biosci* 7: 12-23.
- Ito J, Nagayasu Y, Kato K, Sato R, Yokoyama S (2002) Apolipoprotein A-I induces translocation of cholesterol, phospholipid, and caveolin-1 to cytosol in rat astrocytes. *J Biol Chem* 277: 7929-7935.
- Ivins JK, Colognato H, Kreidberg JA, Yurchenco PD, Lander AD (1998) Neuronal receptors mediating responses to antibody-activated laminin-1. *J Neurosci* 18: 9703-9715.
- Jacobson M (1991) *Developmental Neurobiology*. New York: Plenum Press.
- Jan YN, Jan LY (2003) The control of dendrite development. *Neuron* 40: 229-242.
- Kageyama H, Hiwasa T, Tokunaga K, Sakiyama S (1988) Isolation and characterization of a complementary DNA clone for a Mr 32,000 protein which is induced with tumor promoters in BALB/c 3T3 cells. *Cancer Res* 48: 4795-4798.
- Kaplan MR, Cho MH, Ullian EM, Isom LL, Levinson SR, Barres BA (2001) Differential control of clustering of the sodium channels Na(v)1.2 and Na(v)1.6 at developing CNS nodes of Ranvier. *Neuron* 30: 105-119.
- Kaplan MR, Meyer-Franke A, Lambert S, Bennett V, Duncan ID, Levinson SR, Barres BA (1997) Induction of sodium channel clustering by oligodendrocytes. *Nature* 386: 724-728.
- Kaprielian Z, Runko E, Imondi R (2001) Axon guidance at the midline choice point. *Dev Dyn* 221: 154-181.
- Kaur C, Hao AJ, Wu CH, Ling EA (2001) Origin of microglia. *Microsc Res Tech* 54: 2-9.

- Keith CH, Wilson MT (2001) Factors controlling axonal and dendritic arbors. *Int Rev Cytol* 205: 77-147.
- Kelly MJ, Wagner EJ (1999) Estrogen Modulation of G-protein-coupled Receptors. *Trends Endocrinol Metab* 10: 369-374.
- Keyse SM, Tyrrell RM (1989) Heme oxygenase is the major 32-kDa stress protein induced in human skin fibroblasts by UVA radiation, hydrogen peroxide, and sodium arsenite. *Proc Natl Acad Sci U S A* 86: 99-103.
- Kidd T, Bland KS, Goodman CS (1999) Slit is the midline repellent for the robo receptor in *Drosophila*. *Cell* 96: 785-794.
- Kidd T, Brose K, Mitchell KJ, Fetter RD, Tessier-Lavigne M, Goodman CS, Tear G (1998) Roundabout controls axon crossing of the CNS midline and defines a novel subfamily of evolutionarily conserved guidance receptors. *Cell* 92: 205-215.
- Klopfenstein DR, Tomishige M, Stuurman N, Vale RD (2002) Role of phosphatidylinositol(4,5)bisphosphate organization in membrane transport by the Unc104 kinesin motor. *Cell* 109: 347-358.
- Klucken J, Buchler C, Orso E, Kaminski WE, Porsch-Ozcurumez M, Liebisch G, Kapinsky M, Diederich W, Drobnik W, Dean M, Allikmets R, Schmitz G (2000) ABCG1 (ABC8), the human homolog of the *Drosophila* white gene, is a regulator of macrophage cholesterol and phospholipid transport. *Proc Natl Acad Sci U S A* 97: 817-822.
- Ko CP, Propst JW (1986) Absence of sterol-specific complexes at active zones of degenerating and regenerating frog neuromuscular junctions. *J Neurocytol* 15: 231-240.
- Koch M, Murrell JR, Hunter DD, Olson PF, Jin W, Keene DR, Brunken WJ, Burgeson RE (2000) A novel member of the netrin family, beta-netrin, shares homology with the beta chain of laminin: identification, expression, and functional characterization. *J Cell Biol* 151: 221-234.
- Komada M, Soriano P (2002) [Beta]IV-spectrin regulates sodium channel clustering through ankyrin-G at axon initial segments and nodes of Ranvier. *J Cell Biol* 156: 337-348.
- Kordeli E, Lambert S, Bennett V (1995) AnkyrinG. A new ankyrin gene with neural-specific isoforms localized at the axonal initial segment and node of Ranvier. *J Biol Chem* 270: 2352-2359.
- Koroll M, Rathjen FG, Volkmer H (2001) The neural cell recognition molecule neurofascin interacts with syntenin-1 but not with syntenin-2, both of which reveal self-associating activity. *J Biol Chem* 276: 10646-10654.
- Kothary RK, Candido EP (1982) Induction of a novel set of polypeptides by heat shock or sodium arsenite in cultured cells of rainbow trout, *Salmo gairdnerii*. *Can J Biochem* 60: 347-355.
- LaDu MJ, Gilligan SM, Lukens JR, Cabana VG, Reardon CA, Van Eldik LJ, Holtzman DM (1998) Nascent astrocyte particles differ from lipoproteins in CSF. *J Neurochem* 70: 2070-2081.

- Laemmli UK (1970) Cleavage of structural proteins during the assembly of the head of bacteriophage T4. *Nature* 227: 680-685.
- Lang DM, Lommel S, Jung M, Ankerhold R, Petrusch B, Laessing U, Wiechers MF, Plattner H, Stuermer CA (1998) Identification of reggie-1 and reggie-2 as plasmamembrane-associated proteins which cocluster with activated GPI-anchored cell adhesion molecules in non-caveolar micropatches in neurons. *J Neurobiol* 37: 502-523.
- Lang T, Bruns D, Wenzel D, Riedel D, Holroyd P, Thiele C, Jahn R (2001) SNAREs are concentrated in cholesterol-dependent clusters that define docking and fusion sites for exocytosis. *EMBO J* 20: 2202-2213.
- Le Roux P, Behar S, Higgins D, Charette M (1999) OP-1 enhances dendritic growth from cerebral cortical neurons in vitro. *Exp Neurol* 160: 151-163.
- Le Roux PD, Esquenazi S (2002) Astrocytes mediate cerebral cortical neuronal axon and dendrite growth, in part, by release of fibroblast growth factor. *Neurol Res* 24: 81-92.
- Le Roux PD, Reh TA (1994) Regional differences in glial-derived factors that promote dendritic outgrowth from mouse cortical neurons in vitro. *J Neurosci* 14: 4639-4655.
- Lein PJ, Beck HN, Chandrasekaran V, Gallagher PJ, Chen HL, Lin Y, Guo X, Kaplan PL, Tiedge H, Higgins D (2002) Glia induce dendritic growth in cultured sympathetic neurons by modulating the balance between bone morphogenetic proteins (BMPs) and BMP antagonists. *J Neurosci* 22: 10377-10387.
- Lein PJ, Johnson M, Guo X, Rueger D, Higgins D (1995) Osteogenic protein-1 induces dendritic growth in rat sympathetic neurons. *Neuron* 15: 597-605.
- Leitinger B, Hogg N (2002) The involvement of lipid rafts in the regulation of integrin function. *J Cell Sci* 115: 963-972.
- Lesuisse C, Qiu D, Bose CM, Nakaso K, Rupp F (2000) Regulation of agrin expression in hippocampal neurons by cell contact and electrical activity. *Brain Res Mol Brain Res* 81: 92-100.
- Levin ER (1999) Cellular Functions of the Plasma Membrane Estrogen Receptor. *Trends Endocrinol Metab* 10: 374-377.
- Li X, Clark JD (2002) Spinal cord heme oxygenase participates in glutamate-induced pain-related behaviors. *Eur J Pharmacol* 450: 43-48.
- Li YX, Schaffner AE, Barker JL (1999) Astrocytes regulate the developmental appearance of GABAergic and glutamatergic postsynaptic currents in cultured embryonic rat spinal neurons. *Eur J Neurosci* 11: 2537-2551.
- Libby RT, Champlaud MF, Claudepierre T, Xu Y, Gibbons EP, Koch M, Burgeson RE, Hunter DD, Brunken WJ (2000) Laminin expression in adult and developing retinae: evidence of two novel CNS laminins. *J Neurosci* 20: 6517-6528.
- Libersat F, Duch C (2004) Mechanisms of dendritic maturation. *Mol Neurobiol* 29: 303-320.

- Liesi P, Dahl D, Vaheri A (1983) Laminin is produced by early rat astrocytes in primary culture. *J Cell Biol* 96: 920-924.
- Liesi P, Narvanen A, Soos J, Sariola H, Snounou G (1989) Identification of a neurite outgrowth-promoting domain of laminin using synthetic peptides. *FEBS Lett* 244: 141-148.
- Lim DA, Alvarez-Buylla A (1999) Interaction between astrocytes and adult subventricular zone precursors stimulates neurogenesis. *Proc Natl Acad Sci U S A* 96: 7526-7531.
- Lin W, Sanchez HB, Deerinck T, Morris JK, Ellisman M, Lee KF (2000) Aberrant development of motor axons and neuromuscular synapses in erbB2-deficient mice. *Proc Natl Acad Sci U S A* 97: 1299-1304.
- Luckenbill-Edds L (1997) Laminin and the mechanism of neuronal outgrowth. *Brain Res Brain Res Rev* 23: 1-27.
- Lund RD, Lund JS (1972) Development of synaptic patterns in the superior colliculus of the rat. *Brain Res* 42: 1-20.
- Luo G, D'Souza R, Hogue D, Karsenty G (1995) The matrix Gla protein gene is a marker of the chondrogenesis cell lineage during mouse development. *J Bone Miner Res* 10: 325-334.
- Majewska MD, Harrison NL, Schwartz RD, Barker JL, Paul SM (1986) Steroid hormone metabolites are barbiturate-like modulators of the GABA receptor. *Science* 232: 1004-1007.
- Mangold HK, Malis C (1960) Fraction of fats, oils and waxes on thin layers of silicic acid. *J Am Oil Chem Soc* 37: 383-385
- Manthorpe M, Engvall E, Ruoslahti E, Longo FM, Davis GE, Varon S (1983) Laminin promotes neuritic regeneration from cultured peripheral and central neurons. *J Cell Biol* 97: 1882-1890.
- Marcus RC, Blazeski R, Godement P, Mason CA (1995) Retinal axon divergence in the optic chiasm: uncrossed axons diverge from crossed axons within a midline glial specialization. *J Neurosci* 15: 3716-3729.
- Marcus RC, Mason CA (1995) The first retinal axon growth in the mouse optic chiasm: axon patterning and the cellular environment. *J Neurosci* 15: 6389-6402.
- Maslim J, Webster M, Stone J (1986) Stages in the structural differentiation of retinal ganglion cells. *J Comp Neurol* 254: 382-402.
- Mathis C, Hindelang C, LeMeur M, Borrelli E (2000) A transgenic mouse model for inducible and reversible dysmyelination. *J Neurosci* 20: 7698-7705.
- Mauch DH, Nägler K, Schumacher S, Göritz C, Müller EC, Otto A, Pfrieder FW (2001) CNS synaptogenesis promoted by glia-derived cholesterol. *Science* 294: 1354-1357.
- McCarthy KD, de Vellis J (1980) Preparation of separate astroglial and oligodendroglial cell cultures from rat cerebral cortex. *J Cell Biol* 85: 890-902.

- McCoubrey WK, Jr., Huang TJ, Maines MD (1997) Isolation and characterization of a cDNA from the rat brain that encodes hemoprotein heme oxygenase-3. *Eur J Biochem* 247: 725-732.
- McEwen B, Akama K, Alves S, Brake WG, Bulloch K, Lee S, Li C, Yuen G, Milner TA (2001) Tracking the estrogen receptor in neurons: implications for estrogen-induced synapse formation. *Proc Natl Acad Sci U S A* 98: 7093-7100.
- Menegoz M, Gaspar P, Le Bert M, Galvez T, Burgaya F, Palfrey C, Ezan P, Arnos F, Girault JA (1997) Paranodin, a glycoprotein of neuronal paranodal membranes. *Neuron* 19: 319-331.
- Meyer-Franke A, Kaplan MR, Pfrieger FW, Barres BA (1995) Characterization of the signaling interactions that promote the survival and growth of developing retinal ganglion cells in culture. *Neuron* 15: 805-819.
- Miller FD, Kaplan DR (2003) Signaling mechanisms underlying dendrite formation. *Curr Opin Neurobiol* 13: 391-398.
- Milner TA, McEwen BS, Hayashi S, Li CJ, Reagan LP, Alves SE (2001) Ultrastructural evidence that hippocampal alpha estrogen receptors are located at extranuclear sites. *J Comp Neurol* 429: 355-371.
- Mitchell KJ, Doyle JL, Serafini T, Kennedy TE, Tessier-Lavigne M, Goodman CS, Dickson BJ (1996) Genetic analysis of Netrin genes in *Drosophila*: Netrins guide CNS commissural axons and peripheral motor axons. *Neuron* 17: 203-215.
- Mitter D, Reisinger C, Hinz B, Hollmann S, Yelamanchili SV, Treiber-Held S, Ohm TG, Herrmann A, Ahnert-Hilger G (2003) The synaptophysin/synaptobrevin interaction critically depends on the cholesterol content. *J Neurochem* 84: 35-42.
- Monnet FP, Mahe V, Robel P, Baulieu EE (1995) Neurosteroids, via sigma receptors, modulate the [3H]norepinephrine release evoked by N-methyl-D-aspartate in the rat hippocampus. *Proc Natl Acad Sci U S A* 92: 3774-3778.
- Muller CP, Stephany DA, Winkler DF, Hoeg JM, Demosky SJ, Jr., Wunderlich JR (1984) Filipin as a flow microfluorometry probe for cellular cholesterol. *Cytometry* 5: 42-54.
- Murphy DD, Segal M (1996) Regulation of dendritic spine density in cultured rat hippocampal neurons by steroid hormones. *J Neurosci* 16: 4059-4068.
- Nadarajah B, Parnavelas JG (2002) Modes of neuronal migration in the developing cerebral cortex. *Nat Rev Neurosci* 3: 423-432.
- Nagler K, Mauch DH, Pfrieger FW (2001) Glia-derived signals induce synapse formation in neurones of the rat central nervous system. *J Physiol* 533: 665-679.
- Nagy A, Baker RR, Morris SJ, Whittaker VP (1976) The preparation and characterization of synaptic vesicles of high purity. *Brain Res* 109: 285-309.
- Nakajima Y, Bridgman PC (1981) Absence of filipin-sterol complexes from the membranes of active zones and acetylcholine receptor aggregates at frog neuromuscular junctions. *J Cell Biol* 88: 453-458.

- Nathanson JA, Scavone C, Scanlon C, McKee M (1995) The cellular Na⁺ pump as a site of action for carbon monoxide and glutamate: a mechanism for long-term modulation of cellular activity. *Neuron* 14: 781-794.
- Niethammer P, Delling M, Sytnyk V, Dityatev A, Fukami K, Schachner M (2002) Cosignaling of NCAM via lipid rafts and the FGF receptor is required for neuritogenesis. *J Cell Biol* 157: 521-532.
- Norman AW, Demel RA, de Kruyff B, van Deenen LL (1972) Studies on the biological properties of polyene antibiotics. Evidence for the direct interaction of filipin with cholesterol. *J Biol Chem* 247: 1918-1929.
- Ohara-Imaizumi M, Nishiwaki C, Kikuta T, Kumakura K, Nakamichi Y, Nagamatsu S (2004) Site of docking and fusion of insulin secretory granules in live MIN6 beta cells analyzed by TAT-conjugated anti-syntaxin 1 antibody and total internal reflection fluorescence microscopy. *J Biol Chem* 279: 8403-8408.
- Oram JF (1986) Receptor-mediated transport of cholesterol between cultured cells and high-density lipoproteins. *Methods Enzymol* 129: 645-659.
- Paratcha G, Ibanez CF (2002) Lipid rafts and the control of neurotrophic factor signaling in the nervous system: variations on a theme. *Curr Opin Neurobiol* 12: 542-549.
- Parfenova H, Neff RA, III, Alonso JS, Shlopov BV, Jamal CN, Sarkisova SA, Leffler CW (2001) Cerebral vascular endothelial heme oxygenase: expression, localization, and activation by glutamate. *Am J Physiol Cell Physiol* 281: C1954-C1963.
- Parnavelas JG, Luder R, Pollard SG, Sullivan K, Lieberman AR (1983) A qualitative and quantitative ultrastructural study of glial cells in the developing visual cortex of the rat. *Philos Trans R Soc Lond B Biol Sci* 301: 55-84.
- Patton BL (2000) Laminins of the neuromuscular system. *Microsc Res Tech* 51: 247-261.
- Peng HB, Yang JF, Dai Z, Lee CW, Hung HW, Feng ZH, Ko CP (2003) Differential effects of neurotrophins and schwann cell-derived signals on neuronal survival/growth and synaptogenesis. *J Neurosci* 23: 5050-5060.
- Perry VH, Linden R (1982) Evidence for dendritic competition in the developing retina. *Nature* 297: 683-685.
- Pfriegeer FW (2003a) Cholesterol homeostasis and function in neurons of the central nervous system. *Cell Mol Life Sci* 60: 1158-1171.
- Pfriegeer FW (2003b) Role of cholesterol in synapse formation and function. *Biochim Biophys Acta* 1610: 271-280.
- Pfriegeer FW, Barres BA (1996) New views on synapse-glia interactions. *Curr Opin Neurobiol* 6: 615-621.
- Pfriegeer FW, Barres BA (1997) Synaptic efficacy enhanced by glial cells in vitro. *Science* 277: 1684-1687.

- Plump AS, Erskine L, Sabatier C, Brose K, Epstein CJ, Goodman CS, Mason CA, Tessier-Lavigne M (2002) Slit1 and Slit2 cooperate to prevent premature midline crossing of retinal axons in the mouse visual system. *Neuron* 33: 219-232.
- Porter JT, McCarthy KD (1996) Hippocampal astrocytes in situ respond to glutamate released from synaptic terminals. *J Neurosci* 16: 5073-5081.
- Powell SK, Kleinman HK (1997) Neuronal laminins and their cellular receptors. *Int J Biochem Cell Biol* 29: 401-414.
- Price PA, Williamson MK (1985) Primary structure of bovine matrix Gla protein, a new vitamin K-dependent bone protein. *J Biol Chem* 260: 14971-14975.
- Rakic P, Bourgeois JP, Eckenhoff MF, Zecevic N, Goldman-Rakic PS (1986) Concurrent overproduction of synapses in diverse regions of the primate cerebral cortex. *Science* 232: 232-235.
- Rasband K, Hardy M, Chien CB (2003) Generating X: formation of the optic chiasm. *Neuron* 39: 885-888.
- Reddy LV, Koirala S, Sugiura Y, Herrera AA, Ko CP (2003) Glial cells maintain synaptic structure and function and promote development of the neuromuscular junction in vivo. *Neuron* 40: 563-580.
- Reese BE, Maynard TM, Hocking DR (1994) Glial domains and axonal reordering in the chiasmatic region of the developing ferret. *J Comp Neurol* 349: 303-324.
- Rios JC, Melendez-Vasquez CV, Einheber S, Lustig M, Grumet M, Hemperly J, Peles E, Salzer JL (2000) Contactin-associated protein (Caspr) and contactin form a complex that is targeted to the paranodal junctions during myelination. *J Neurosci* 20: 8354-8364.
- Rios JC, Rubin M, St Martin M, Downey RT, Einheber S, Rosenbluth J, Levinson SR, Bhat M, Salzer JL (2003) Paranodal interactions regulate expression of sodium channel subtypes and provide a diffusion barrier for the node of Ranvier. *J Neurosci* 23: 7001-7011.
- Rochon D, Rousse I, Robitaille R (2001) Synapse-glia interactions at the mammalian neuromuscular junction. *J Neurosci* 21: 3819-3829.
- Rogers SL, Letourneau PC, Palm SL, McCarthy J, Furcht LT (1983) Neurite extension by peripheral and central nervous system neurons in response to substratum-bound fibronectin and laminin. *Dev Biol* 98: 212-220.
- Rosenbluth J (1999) A brief history of myelinated nerve fibers: one hundred and fifty years of controversy. *J Neurocytol* 28: 251-262.
- Rotenberg MO, Maines MD (1990) Isolation, characterization, and expression in *Escherichia coli* of a cDNA encoding rat heme oxygenase-2. *J Biol Chem* 265: 7501-7506.
- Sakakura Y, Shimano H, Sone H, Takahashi A, Inoue N, Toyoshima H, Suzuki S, Yamada N (2001) Sterol regulatory element-binding proteins induce an entire pathway of cholesterol synthesis. *Biochem Biophys Res Commun* 286: 176-183.

- Sakamoto H, Ukena K, Tsutsui K (2001) Effects of progesterone synthesized de novo in the developing Purkinje cell on its dendritic growth and synaptogenesis. *J Neurosci* 21: 6221-6232.
- Sanes JR, Lichtman JW (1999) Development of the vertebrate neuromuscular junction. *Annu Rev Neurosci* 22: 389-442.
- Scherer SS, Arroyo EJ (2002) Recent progress on the molecular organization of myelinated axons. *J Peripher Nerv Syst* 7: 1-12.
- Schmitz G, Langmann T, Heimerl S (2001) Role of ABCG1 and other ABCG family members in lipid metabolism. *J Lipid Res* 42: 1513-1520.
- Schmitz G, Orso E (2001) Intracellular cholesterol and phospholipid trafficking: comparable mechanisms in macrophages and neuronal cells. *Neurochem Res* 26: 1045-1068.
- Scott EK, Luo L (2001) How do dendrites take their shape? *Nat Neurosci* 4: 359-365.
- Seil FJ (1998) The extracellular matrix molecule, laminin, induces purkinje cell dendritic spine proliferation in granule cell depleted cerebellar cultures. *Brain Res* 795: 112-120.
- Selak I, Foidart JM, Moonen G (1985) Laminin promotes cerebellar granule cells migration in vitro and is synthesized by cultured astrocytes. *Dev Neurosci* 7: 278-285.
- Sephel GC, Tashiro KI, Sasaki M, Greatorex D, Martin GR, Yamada Y, Kleinman HK (1989) Laminin A chain synthetic peptide which supports neurite outgrowth. *Biochem Biophys Res Commun* 162: 821-829.
- Serafini T, Colamarino SA, Leonardo ED, Wang H, Beddington R, Skarnes WC, Tessier-Lavigne M (1996) Netrin-1 is required for commissural axon guidance in the developing vertebrate nervous system. *Cell* 87: 1001-1014.
- Sernagor E, Eglén SJ, Wong RO (2001) Development of retinal ganglion cell structure and function. *Prog Retin Eye Res* 20: 139-174.
- Severs NJ, Robenek H (1983) Detection of microdomains in biomembranes. An appraisal of recent developments in freeze-fracture cytochemistry. *Biochim Biophys Acta* 737: 373-408.
- Shea-Eaton WK, Trinidad MJ, Lopez D, Nackley A, McLean MP (2001) Sterol regulatory element binding protein-1a regulation of the steroidogenic acute regulatory protein gene. *Endocrinology* 142: 1525-1533.
- Shibahara S, Muller R, Taguchi H, Yoshida T (1985) Cloning and expression of cDNA for rat heme oxygenase. *Proc Natl Acad Sci U S A* 82: 7865-7869.
- Shimano H, Horton JD, Shimomura I, Hammer RE, Brown MS, Goldstein JL (1997) Isoform 1c of sterol regulatory element binding protein is less active than isoform 1a in livers of transgenic mice and in cultured cells. *J Clin Invest* 99: 846-854.

- Simoncini T, Hafezi-Moghadam A, Brazil DP, Ley K, Chin WW, Liao JK (2000) Interaction of oestrogen receptor with the regulatory subunit of phosphatidylinositol-3-OH kinase. *Nature* 407: 538-541.
- Simons K, Ikonen E (1997) Functional rafts in cell membranes. *Nature* 387: 569-572.
- Simons K, Toomre D (2000) Lipid rafts and signal transduction. *Nat Rev Mol Cell Biol* 1: 31-39.
- Skoff RP (1990) Gliogenesis in rat optic nerve: astrocytes are generated in a single wave before oligodendrocytes. *Dev Biol* 139: 149-168.
- Slezak M, Pfrieder FW (2003) New roles for astrocytes: regulation of CNS synaptogenesis. *Trends Neurosci* 26: 531-535.
- Smalheiser NR, Crain SM, Reid LM (1984) Laminin as a substrate for retinal axons in vitro. *Brain Res* 314: 136-140.
- Song HJ, Stevens CF, Gage FH (2002) Neural stem cells from adult hippocampus develop essential properties of functional CNS neurons. *Nat Neurosci* 5: 438-445.
- Spector AA, Yorek MA (1985) Membrane lipid composition and cellular function. *J Lipid Res* 26: 1015-1035.
- Sretavan DW (1990) Specific routing of retinal ganglion cell axons at the mammalian optic chiasm during embryonic development. *J Neurosci* 10: 1995-2007.
- Sretavan DW, Reichardt LF (1993) Time-lapse video analysis of retinal ganglion cell axon pathfinding at the mammalian optic chiasm: growth cone guidance using intrinsic chiasm cues. *Neuron* 10: 761-777.
- Stocco DM (2001) StAR protein and the regulation of steroid hormone biosynthesis. *Annu Rev Physiol* 63: 193-213.
- Sugawara T, Lin D, Holt JA, Martin KO, Javitt NB, Miller WL, Strauss JF, III (1995) Structure of the human steroidogenic acute regulatory protein (StAR) gene: StAR stimulates mitochondrial cholesterol 27-hydroxylase activity. *Biochemistry* 34: 12506-12512.
- Sun Y, Hao M, Luo Y, Liang CP, Silver DL, Cheng C, Maxfield FR, Tall AR (2003) Stearoyl-CoA desaturase inhibits ATP-binding cassette transporter A1-mediated cholesterol efflux and modulates membrane domain structure. *J Biol Chem* 278: 5813-5820.
- Surchev L, Dontchev V, Ichev K, Dolapchieva S, Bozhilova-Pastirova A, Vankova M, Kirazov E, Vassileva E, Venkov L (1995) Changes in the neuronal plasma membrane during synaptogenesis. *Cell Mol Biol (Noisy-le-grand)* 41: 1073-1080.
- Suzuki T, Ito J, Takagi H, Saitoh F, Nawa H, Shimizu H (2001) Biochemical evidence for localization of AMPA-type glutamate receptor subunits in the dendritic raft. *Brain Res Mol Brain Res* 89: 20-28.

- Tait S, Gunn-Moore F, Collinson JM, Huang J, Lubetzki C, Pedraza L, Sherman DL, Colman DR, Brophy PJ (2000) An oligodendrocyte cell adhesion molecule at the site of assembly of the paranodal axo-glia junction. *J Cell Biol* 150: 657-666.
- Tenhunen R, Marver HS, Schmid R (1968) The enzymatic conversion of heme to bilirubin by microsomal heme oxygenase. *Proc Natl Acad Sci U S A* 61: 748-755.
- Thiele C, Hannah MJ, Fahrenholz F, Huttner WB (2000) Cholesterol binds to synaptophysin and is required for biogenesis of synaptic vesicles. *Nat Cell Biol* 2: 42-49.
- Thomson M (2003) Does cholesterol use the mitochondrial contact site as a conduit to the steroidogenic pathway? *Bioessays* 25: 252-258.
- Toda H, Takahashi J, Mizoguchi A, Koyano K, Hashimoto N (2000) Neurons generated from adult rat hippocampal stem cells form functional glutamatergic and GABAergic synapses in vitro. *Exp Neurol* 165: 66-76.
- Tropea M, Johnson MI, Higgins D (1988) Glial cells promote dendritic development in rat sympathetic neurons in vitro. *GLIA* 1: 380-392.
- Tsui-Pierchala BA, Encinas M, Milbrandt J, Johnson EM, Jr. (2002) Lipid rafts in neuronal signaling and function. *Trends Neurosci* 25: 412-417.
- Tucker RP, Matus AI (1988) Microtubule-associated proteins characteristic of embryonic brain are found in the adult mammalian retina. *Dev Biol* 130: 423-434.
- Ullian EM, Christopherson KS, Barres BA (2004) Role for glia in synaptogenesis. *GLIA* 47: 209-216.
- Ullian EM, Sapperstein SK, Christopherson KS, Barres BA (2001) Control of synapse number by glia. *Science* 291: 657-661.
- Ullian EM, Harris BT, Wu A, Chan JR, Barres BA (2004) Schwann cells and astrocytes induce synapse formation by spinal motor neurons in culture. *Mol.Cell.Neurosci.* 25: 241-251
- Urist MR, Huo YK, Brownell AG, Hohl WM, Buyske J, Lietze A, Tempst P, Hunkapiller M, DeLange RJ (1984) Purification of bovine bone morphogenetic protein by hydroxyapatite chromatography. *Proc Natl Acad Sci U S A* 81: 371-375.
- Vance DE, Vance JE (2002) *Biochemistry of lipids, lipoproteins and membranes*. 4th edition, Elsevier Science
- van den Pol AN, Spencer DD (2000) Differential neurite growth on astrocyte substrates: interspecies facilitation in green fluorescent protein-transfected rat and human neurons. *Neuroscience* 95: 603-616.
- Verderio C, Coco S, Pravettoni E, Bacci A, Matteoli M (1999) Synaptogenesis in hippocampal cultures [In Process Citation]. *Cell Mol Life Sci* 55: 1448-1462.
- Verma A, Hirsch DJ, Glatt CE, Ronnett GV, Snyder SH (1993) Carbon monoxide: a putative neural messenger. *Science* 259: 381-384.

- Virchow R (1856) *Gesammelte Abhandlungen zur wissenschaftlichen Medizin*. Frankfurt am Main: Hamm.
- Wagner JA, Carlson SS, Kelly RB (1978) Chemical and physical characterization of cholinergic synaptic vesicles. *Biochemistry* 17: 1199-1206.
- Wang N, Silver DL, Costet P, Tall AR (2000a) Specific binding of ApoA-I, enhanced cholesterol efflux, and altered plasma membrane morphology in cells expressing ABC1. *J Biol Chem* 275: 33053-33058.
- Wang N, Silver DL, Thiele C, Tall AR (2001) ATP-binding cassette transporter A1 (ABCA1) functions as a cholesterol efflux regulatory protein. *J Biol Chem* 276: 23742-23747.
- Wang Y, Thiele C, Huttner WB (2000b) Cholesterol is required for the formation of regulated and constitutive secretory vesicles from the trans-Golgi network. *Traffic* 1: 952-962.
- Warton SS, McCart R (1989) Synaptogenesis in the stratum griseum superficiale of the rat superior colliculus. *Synapse* 3: 136-148.
- Whitford KL, Dijkhuizen P, Polleux F, Ghosh A (2002) Molecular control of cortical dendrite development. *Annu Rev Neurosci* 25: 127-149.
- Williams SE, Mann F, Erskine L, Sakurai T, Wei S, Rossi DJ, Gale NW, Holt CE, Mason CA, Henkemeyer M (2003) Ephrin-B2 and EphB1 mediate retinal axon divergence at the optic chiasm. *Neuron* 39: 919-935.
- Withers GS, Higgins D, Charette M, Banker G (2000) Bone morphogenetic protein-7 enhances dendritic growth and receptivity to innervation in cultured hippocampal neurons. *Eur J Neurosci* 12: 106-116.
- Wong RO, Ghosh A (2002) Activity-dependent regulation of dendritic growth and patterning. *Nat Rev Neurosci* 3: 803-812.
- Wood WG, Schroeder F, Hogg L, Rao AM, Nemezc G (1990) Asymmetric distribution of a fluorescent sterol in synaptic plasma membranes: effects of chronic ethanol consumption. *Biochim Biophys Acta* 1025: 243-246.
- Woolley CS, McEwen BS (1992) Estradiol mediates fluctuation in hippocampal synapse density during the estrous cycle in the adult rat. *J Neurosci* 12: 2549-2554.
- Wu FS, Gibbs TT, Farb DH (1991) Pregnenolone sulfate: a positive allosteric modulator at the N-methyl-D-aspartate receptor. *Mol Pharmacol* 40: 333-336.
- Yagami K, Suh JY, Enomoto-Iwamoto M, Koyama E, Abrams WR, Shapiro IM, Pacifici M, Iwamoto M (1999) Matrix GLA protein is a developmental regulator of chondrocyte mineralization and, when constitutively expressed, blocks endochondral and intramembranous ossification in the limb. *J Cell Biol* 147: 1097-1108.
- Yeagle PL (1985) Cholesterol and the cell membrane. *Biochim Biophys Acta* 822: 267-287.

- Yeagle PL (1989) Lipid regulation of cell membrane structure and function. *FASEB J* 3: 1833-1842.
- Yin Y, Kikkawa Y, Mudd JL, Skarnes WC, Sanes JR, Miner JH (2003) Expression of laminin chains by central neurons: analysis with gene and protein trapping techniques. *Genesis* 36: 114-127.
- Yin Y, Miner JH, Sanes JR (2002) Laminets: laminin- and netrin-related genes expressed in distinct neuronal subsets. *Mol Cell Neurosci* 19: 344-358.
- Yokoyama C, Wang X, Briggs MR, Admon A, Wu J, Hua X, Goldstein JL, Brown MS (1993) SREBP-1, a basic-helix-loop-helix-leucine zipper protein that controls transcription of the low density lipoprotein receptor gene. *Cell* 75: 187-197.
- Zakhary R, Poss KD, Jaffrey SR, Ferris CD, Tonegawa S, Snyder SH (1997) Targeted gene deletion of heme oxygenase 2 reveals neural role for carbon monoxide. *Proc Natl Acad Sci U S A* 94: 14848-14853.
- Zhang J, Madden TL (1997) PowerBLAST: a new network BLAST application for interactive or automated sequence analysis and annotation. *Genome Res* 7: 649-656.
- Zheng P, Horwitz A, Waelde CA, Smith JD (2001) Stably transfected ABCA1 antisense cell line has decreased ABCA1 mRNA and cAMP-induced cholesterol efflux to apolipoprotein AI and HDL. *Biochim Biophys Acta* 1534: 121-128.
- Ziv NE, Smith SJ (1996) Evidence for a role of dendritic filopodia in synaptogenesis and spine formation. *Neuron* 17: 91-102.
- Zwain IH, Yen SS (1999) Neurosteroidogenesis in astrocytes, oligodendrocytes, and neurons of cerebral cortex of rat brain. *Endocrinology* 140: 3843-3852.

VII. A C K N O W L E D G E M E N T S

Many Thanks, Merci Beaucoup, Vielen Dank

- an meinen Doktorvater Frank W. Pfrieder, einen großartigen Wissenschaftler und Mentor, der mich förderte und forderte
- an Herrn Prof. Hucho für die Anfertigung des Zweitgutachtens
- to the Région d'Alsace for financial support over the last three years
- to the European Doctoral College for financial support and education in European affairs with many interesting views in European institutions
- to all my colleagues for the wonderful time in the great Pfrieder-team
- an meine Eltern, die mich in Frankreich abgesetzt haben, mich aber dennoch nie alleine ließen
- an meine Schwester für Eulen aus Hamburg und alles andere, das man unter Geschwistern nicht aufzählt
- an meinen HH für den H im Leben

VIII. CURRICULUM VITAE

Family Name	Göritz
First Name	Christian
Date of Birth	25 February 1974
Place of Birth	Berlin, Germany
Nationality	German
Address	10, rue De Bruges; 67000 Strasbourg; France

EDUCATION

since 2001	Thesis at the Centre de Neurochimie in Strasbourg, in the Max Planck/CNRS Group under supervision of Dr. Frank W. Pfrieger. In co-support of the Free University of Berlin and the University Louis Pasteur of Strasbourg, with financial support from the Region Alsace and the European Doctoral College.
1999 – 2000	Diploma in Biochemistry; Title: »Identification of Neuronal Proteins Controlled by Glial Signals Using 2D-Gelelectrophoresis and Mass Spectrometry«. Faculty of Biology, Chemistry and Pharmacy, Free University of Berlin and MDC for Molecular Medicine, Berlin. Advisors: Prof. Dr. F. Hucho and Dr. F. W. Pfrieger.
1994 – 1999	Study of Biochemistry at the Free University of Berlin
1990 – 1992	Gymnasium Bernau (at Berlin), Germany
1980 – 1990	Realschule Klosterfelde, Germany

PUBLICATIONS

Mauch DH, Nägler K, Schumacher S, Göritz C, Müller EC, Otto A, Pfrieger FW (2001). CNS synaptogenesis promoted by glia-derived cholesterol. *Science* 294, 1354-1357.

Göritz C, Mauch DH, Nägler K, Pfrieger FW (2002) Role of glia-derived cholesterol in synaptogenesis: new revelations in the synapse-glia affair. *J Physiol (Paris)* 96: 257-263.

Göritz C, Mauch DH, Pfrieger FW. Multiple mechanisms mediate glia-induced synaptogenesis in a CNS neuron (in press)